

The following article is hosted by PTB.

DOI: 10.7795/530.20240206A

Good Practice Guide for setting up an uncertainty budget for the measurement of luminance distributions including correlation of the 2D datasets

Christian Schrader¹, Johannes Ledig¹, Armin Sperling¹, Udo Krüger², Tobias Schneider³, Fabien Eloi⁴, Zühal Alpaslan Kösemen⁵, Olivier Pellegrino⁶, Teresa Molina-Jimenez⁷

¹ Physikalisch-Technische Bundesanstalt, Braunschweig and Berlin, Germany

² TechnoTeam Bildverarbeitung GmbH, Ilmenau, Germany

³ Instrument Systems Optische Messtechnik GmbH, München, Germany

⁴ Laboratoire National de métrologie et d'Essai (LNE), Paris, France

⁵ TÜBİTAK UME, National Metrology Institute of Türkiye, Kocaeli, Türkiye

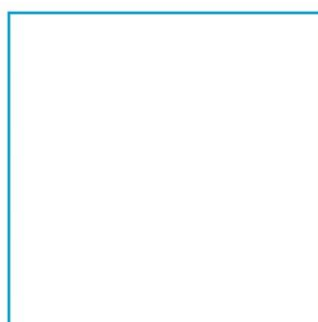
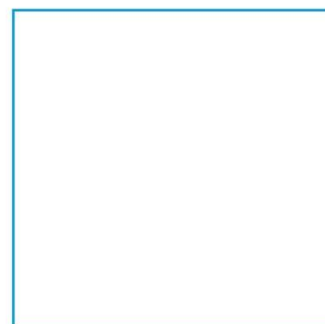
⁶ Instituto Português da Qualidade, Caparica, Portugal

⁷ candelTEC S.L., Valencia, Spain

Acknowledgement: This project has received funding from the EMPIR programme co-financed by the Participating States and from the European Union's Horizon 2020 research and innovation programme.

Available at:

<https://doi.org/10.7795/530.20240206A>





19NRM02 “RevStdLED”



**Good Practice Guide
for
Setting up an Uncertainty Budget for the
Measurement of Luminance Distributions
Part 1**

**Estimation of Measurement Uncertainty Contributions
Originating From the ILMD**

This project has received funding from the EMPIR programme co-financed by the Participating States and from the European Union’s Horizon 2020 research and innovation programme.



The EMPIR initiative is co-funded by the European Union's Horizon 2020 research and innovation programme and the EMPIR Participating States

Table of Contents

1	Introduction.....	3
1.1	Aspects of Correcting for Measurement Errors	3
1.2	Identification of Uncertainty Contributions	4
2	Calibration Uncertainty	5
2.1	Technical Background.....	5
2.2	Proposed Estimate of Uncertainty Contribution:.....	5
3	Shading Error and its Focus Dependence	5
3.1	Technical Background.....	5
3.2	Proposed Estimate of Uncertainty Contribution:.....	8
4	Non-Linearity	9
4.1	Technical Background.....	9
4.2	Proposed Estimate of Uncertainty Contribution:.....	10
5	Spectral Dependence of Non-Linearity	10
5.1	Technical Background.....	10
5.2	Proposed Estimate of Uncertainty Contribution:.....	12
6	Size-of-Source-Effect	12
6.1	Technical Background.....	12
6.2	Proposed Estimate of Uncertainty Contribution:.....	14
7	Straylight into Dark Regions	14
7.1	Technical Background.....	14
7.2	Proposed Estimate of Uncertainty Contribution:.....	15
8	Focus-Setting	16
8.1	Technical Background.....	16
8.2	Proposed estimate of uncertainty contribution:.....	16
9	Other Uncertainty Contributions	17
10	Correlations Between Multiple Measurements	18
11	Relevance of Different Uncertainty Contributions for Exemplary Measurement Applications....	20
12	References.....	22
13	Appendix I: Checklist for the ILMD configuration	23
14	Appendix II: List of Measurement Applications	25

1 Introduction

This document addresses the handling and estimation of critical measurement errors and related uncertainties that are originating from the working principle of an imaging measurement device (ILMD) and consider their relevance for selected applications. It is shown, how information from the instrument manufacturer regarding properties of his Imaging Luminance, Radiance or Colour Measuring Device (IxMD) can be used for such estimations. Further contributions related to the luminance measurement using an ILMD, i.e. mainly originating from the scene and the definition of the measurand in the application and its repeatability, are considered in a separate document (cf. Part 2 of this GPG). Both guidelines are reasonable only in case of a proper state and adequate configuration of the IMLD is ensured, which is addressed in Appendix I: Checklist for the ILMD configuration.

ILMDs are complex measurement devices based on microelectronic pixel matrix sensors as a key-enabling technology. Their complex signal path leads to multiple error sources in the optical path, the spectral weighting, the analogue signal processing and the digitalization that significantly affect the signal in an unintended way. Manufacturers design an internal model of evaluation which transforms the sensor signal with respect to internal configuration settings into a luminance signal indicated by the ILMD. Parts of these models apply corrections for relevant systematic signal distortions and therefore reduce corresponding measurement errors. However, this is increasingly problematic (also for the manufacturers) because not enough information about the pixel sensor is provided for this, and the measurement systems are becoming more complex. These models need to be parametrized by an adjustment procedure. The characterization for this adjustment is a complex task that requires a suitable setup and may take a significant amount of effort. The amount of details required depend on the number of different configurations that need to be characterized and the availability of automation.

Some of the distortions depend on internal quantities which are known (i.e. device parameters and configuration) or can be estimated during measurement. These are candidates to be corrected for. Other distortions depend on environmental condition or the scene to be measured itself, which are not known during the measurement. Here an intrinsic correction is difficult. Some corrections may be generally possible but require some computational effort. The temporal stability of the device regarding its properties is also a limiting factor for the level of detail. From these facts follows that the manufacturer has to select an internal model and the corrections to be applied that balance the effort during characterization and application and the benefit obtained. The weighting of these boundary conditions may depend on the targeted measurement task. As a consequence of this, despite internal corrections being applied, the devices will have residual systematic deviations that lead to measurement uncertainties depending namely on the extent and the quality of the internal corrections.

1.1 Aspects of Correcting for Measurement Errors

For the user there are two ways to deal with these systematic measurement errors of the readings from the device. The first is to correct for them. From the metrological standpoint this is the preferred way because the propagation of variance according to GUM requires a correction of all relevant systematic effects and propagate only stochastic components to a measurement uncertainty. This correction requires their determination and modelling by means of characteristic functions to calculate the correction for a specific measurement. Different problems come together at this task. First of all, the result depends on the internal configuration of the device and its internal adjustments. If this changes between characterization and measurement, the result may not be transferable to this new configuration. This means, the user has to make assumptions that are not based on knowledge of internal parameters. It is a contradiction to use a device just "as is", as a black-box, and then use assumptions about the internal behaviour when it seems to be useful. The second issue is that it is very challenging to stimulate the system in a way that the change of the acquired signal (luminance value) can be

attributed to a specific influential quantity or mechanism. But this selective stimulation is required to determine the related characteristic without considering other mechanisms. If each influential quantity cannot be handled independently the parameter space to be scanned gets vastly large. A change of the scene/stimulus will usually affect multiple mechanisms simultaneously. If the residual systematic measurement errors are determined the uncertainty of this correction and the remaining stochastic components need to be quantified. This characterization might be possible for some devices, influential mechanisms, and measurement tasks, but it cannot be recommended as a general approach to handle measurement uncertainties.

For many users a second way to handle systematic measurement errors might be preferable. Here the systematic deviations of the readings from the device are *not corrected* but they are entirely handled as uncertainties, namely for such already corrected inside the ILMD. To determine these uncertainties, in principle one could measure a set of known luminance levels in different configurations (vary the objective lens, distance, size in the image, position in the image, integration time, ambient conditions, ...) but here the same issue arises like above, i.e. the parameter space gets huge and cannot be sampled sufficiently densely. Therefore, this sampling needs to systematically cover critical measurement conditions regarding specific influential mechanisms with the goal to estimate intervals for the maximum error that can be expected from each mechanism, not to determine detailed correction functions. Because the origin of these uncertainties lies in systematic deviations, the resulting uncertainty distributions will often be asymmetric, but, resulting from missing knowledge, the underlying distributions of these errors are treated as uniform. The resulting standard deviation for an interval [*min* .. *max*] is then given by

$$\sigma = u = \frac{\text{max}-\text{min}}{\sqrt{12}}. \quad (1)$$

1.2 Identification of Uncertainty Contributions

The information of what the critical conditions are is based on the knowledge of full characterizations and an understanding of the general inner working principle of an ILMD. A possible source for aspects of these characterizations is the CIE 244:2021 “Characterization of Imaging Luminance Measurement Devices (ILMDs)” [1]. The quality indices introduced there are designed to trigger different error sources and quantify the device’s performance regarding these error sources. They are designed to compare devices. The quality indexes are explicitly not usable to correct measurement results or to estimate the measurement uncertainty for a specific measurement. They also are only valid for a specific configuration. If some quality indices are provided for a device, they are not necessarily determined in a most critical configuration nor in the configuration used for a measurement. Also, not every quality index is generally relevant for the application.

This guide will select the most critical error sources that can be evaluated by the user with a reasonable amount on effort and guidance on how to estimate them. The evaluations will/may be similar to ones of the CIE 244:2021 quality indices but with variations to measure with critical configurations. For each measurement, an explanation is provided why the proposed measurement configuration is a critical one.

For effects that scale the transfer function for the pixels just by a factor, the uncertainty contributions can be expressed as a relative contribution u_{rel} . They can be transferred to absolute uncertainty contribution by just multiplying them with the output quantity Y (luminance signal) related to the pixel (or the evaluation region). For effects that are purely additive this is not helpful because the sensitivity of the output quantity to the uncertainty of the input quantity and therefore the value of the absolute uncertainty contribution u_{abs} does not just scale with the pixel signal itself. It can also depend on the signal of other pixels or on regions completely out of the measurement field (as for stray light). They

have to be estimated during the measurements for the specific device configuration and scene. The overall standard uncertainty of a single luminance measurement then is given by

$$u_{\text{abs}}(Y) = \sqrt{Y^2(u_{\text{rel},1}^2 + u_{\text{rel},2}^2 + \dots) + u_{\text{abs},1}^2 + \dots} \quad (2)$$

All uncertainty components of a measurement Y (single pixel or evaluation region) are treated as uncorrelated, c.f. Section 9 “Correlations Between Multiple Measurements”.

The approach of not correcting for systematic effects might be not ideal in the metrological view [2], but this correction can only be done on sufficiently extensive and reliable characterization. According to VIM 2.26 [3], Measurement uncertainty is a “non-negative parameter characterizing the dispersion of the quantity values being attributed to a measurand, based on the information used”. The proposed approach works on an intentionally limited amount of “information used”.

2 Calibration Uncertainty

2.1 Technical Background

The ILMD system needs to be adjusted by the manufacturer. The determined characterization data is used to adjust the device to be able to transform the luminance at the measured scene into luminance values that are indicated by the measurement device (and taken as a reading by the operator). The complexity of this adjustment differs significantly for each ILMD model/manufacturer and its configuration, i.e. lens type. One part of this process is the “absolute calibration” to establish a link to the unit by measuring a traceable luminance standard, e.g. by the determination of a global adjustment factor and subsequent calibration of the well-adjusted ILMD. This standard itself is calibrated with a given uncertainty. Additionally, the calibration process adds uncertainties by differences between the realized measurement conditions during absolute calibration of the ILMD and the conditions with that the luminance standard was calibrated. This uncertainty of the manufacturer’s absolute calibration establishes the base uncertainty of the ILMD system.

2.2 Proposed Estimate of Uncertainty Contribution:

The information on the (relative) calibration uncertainty $u_{\text{rel,cal}}$ should be stated in the manufacturer’s calibration certificate. It might be given as an expanded uncertainty which then has to be converted to standard uncertainty. This uncertainty might be given as the uncertainty of an initial adjustment index f_{adj} from [1] which should be zero itself for an individual adjusted device.

3 Shading Error and its Focus Dependence

3.1 Technical Background

For the underlying camera system forming an ILMD the responsivity to luminance varies between the pixels. One part of this variation is the varying responsivity of each pixel of the sensor (photo response non-uniformity, PRNU) which renders in a high frequency image noise. A second part, called “shading”, is caused by the changing transmissivity of the optical path through the objective lens (lenses and aperture) and the spectral weighting filter into the pixel matrix sensor. Here the main part is caused by the varying effective/projected aperture size into the viewing direction. This effect is known as \cos^4 -law and leads to a decline of the signal with increasing viewing angle and therefore with larger distance to the optical axis (image centre) and shorter focus lengths. A smaller contribution to the shading comes from the changing path length through the optical filters and other local variations, e.g. the pixel structure including the alignment of micro-lenses that are placed on the pixels to increase the effective light collecting area and therefore the responsivity.

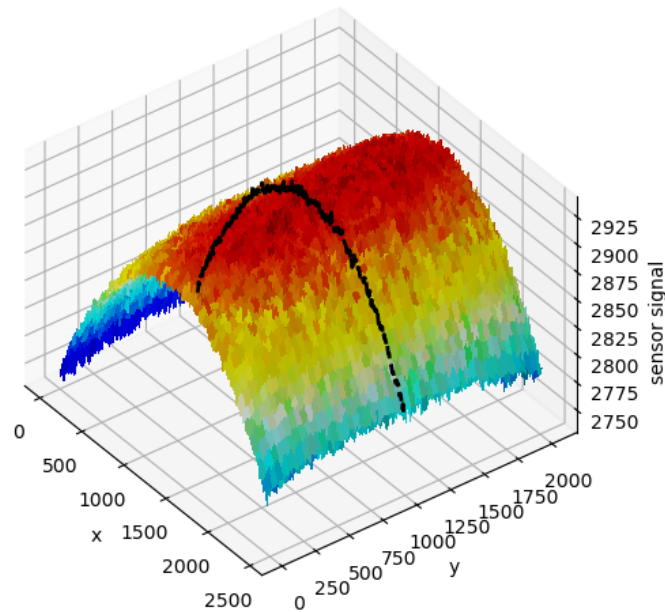


Figure 1: Example of the shading characteristic of an ILMD

To initially adjust an ILMD, the relation of the sensor signal (after some corrections) to the input luminance needs to be determined. For this one would ideally use a calibrated and homogeneous source that is extended enough to fill the whole measurement field of the ILMD. This combination is not generally available. Therefore, the adjustment gets split into the determination of the relative responsivity between the pixels and an absolute link to the SI unit for a small (usually central) pixel region (see previous section). The relative responsivity can be determined by imaging into an Ulbricht-sphere. Figure 1 shows an exemplary result of such measurement as a 3D plot. The black line shows the position of a central horizontal profile line that will be used in the next figures for better illustration. Please note that the size and the general shape of the shading effects depend strongly on the specific objective lens type and that the shown examples cannot be taken as “typical”!

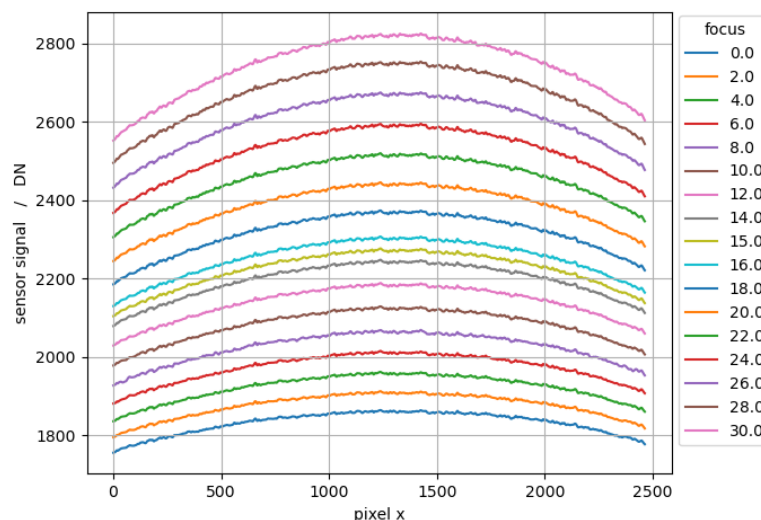


Figure 2: Focus dependence of the shading characteristic, absolute and relative

Figure 2 shows these shading profile lines for a series of measurements at different focus. It is apparent that the absolute values and the relative shapes change with the focus. For each shading dataset an average value of a small central region can be calculated as a reference value. When the shading datasets are normalized to this reference value, only the relative changes remain. Figure 3 shows the normalized profile lines where their relative change regarding to the focus gets more evident.

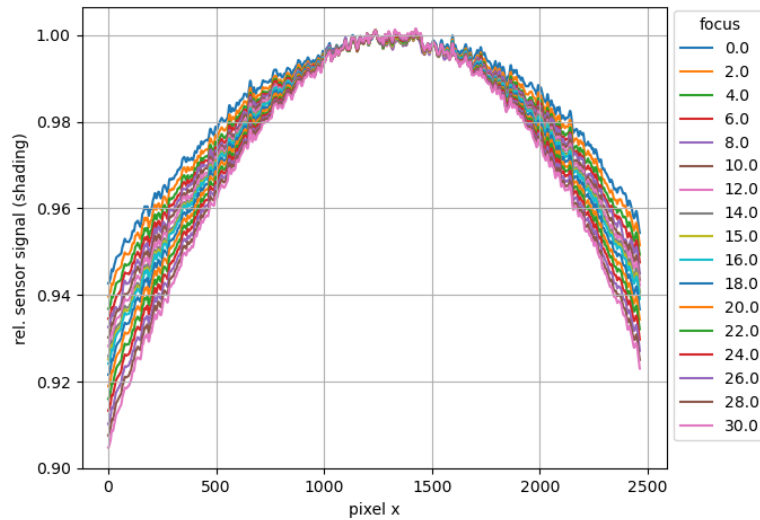


Figure 3: Focus dependency of the relative shading characteristic across the image

The reference values itself characterize the change of the absolute responsivity regarding the focus. They can get normalized themselves to the reference value of one focus setting to get a relative correction factor versus to the focus setting (Figure 4). In the ILM D control software this factor is usually implemented as a correction which value gets selected by an automated read-out or a manual selection of the current focus value of the objective lens.

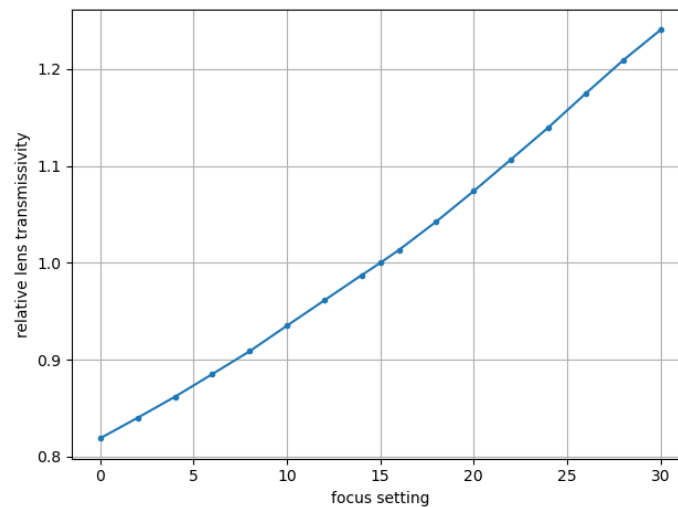


Figure 4: Relative lens transmissivity versus focus setting

Such characterization data regarding the ILM D responsivity can be used internally as an adjustment to compensate for the shading effects on a per pixel basis. Here, a balance between the effort for the characterization and handling of the data and the improvement that can be achieved is targeted. Often only one of these two-dimensional shading data sets is determined and used in combination with a global focus dependent scaling. The remaining change in the outer image regions remain as an uncertainty component.

These remaining shading errors with enabled internal correction can be determined by rotating the ILM D horizontally and vertically around its projection centre and measure the average luminance of a small homogeneous light source in different distances (small, medium, large, according to the objective's focus scale). Figure 5 shows the result of such measurements for horizontal and vertical scanning where the regions average values are normalized to the value at the image centre. With the central focus value 15 (complies to the calibration condition for this example) the shading is well compensated

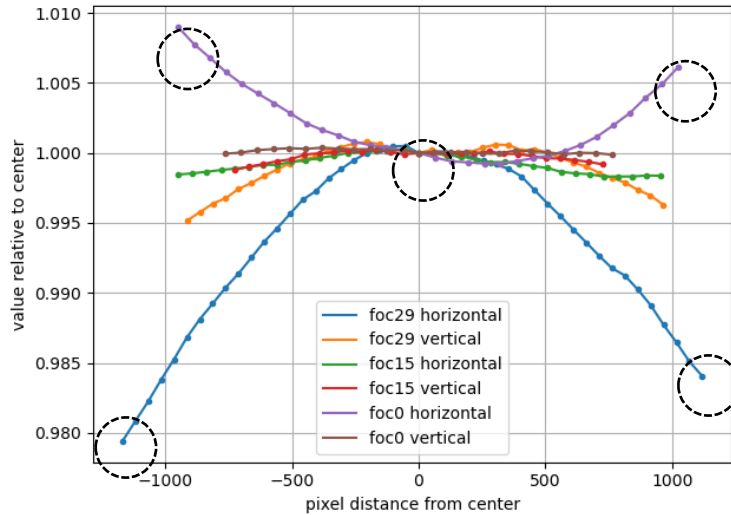


Figure 5: Relative residual shading error for different focus with respect to that at a focus value of 15

and only a very small shading error remains. With focus value 0 (small distance) the shading gets overcompensated and with focus value 29 (large distance) the shading gets undercompensated. Shading is also different in vertical and horizontal direction, and both must be investigated to properly determine the maximum shading error.

3.2 Proposed Estimate of Uncertainty Contribution:

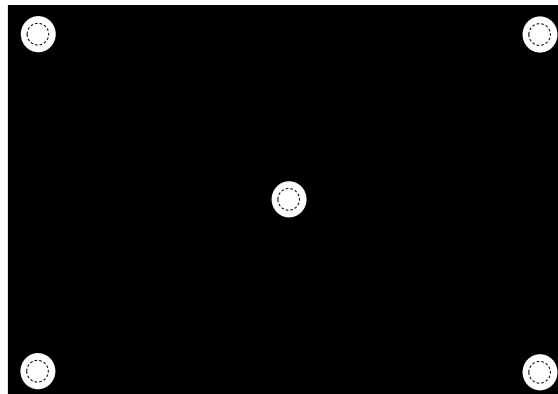


Figure 6: Measurement locations of homogenous light source by rotation around projection centre

The circular marked regions in Figure 5 correspond to the critical regions for a single axis scan. These demonstrate that the largest uncertainty contributions can be expected in the image corners. Therefore, the maximum relative errors can be estimated by, for each lens, measuring the average luminance of a small spot region in the image centre and near the image corners. Figure 6 shows these locations. The image regions should not touch the image corner. The evaluation region should be significantly smaller than the image of the source ($\approx 50\%$ of source).

To ensure that the source has the same luminance for all measurements, the change of the sources location in the image should be reached by rotating the ILMD (nearly) around its projection centre. This is important especially for small distances and can i.e. be realized by using a nodal point adapter for this rotation while placing the ILMD projection centre into the pivot point of the adapter to maintain the viewing position. By this the measurement direction with respect to the source is kept constant, in opposite to a translation of the ILMD. These measurements give one value for the centre Y_{centre} and multiple values Y_i for the corners (additional locations are possible). This series of single point measurements needs to be repeated for different focus settings and corresponding source distances k .

The maximum error is then given by

$$E_{\text{rel,shading}} = \max \left(\left| \frac{Y_{\text{centre}} - Y_i}{Y_{\text{centre}}} \right|_k \right) \quad (3)$$

With this the relative uncertainty follows for a uniform distribution as

$$u_{\text{rel,shading}} = \frac{2 E_{\text{rel,shading}}}{\sqrt{12}} = \frac{E_{\text{rel,shading}}}{\sqrt{3}} \quad (4)$$

In general, the distances should be varied from the lowest possible focus distance to a large one near infinity. If the adjustment distance is known, it should be used as a reference. Here the lowest residual shading error can be expected. For each distance the correct focus setting of the objective lens needs to be set in the ILM software. It might be helpful to use additional locations on the image diagonals or the image in general (see also definition of f_{22} in [1]). This will increase the needed effort for the characterization but allows later to select appropriate subregions that correspond to a specific measurement task for the determination of $u_{\text{rel,shading}}$. The same applies for the focus distances. The definition of f_{22} uses a very similar formulation to eqn. 3, but there is no requirement to determine it at different focus distances to detect the maximum values at critical focus distances. Therefore, no general recommendation can be given to use f_{22} as $E_{\text{rel,shading}}$. If it can be ensured that f_{22} was determined using multiple and critical focus distances, then it would be possible to use it rather than doing the characterisation on one's own.

During the variation of the distances the imaged size of the source needs to be held in a similar range to ensure that a sufficient local resolution is achieved. This can be achieved by using different sources or placing apertures in front of the source for smaller distances.

4 Non-Linearity

4.1 Technical Background

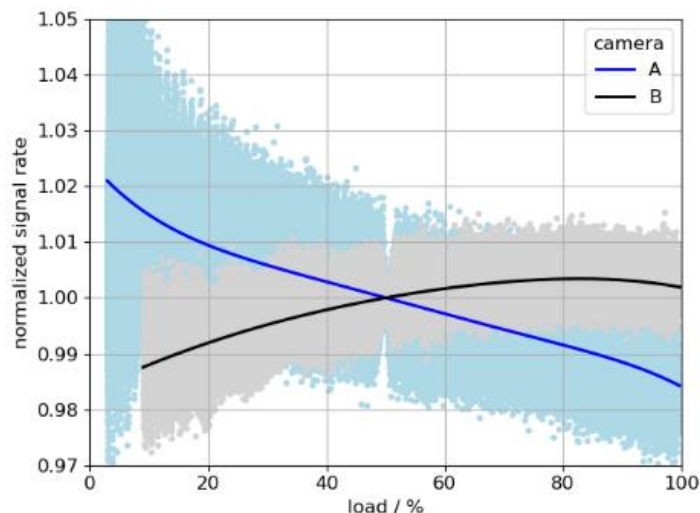


Figure 7: Examples for non-linearity characteristics

The internal components of an ILM may show deviations from an ideal linear behaviour versus the presented luminance. This means that the respective transfer function of that component changes depending on its operating point. This operating point can usually be described by its input or output quantity. The main sources of non-linearity are the signal processing (analogue amplification and AD-conversion) and non-linear properties of the pixels photo diodes. The quantity that defines the operating point is the number of accumulated charges or, transformed by an internal gain factor, the

sensors raw (count-) signal. Figure 7 shows the normalized signal rate representing the non-linearity versus the signal load of two different pixel matrix sensors that are also used in ILMDs. The non-linearity might be corrected by the device internally.

4.2 Proposed Estimate of Uncertainty Contribution:

To determine the residual non-linearity error, the average luminance of a stable homogenous light source needs to be measured while changing the internal operating point. Instead of changing the luminance level this is achieved by a variation of the integration time in multiple steps ($n_{ti} = 5 \dots 20$) to result in a signal from $\approx 10\%$ load to $\approx 90\%$ load of the dynamic range (available range of count values). For an ideal ILMD, the measured average luminance should be independent of the integration time. In case of a suitable internal configuration the non-linearity will not depend on the luminance level, except than for extreme low or high luminance.

To convert the averaged luminance values into a relative non-linearity, they would have to be normalized to the value corresponding to a reference point. At this reference point the non-linearity correction factor would be exactly 1. This reference point is ambiguous and the one used by the manufacturer for the internal calibration cannot be reconstructed.

A good estimation for residual non-linearity error of an ILMD is half of the range between the maximum and minimum values, normalized to the centre between maximum and minimum:

$$E_{rel,nl} = \frac{(Y_{max}-Y_{min})/2}{(Y_{max}+Y_{min})/2} = \frac{Y_{max}-Y_{min}}{Y_{max}+Y_{min}} \quad (5)$$

If available, the quality index f_3 from [1] can be used as a good replacement of $E_{rel,nl}$. With this the relative uncertainty follows as

$$u_{rel,nl} = \frac{2 E_{rel,nl}}{\sqrt{12}} = \frac{E_{rel,nl}}{\sqrt{3}} \quad (6)$$

The measurements need to be done with sufficient spatial averaging (size of the measurement region by means of number of pixels) or temporal averaging (repetitive measurements) to get stable values, not significantly influenced by photon noise. For devices with electronic shutter, the luminance should be chosen at a level that the integration time is larger than ≈ 10 ms. Devices with mechanical shutter might need larger integration times. This reduces the influence of the smear effect (for CCD sensors) at short integration times and the relative error on the realized integration time itself. To ensure that the result is not an issue of an integration time error, or a related internal configuration change, the measurement can be repeated using a different luminance (i.e. realized by a neutral density filter). The spectral distribution should match that of the typical objects to measure or illuminant "A" (see next section).

5 Spectral Dependence of Non-Linearity

5.1 Technical Background

As stated in the previous section the effective overall non-linearity is the superposition of different internal mechanisms. One of these is the charge generation/collection inside the pixel photodiode. The incoming light is absorbed in the silicon of the pixel with different absorption coefficient and therefore at different depths, depending on the wavelength. Blue light has only a very limited penetration depth below $<1 \mu\text{m}$ but for red light it increases to some $10 \mu\text{m}$. So, the charge generation occurs at different regions inside the pixel. During the collection of the charges the location of the internal depletion zone may move and overlap with the zone of charge generation. This leads to a reduction of the charge collection efficiency during the integration time. Despite the real non-linearity evolving during the integration time, at the end of the integration time the overall number of collected charged

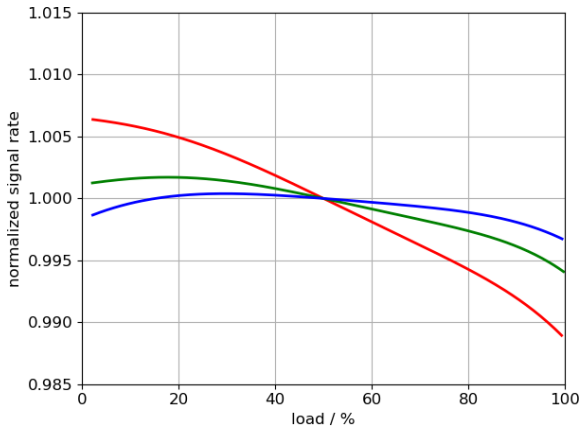


Figure 8: Example for different non-linearities for red, green and blue light

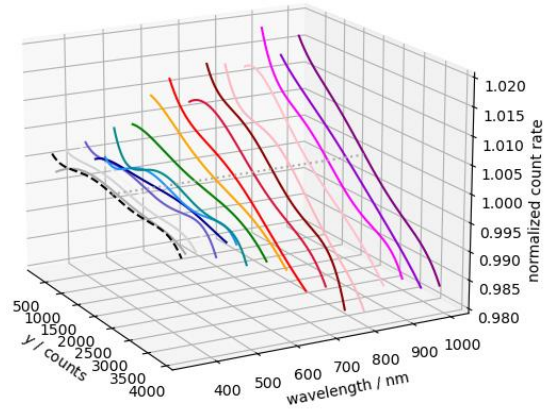


Figure 9: Wavelength dependency of the non-linearity

reduces for light with larger penetration depth (respectively wavelength), which resembles a non-linearity over the count signal [4].

Figure 8 shows an example for the effective measured non-linearities for an ILMD at the sensor's raw count signal for red, green and blue light. For blue light the non-linearity is only a few parts per thousand and thus neglectable. The non-linearity for red light is in a range from +0.7 % to -1 % and with this very similar to that measured with incandescent light. For this specific system it can be stated that most of the non-linearity is not caused by the internal signal processing but by the spectral properties of the pixel. Figure 9 shows a measurement with higher spectral resolution using a monochromator. Here it is to see that up to 500 nm wavelength the non-linearity is nearly flat but above that wavelength the spectral dependency sets in and increases until 800 nm. Above that wavelength there is no further increase.

This effect is not mandatory to exist, but it may occur. This depends on the internal structure of the pixel. If an internal correction for non-linearity takes place in an ILMD, one can expect that its characteristics is usually determined with an incandescent lamp or a source similar to standard illuminant A which might have a significant spectral dependent component. Figure 10 shows an example of this effect on a device. The measured luminance values are here normalized to the value nearest to 50% load to make the characteristics easier to compare. For illuminant "A" a nearly perfect compensation can be stated, but for red and blue light, an under- and overcompensation occurs.

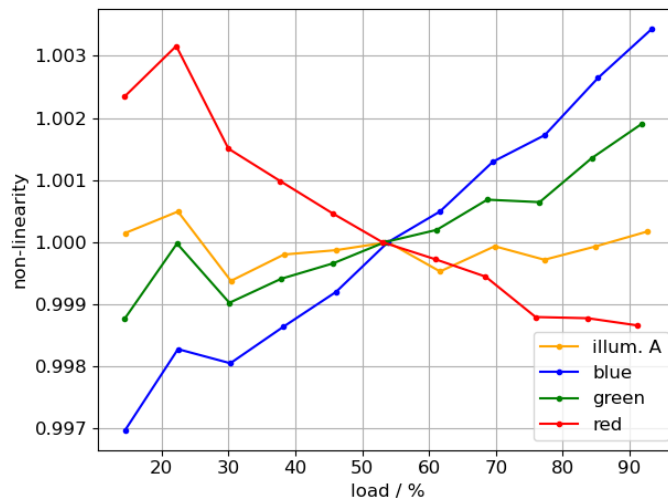


Figure 10: Residual non-linearity error for different spectral distributions

5.2 Proposed Estimate of Uncertainty Contribution:

The presence of this effect can be tested, and the resulting uncertainty contribution can be determined, by measuring the non-linearity error like in the previous section but using additionally sources with blue and red light, e.g. single colour LED-based luminance standards.

The relative uncertainty is then given as the maximum error value of all colour series k :

$$E_{\text{rel,nl}} = \max \left(\frac{Y_{\text{max}} - Y_{\text{min}}}{Y_{\text{max}} + Y_{\text{min}}} \Big|_k \right) \quad (7)$$

With this the relative uncertainty follows as

$$u_{\text{rel,nl}} = \frac{2 E_{\text{rel,nl}}}{\sqrt{12}} = \frac{E_{\text{rel,nl}}}{\sqrt{3}} \quad (8)$$

This replaces the uncertainty contribution of the previous section. The spectral dependency is a property of the sensor and the knowledge of the existence of a spectral dependency therefore can be transferred to other devices if their sensor type is known to be the same.

6 Size-of-Source-Effect

6.1 Technical Background

Because of diffuse scattering, optical aberrations and diffraction (described by the point spread function, PSF), parts of the light that are intended to be imaged onto a specific pixel assuming an ideal system gets instead dispersed to adjacent pixels. For larger evaluation regions that are compact (small border length in relation to the area) and relatively homogeneously illuminated these effects cancel out to a certain extend between adjacent pixels.

If the evaluation region is near the border of the illuminated region the effects gets more prominent. The effect works in both directions: dark regions surrounded by bright regions get brighter and bright regions surrounded by dark regions get darker. The overall luminous flux is constant but the distribution in the image differs from an ideal imaging.



Figure 11: Photo of an iris in front of a light source used to illustrate the size-of-source effect

To demonstrate and estimate the significance of this effect an iris is to be placed in front of a homogeneous illuminated surface (Figure 11). The ILMD is focused to the aperture of the iris. Then the iris is closed to minimum aperture, so that the aperture's size in the image is just one pixel (Figure 13, left). A measurement line through this central pixel is defined, wide enough to cover the full diameter of the

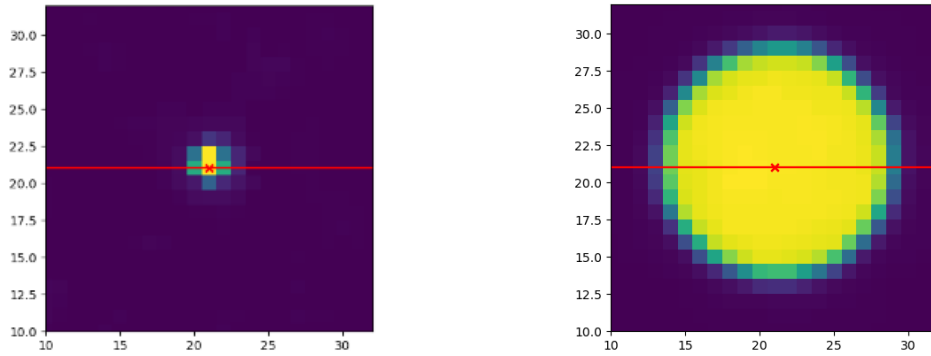


Figure 13: profile line through measurement region of variable aperture
left: smallest possible iris size ≈ 1 pixel, right: largest possible iris size

open iris (Figure 13, right). Then a series of measurements with increasing iris diameter is done and the line profiles are plotted, normalized to the maximum value of all profile lines at the central pixel.

In the example images of Figure 12 the width of the edge appears to be about three pixels wide. One might expect that for an iris diameter larger than twice the border width the central pixel's value keeps constant with increasing iris diameter and inner region show a plateau, because of the homogenous background luminance. But this is not the case and the establishment of a plateau requires in this example a source diameter (full width at half maximum in the image) of at least 15 pixels (iris diameter 7.0 mm, red line). Taking into account that two to three pixels are needed to define a flat plateau at the top, one ends up with an edge width of about five to six pixels. This defines the minimum distance, for this sensor/lens combination, that the evaluation region needs to have from strong gradients. If the imaged size of the source gets smaller, the measured value in the centre drops down rapidly (iris diameter ≤ 5 mm). A consequence from this is, that this effect cannot be handled as an uncertainty, and that *it is not reasonable to measure average luminances of sources with only a few pixels in size!* Despite that it might be common to gain geometrical information on the scene (e.g. angles between light sources) and luminance measurements out of the same image, this might lead to large errors if the source sizes in the image are too small. A better strategy here is to change the lens between wide angle lens for the geometrical information and an appropriate tele lens for the luminance measurements.

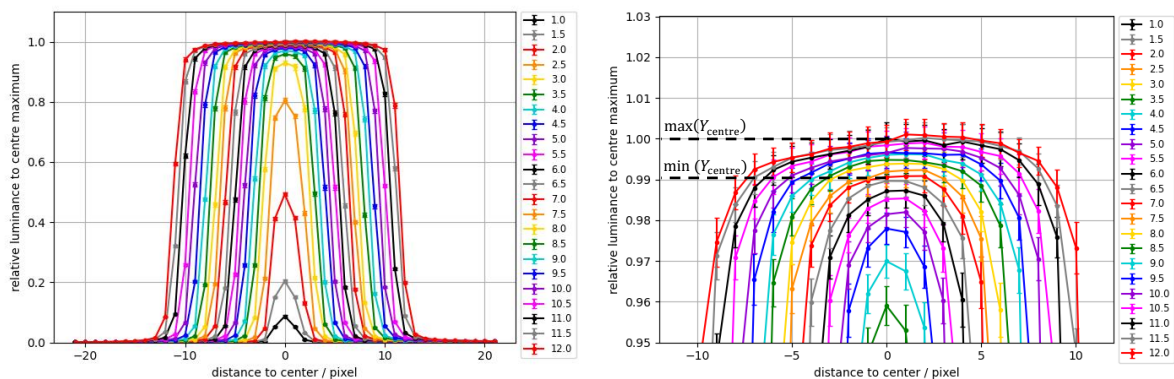


Figure 12: Measured profiles for different iris diameters, left: full profile, right: zoomed in

The second aspect that can be seen in Figure 12 is that the central value further increases for iris diameters larger than 7 mm where the plateau evolved. The increment gets smaller with the iris diameter but to reach limit value the diameter needs to be very large. The correct value lies in this range and depends on the device's calibration conditions. This can be handled as an uncertainty component.

6.2 Proposed Estimate of Uncertainty Contribution:

A measurement like shown before should be done with a reduced set of apertures. The apertures can be realized by an iris or a few fixed apertures. The goal is *not* to measure a full series like shown in Figure 12 but to determine two parameters:

1. The lower size limit where for a homogenous source a plateau gets established. This is to estimate the minimum distance of the evaluation region to the source border.
2. The relative change of that centre value between that lower size limit and a maximum source size (up to full measurement field).

The iris is usually required to realize diameters down to 1 mm. Depending on the measurement field of the ILM, the distance has to be adjusted to realize image sizes of the aperture in the range of a few pixels. For this test only the central pixel or at maximum a region of 3 by 3 pixels is measured. Therefore, a sufficient temporal averaging is required to reduce the influence of the photon noise ($n = 100$). Appropriate baffles have to be used to ensure that no light that passes the iris at the outside should hit the lens. It is recommended for this characterization to check and remove any post-processing from the software if activated such as smoothening, averaging, spike elimination etc.

The maximum source size can be simply realized by removing the iris and baffles. The size of the light source should fit the maximum size expected to be measured (regarding the imaged size). Diffuse LED panels might be suitable if their LEDs are operated by a direct current (i.e. no PWM). A sufficient homogeneity is only required for the central region to be measured, not for the whole source. The source should not be directly behind the iris to prevent backlash from the iris to the source that would change the luminance of the measured central pixel/region. This distance also improves the homogeneity by putting the source out of focus. The point spread function might broaden towards the edges/corners of the image. The size-of-source effect might change/increase at outer image locations. Therefore, this characterization might be repeated with imaging the aperture at a corner.

The relative maximum error is then given by half the ratio of the span to the mean value:

$$E_{\text{rel},\text{sos}} = \frac{\max(Y_{\text{centre}}) - \min(Y_{\text{centre}})}{\max(Y_{\text{centre}}) + \min(Y_{\text{centre}})} \quad (9)$$

This leads to the relative uncertainty

$$u_{\text{rel},\text{nl}} = \frac{2 E_{\text{rel},\text{sos}}}{\sqrt{12}} = \frac{E_{\text{rel},\text{sos}}}{\sqrt{3}} \quad (10)$$

For the shown example this gives a $E_{\text{rel},\text{sos}}$ of $\pm 0.5\%$ for region sizes between 15 (iris 7) and 22 (iris 12) pixels (ignoring the fact that the upper limit is defined by the maximum iris diameter, which is much smaller than the measurement field). This leads to an $u_{\text{rel},\text{nl}}$ of 0.29%.

7 Straylight into Dark Regions

7.1 Technical Background

The Size-of-Source effect of the previous section was induced by straylight from surrounding bright regions into the *bright* evaluation region of the same source. In the same way light might get dispersed from bright regions into neighbouring regions of lower luminance. This is usually a smaller absolute error than in the size-of source effect, but it gets relevant when measuring background luminances in a scene with large bright sources.

7.2 Proposed Estimate of Uncertainty Contribution:

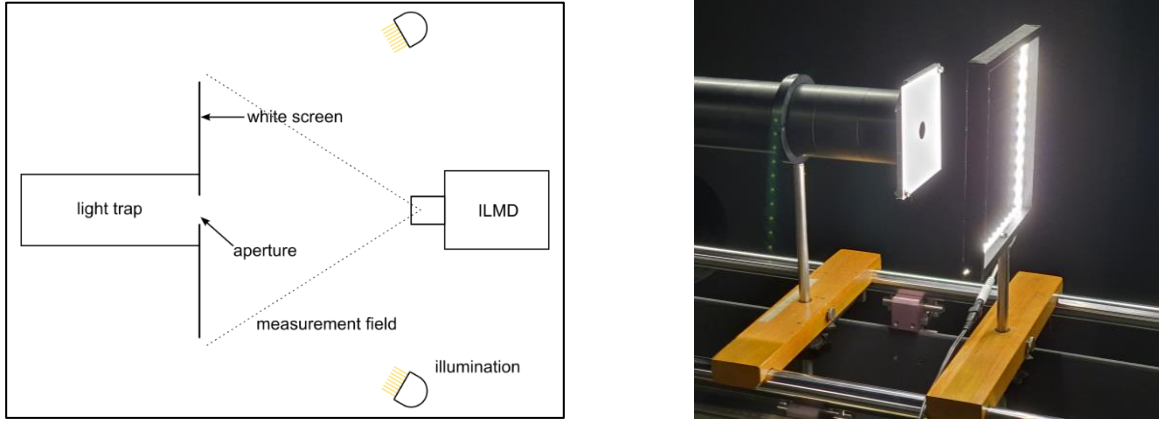


Figure 14: Measurement of negative contrast; left: sketch of setup, right: example setup

For ILMDs without internal straylight correction, an approach to estimate the straylight from surrounding bright regions into dark evaluation regions is to determine the negative contrast by measuring the average luminance in a light trap (Y_{trap}) and the surrounding relatively homogeneous large bright white area (Y_{bright}), similar to quality index f_{24} of [1]. Figure 14 shows a sketch and a realisation of the measurement setup and Figure 15 depicts the evaluation regions.

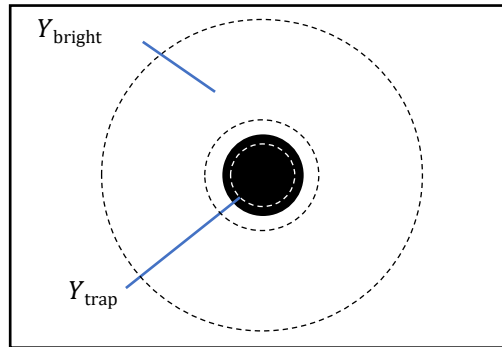


Figure 15: Measurement of negative contrast, defining evaluation regions

The luminance ratio $\frac{Y_{\text{trap}}}{Y_{\text{bright}}}$ describes the negative contrast for this extreme case where large portions of the imaged scene are bright illuminated and generate straylight into the small dark region. If the quality index f_{24} is available for the device, it can be directly used as this luminance ratio.

This device property can be used to scale a surrounding luminance of another scene for estimating its resulting absolute straylight contribution:

$$L_{\text{abs,stray}} = \frac{Y_{\text{trap}}}{Y_{\text{bright}}} Y_{\text{surround}} \quad (11)$$

Strictly speaking, Y_{surround} would be the average luminance outside of the dark evaluation region but it can be approximated by the average luminance of the whole image. $L_{\text{abs,stray}}$ is the estimated straylight “floor” for the whole image.

This gives the resulting absolute uncertainty as:

$$u_{\text{abs,stray}} = \frac{2 L_{\text{abs,stray}}}{\sqrt{12}} = \frac{L_{\text{abs,stray}}}{\sqrt{3}} \quad (12)$$

8 Focus-Setting

8.1 Technical Background

As shown in Figure 4, the optical transmissivity of the lens may change with the focus setting. The overall change of this transmissivity can be from some ten percent down to a few percent. The lens focus is usually adopted so that the detail to be measured is in focus and therefore arbitrary, except for special cases. Depending on the lens properties the focus setting of the lens can be read out electronically or has to be entered by the user into the ILM software. For manual input the focus setting has to be read by the user from a scale at the lens.

Here we assume that the focus scale divides the total angular range of the focus ring evenly into small steps and allows a numerical reading. Scales that display the focus distance are strongly non-linear and usually made for informational purposes, not for precise reading of the setting. Because the focus rings of the lenses usually do not provide vernier scales, the error of this focus reading E_f will be above ± 0.2 step. The ILM software may only allow the input or selection of integer focus values which increases the possible error of the focus value parameter inside the ILM software to ± 0.5 steps with a uniform distribution.

This uncertainty of the focus value parameter available to the ILM translates into an uncertainty of the internal focus correction and therefore of the measured luminances.

8.2 Proposed estimate of uncertainty contribution:

In case the manufacturer provides values for the relative transmissivity or their inverse as a corresponding correction factor, then they can be used to determine the delta of the focus correction per focus step. If this data is not provided, it can be estimated by measure a constant source and vary the focus setting in the ILM software. What usually would be an error when operating the ILM is done intentionally to reveal the range of the internal focus correction. The change in the measured values is directly proportional to the change of the internal focus correction factor.

To do this estimation the following steps are necessary:

- Place the ILM in front of an extended light source that is constant during the measurement. Homogeneity and focusing are not relevant here.
- Define an evaluation region, sufficiently large to reduce influence of photon noise.
- Measure the average luminance Y in that region for at least minimum and maximum focus setting (f_{\min}, f_{\max}). Some additional measurements at intermediate focus settings might be helpful to verify the absence of a strongly non-linear dependence.
- Normalize the difference of the measured luminance values to their average. This gives the relative change of

$$\Delta_{\text{rel},Y} = \frac{Y(f_{\max}) - Y(f_{\min})}{\bar{Y}} \quad (13)$$

The resulting uncertainty of the focus correction and therefore of the measured luminance is then given by

$$u_{\text{rel},\text{foc}} = \frac{E_f}{\sqrt{3}} \frac{\Delta_{\text{rel},Y}}{f_{\max} - f_{\min}} \quad (14)$$

Figure 16 shows two examples of these measurements for two lenses with different amount of the change of relative transmissivity. To make the characteristics comparable to the device data provided by the manufacturer, the luminance values are normalized to a focus setting at device calibration, not the average value. It is evident, that the estimated characteristics match the calibration data very well.

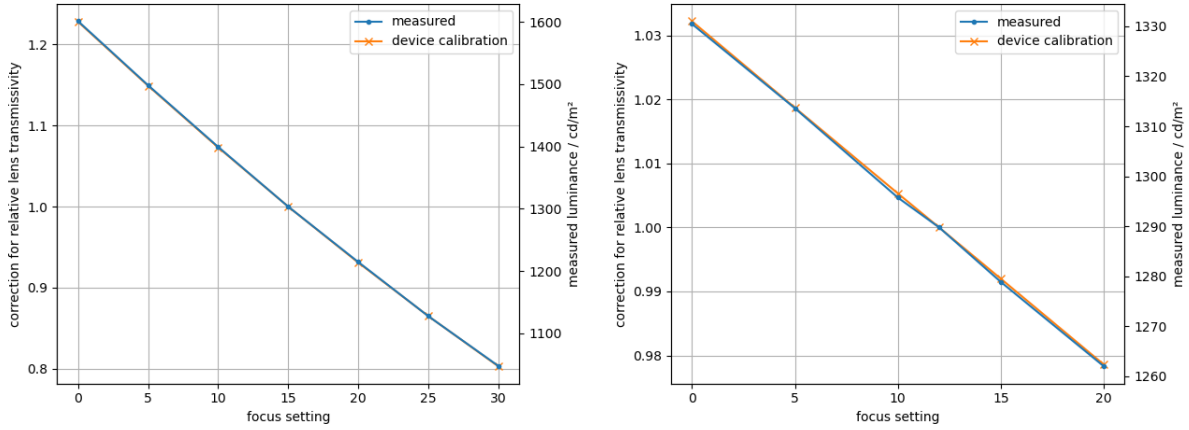


Figure 16: Examples for lens transmissivity for two lenses; estimated by changing the internal focus setting for a constant lens/scene setting compared with manufacturer-provided device data for comparison

For an expected maximum error of the focus reading of $E_f = 0.5$ we get for the left example with a relatively large focus dependency and using measured luminance values or correction data:

$$u_{\text{rel,foc}} = \frac{0.5}{\sqrt{3}} \cdot \frac{1601 - 1047}{1601 + 1047} \cdot \frac{2}{30} = \frac{0.5}{\sqrt{3}} \cdot \frac{1.2285 - 0.8035}{1.2285 + 0.8035} \cdot \frac{2}{30} = 0.0040 \quad (15)$$

For the right example we get:

$$u_{\text{rel,foc}} = \frac{0.5}{\sqrt{3}} \cdot \frac{1331 - 1262}{1331 + 1262} \cdot \frac{2}{20} = \frac{0.5}{\sqrt{3}} \cdot \frac{1.0320 - 0.9785}{1.0320 + 0.9785} \cdot \frac{2}{20} = 0.00077 \quad (16)$$

which is neglectable in most cases.

9 Other Uncertainty Contributions

The shown uncertainty contributions in the sections before are a selection of prevalent contributions that can be estimated by the user of an ILMD with reasonable amount of effort. One generally relevant contribution is the spectral mismatch but the determination of the normalized spectral responsivity of an ILMD requires specialized complex setups that are not commonly available/affordable. Therefore, for the spectral responsivity the user usually has to rely on data provided the manufacturer or other laboratories. With this and knowledge about the source spectrum it is possible to determine the spectral mismatch and handle this as an uncertainty, like in this document, or to correct for and then needs to state the residual uncertainty.

Other contributions that might be relevant for a specific device, relate to the mechanical stability of the ILMD or the repeatability of settings like aperture repeatability (f_{28}) or shutter repeatability (f_{27}) for mechanical shutters. These indices describe the relative spread of the reading caused by the respective influence and can be used directly as $u_{*,\text{rel}}$ or easily determined according to [1].

Dark signal might get relevant if very long integration times are used. But modern devices implement a sufficient internal correction or allow to measure correction data that fits the current temperature state of the device to a correction. Therefore, this will only be relevant for special applications. Quantisation errors can be considered as neglectable for modern devices.

If some contributions are suspected as relevant, then the task is to find the interval limits of the output signal Y and relate it to a reference point, e.g. the centre of the interval, like shown for the selected contributions before.

10 Correlations Between Multiple Measurements

In the introduction was stated that no correlations between uncertainty components for a single luminance measurement Y are regarded. This was required because the complexity of their determination is the same as the determination of the correction functions, in addition the underlying mechanisms are quite independent and therefore their residual errors are assumed to be uncorrelated to another. But for multiple luminance measurements with the same device the same errors occur in each of them and statements on full correlations between some uncertainty components of these measurements can be made.

For a single luminance measurement, the measurement value L is given by the model of evaluation

$$L = Y \cdot c_a \cdot c_b \cdot \dots \quad (17)$$

where

Y : devices luminance reading

c_a, c_b, \dots : correction factors for uncertainty components, all $c_i \equiv 1$ (no correction applied) but with assigned uncertainty u_a, u_b, \dots

When derived quantities have to be calculated from multiple luminance measurements, e.g. a luminance ratio or a difference of luminance values, the model of evaluation is given by the equation of this derived quantity, e.g. for the luminance ratio:

$$R_{L_1, L_2} = \frac{L_1}{L_2} = \frac{Y_1 \cdot c_{a,1} \cdot c_{b,1} \cdot \dots}{Y_2 \cdot c_{a,2} \cdot c_{b,2} \cdot \dots} \quad (18)$$

or the luminance difference:

$$D_L = L_1 - L_2 = Y_1 \cdot c_{a,1} \cdot c_{b,1} \cdot \dots - Y_2 \cdot c_{a,2} \cdot c_{b,2} \cdot \dots \quad (19)$$

If the critical measurement conditions at the individual measurements are the same, then the corresponding uncertainty components $u_{*,1|2\dots}$ are fully correlated. For example, the calibration uncertainty u_{cal} is for all measurements with the same device fully correlated. If the measurement regions for successive measurements are identical or at a very similar region of the image and the focus setting is identical, then the uncertainty contribution caused by the shading error is fully correlated. For measurement regions near the image centre this is also valid for different focus settings. Measurement regions in different parts of the image have to be treated as uncorrelated regarding the shading error.

Partial correlations cannot be derived by this analytical method. This would require detailed determination on the systematic residual errors. But from the knowledge which critical measurement conditions are identical between different evaluation regions in one or multiple luminance images taken, a correlation matrix can be created to hold the correlation information in a standardized way.

To give an example, assuming a measurement of the average luminance of two different sources of the same type in one image, one evaluation region in the centre and one near the corner. As significant uncertainty components were calibration uncertainty $u_{\text{rel,cal}} = u_a$, residual shading uncertainty $u_{\text{rel,shading}} = u_b$ and a residual spectral nonlinearity $u_{\text{rel,nl}} = u_c$ identified. Because both measurements are done with the same device, $u_{a,1}$ and $u_{a,2}$ are fully correlated. Both measurements are done at different positions in the image, there is no full correlation for the shading errors and we take these as uncorrelated to another. Both sources are the same type and therefore have the same spectral distribution and a similar luminance. Therefore, the sensor will give similar count signal for both regions. With this follows that $u_{c,1}$ and $u_{c,2}$ are fully correlated. This information can be put into a correlation matrix \mathbf{P} by setting the corresponding non-diagonal elements to 1:

$$\mathbf{P} = \begin{matrix} & \begin{matrix} u_{a,1} & u_{b,1} & u_{c,1} & u_{a,2} & u_{b,2} & u_{c,2} \end{matrix} \\ \begin{matrix} u_{a,1} \\ u_{b,1} \\ u_{c,1} \\ u_{a,2} \\ u_{b,2} \\ u_{c,2} \end{matrix} & \begin{bmatrix} 1 & 0 & 0 & 1 & 0 & 0 \\ 0 & 1 & 0 & 0 & 0 & 0 \\ 0 & 0 & 1 & 0 & 0 & 1 \\ 1 & 0 & 0 & 1 & 0 & 0 \\ 0 & 0 & 0 & 0 & 1 & 0 \\ 0 & 0 & 1 & 0 & 0 & 1 \end{bmatrix} \end{matrix} \quad (20)$$

(coloured elements are row/column-captions, not matrix content)

With the diagonal matrix of the input uncertainties

$$\mathbf{D} = \text{diag}(u_{a,1}, u_{b,1}, u_{c,1}, u_{a,2}, u_{b,2}, u_{c,2}) = \begin{bmatrix} u_{a,1} & 0 & 0 & 0 & 0 & 0 \\ 0 & u_{b,1} & 0 & 0 & 0 & 0 \\ 0 & 0 & u_{c,1} & 0 & 0 & 0 \\ 0 & 0 & 0 & u_{a,2} & 0 & 0 \\ 0 & 0 & 0 & 0 & u_{b,2} & 0 \\ 0 & 0 & 0 & 0 & 0 & u_{c,2} \end{bmatrix} \quad (21)$$

the covariance matrix Σ is then given by

$$\Sigma = \mathbf{D P D}$$

This matrix then can be used for uncertainty propagation according to GUM [5]–[7].

11 Relevance of Different Uncertainty Contributions for Exemplary Measurement Applications

From the technical background of the discussed uncertainty sources some criteria can be derived, which one are possibly relevant for a specific measurement application. These criteria focus on single luminance measurement values. Some uncertainty contributions for single measurement may cancel out at the calculated final quantity because of correlations but this is not addressed here.

Absolute Calibration: This has the same importance for all applications.

Focus Setting: This has the same importance for all applications.

Shading: Are evaluation regions located in outer image regions or near centre? For outer regions the shading gets relevant.

Non-Linearity: Are absolute values measured or are evaluation regions with different luminance in same image used? Then non-linearity is relevant.

Spectral Non-Linearity: Sources to be measured have different spectral distributions vs. illuminant A (or similar). Esp. for narrow banded coloured sources spectral-non-linearity can be relevant.

Edge Distance: Allows the size of the source in the image to define an evaluation region that is kept away of strong gradients (edges) or is large enough that the edge region is small compared to the entire area. Of not, this is relevant. This is not an uncertainty component but an evaluation condition that has to be met.

Size-of-Source: What is the ratio of the measurement region to the surrounding source between different evaluation regions? What is the ratio of the measurement region to the surrounding source compared to the calibration condition? If absolute values are measured, this is relevant. If the ratio is changing, this effect might be not relevant for derived quantities because of correlations.

Negative Contrast: If measurements in dark regions are done while bright sources are present in image, then this is relevant.

The following section will give some examples for the application of these criteria to real measurement tasks, by applying them to the applications collected in section 14 (“Appendix II: List of Measurement Applications”).

Laboratory – Uniformity of Sources:

Analysis of uniformity of laboratory luminous sources for calibration at different luminance levels.

- High contrast at source border → edge distance relevant
- Source fills measurement field (vertical) → shading relevant
- Varying size of evaluation regions → size-of-source relevant

- All measurements at similar luminance → for the calculated luminance ratio non-linearity not relevant because of full correlation
- No measurements in dark regions → negative contrast not relevant

Advertising – Luminous Signal:

Measurement of luminance and analysis of uniformity on dynamic luminous signals used in advertising:

- The whole measurement field is used → shading is relevant
- Absolute values are measured → non-linearity relevant
- No strong gradients → edge distance not relevant
- No measurements in dark regions → negative contrast not relevant
- Temporal Light Modulation (TLM) may be relevant (not covered in this document)!

BlackMURA:

Evaluation of the uniformity of displays especially for the dark state. Relative measurements of lowest/highest luminance in image of display:

- The whole image is evaluated → shading across the measurement field is relevant
- Different luminance levels in one image, depend on the inhomogeneity of the DUT → non-linearity is probably relevant
- No small sources or strong gradients → edge distance is not critical
- Broad spectra → spectral non-linearity not relevant

TI (Threshold Increment):

- Measurements of multiple sources (evaluation regions) distributed across the measurement field → shading is relevant
- Measurement of bright and dark sources → non-linearity and straylight (negative contrast) are relevant

L20-Measure:

Measuring luminance values of road surface on tunnel entrance under fixed viewing position for specific viewing direction.

- Measure mostly in the centre → shading not relevant
- Bright and dark regions → non-linearity and negative contrast relevant

UGR-Measurement:

Measurement of background luminance and luminance produced by each luminaire.

- Full measurement field used → shading relevant
- Dark and bright regions measured → non-linearity and negative contrast relevant
- If no coloured sources measured → spectral non-linearity not relevant
- Small sources → edge distance relevant, size-of-source relevant

Luminance Measurements in Tunnels:

Measuring luminance of road surface.

- Large measurement field used → shading relevant

- Absolute values required → non-linearity relevant
- Measurement in areas with low gradient → edge distance not relevant

Street Lighting EN13201 Measuring grid:

Measuring luminance of road surface under fixed viewing conditions for specific point grid raster.

- Measurement of street surface, bright luminaires in image → negative contrast relevant
- Evaluation region only near image centre → shading not relevant
- Absolute values required → non-linearity relevant
- No coloured sources → spectral non-linearity not relevant

Photobiological safety:

Dimensional measurement of the luminous area with emission above 50% of maximum.

- Neutral-density filter might change shading → shading relevant
- White or colour LED → spectral non-linearity relevant
- No measurement in dark regions → negative contrast not relevant

12 References

- [1] CIE, 'CIE 244:2021 Characterization of Imaging Luminance Measurement Devices (ILMDs)'. Jan. 01, 2021. doi: 10.25039/TR.244.2021.
- [2] K. Klauenberg, G. Wübbeler, and C. Elster, 'About not Correcting for Systematic Effects', *Measurement Science Review*, vol. 19, no. 5, pp. 204–208, 2019, doi: doi:10.2478/msr-2019-0026.
- [3] BIPM *et al.*, 'International vocabulary of metrology — Basic and general concepts and associated terms (VIM)'. [Online]. Available: https://www.bipm.org/documents/20126/2071204/JCGM_200_2012.pdf/f0e1ad45-d337-bbeb-53a6-15fe649d0ff1
- [4] Schrader, Christian and Ledig, Johannes, 'Spectral Dependent Non-Linearity of Charge Accumulating Pixel Matrix Sensors', in *Proceedings of CIE Quadrennial Session 2023 (accepted for publication)*, Ljubljana, Slovenia, Sep. 2023.
- [5] BIPM *et al.*, 'Evaluation of measurement data — An introduction to the “Guide to the expression of uncertainty in measurement” and related documents'. [Online]. Available: https://www.bipm.org/documents/20126/2071204/JCGM_104_2009.pdf/19e0a96c-6cf3-a056-4634-4465c576e513
- [6] BIPM *et al.*, 'Evaluation of measurement data — Guide to the expression of uncertainty in measurement'. [Online]. Available: https://www.bipm.org/documents/20126/2071204/JCGM_100_2008_E.pdf/cb0ef43f-baa5-11cf-3f85-4dcd86f77bd6
- [7] BIPM *et al.*, 'Evaluation of measurement data — Supplement 1 to the “Guide to the expression of uncertainty in measurement” — Propagation of distributions using a Monte Carlo method'. [Online]. Available: https://www.bipm.org/documents/20126/2071204/JCGM_101_2008_E.pdf/325dcaad-c15a-407c-1105-8b7f322d651c

13 Appendix I: Checklist for the ILMD configuration

To avoid significant errors which cannot be covered by uncertainties it is necessary to use a configuration that is suitable for the application. Namely the following aspects should be ensured:

Good state of device components

- correct assembly and professional handling, i.e. clean and not damaged
- documentation of usage and relevant aspects of storage/transport
- consider using clean room gloves when handling optical surfaces and blow dust away by N₂ or oil free air

Selection of an adequate objective lens

- focal length → resulting in a measurement field that is fitting to the application, i.e. a focal length as large as possible.

Selection of an adequate neutral-density filter

- to avoid extremely short integration times where the timing uncertainty gets relevant
- to avoid/reduce effects of Temporal Light Modulation (TLM)

Setting of utilized optical components into the control software

- i.e. type and serial number of the objective lens, neutral density filter. This is relevant also for relative measurements inside the image, it might reset to default after start-up.

Adjustment data loaded into the control software

- configuration file, calibration file for internal corrections, user defined corrections belonging to the actual condition (consider aging and replacement/maintenance of components since the characterization)

Stabilized internal temperature for all components

- i.e. ILMD in operation (powered up and initialized, i.e. imaging loop) for more than one hour

Dark signal correction inside the control software

- belonging to the operation mode (i.e. binning, smoothing, integration time) and aging state (pixel characteristic might change)

Parameter values inside the control software correspond to hardware setting

- **Zoom** value of the objective lens
- **Aperture** value of the objective lens
- **Focus** value of the objective lens
(measurement plane in focus, focus setting or focus distance provided to the control software)
- **Integration time**
 - sufficiently long to reach a signal level well above the detection limit but within the dynamic range and to avoid sensor-internal **timing issues in the μ s-domain**
 - integration time should be an integer multiple of the temporal light modulation period
 - avoid blooming as this in general also affects the result from all other pixel) by using an appropriate neutral-density filter (and setting this inside the control software, c.f. neutral density filter).

- **Region of interest**
 - is each evaluation region many pixels in size and homogeneous?
 - Consider smoothing parameters (i.e. averaging or median filtering)

Verification tests to indicate absence of issues:

- Check **zero reading** (dark signal measurement, verify the internal offset correction)
- Check **measurement of luminance standard**
using different signal levels to verify also non-linearity and absence of significant offset issues
(or use a referenced luminance, i.e. by means of an illuminance meter or a luminance spot photometer for a traceability determination of an arbitrary but constant luminance source)
- Check it again >10min later (**stability** of standard and measurement device)
- **Reproducibility** (remount objective lens, reset focus, zoom and aperture, rotate filter wheel)

14 Appendix II: List of Measurement Applications

Table of Contents

- 1 Laboratory - Uniformity of Sources 26
- 2 Advertising – Luminous Signal..... 28
- 3 BlackMURA..... 30
- 4 TI (Threshold Increment)..... 33
- 5 L20 - Measure: Example 1 35
- 6 L20 – Measure: Example 2 38
- 7 UGR Measurement..... 39
- 8 Luminance Measurements in Tunnels 40
- 9 Street Lighting EN13201 Measuring grid..... 42
- 10 Photobiological safety 44
- 11 BLH – Blue light hazard..... 46

1 Laboratory - Uniformity of Sources

	Analysis of uniformity of laboratory luminous sources for calibration at different luminance levels
--	---

ILMD Type	I
Measurand	cd/m ²
FOV / (mm/°)	0.1° to 5° aprox.
Lens type	
Resolution	
L_{min}, L_{max}	10, 10000
Contrast local/ contrast global	local

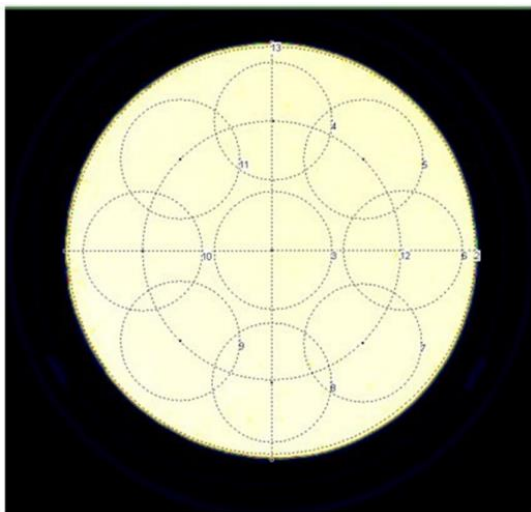
Type of Light Source	Any
Measurement conditions	Typical laboratory conditions
Required Uncertainty / Traceability	Relative measurements
Parameters during the measurement	Constant
	Varying FOV, configuration of exposure time and aperture
Quality indices	

Sample image with evaluation regions:

Examples of evaluation in a reference source used for calibration. In this case: there is a diffuser placed in the outlet port of an integrating sphere. Other types of extended sources could be evaluated following this example.

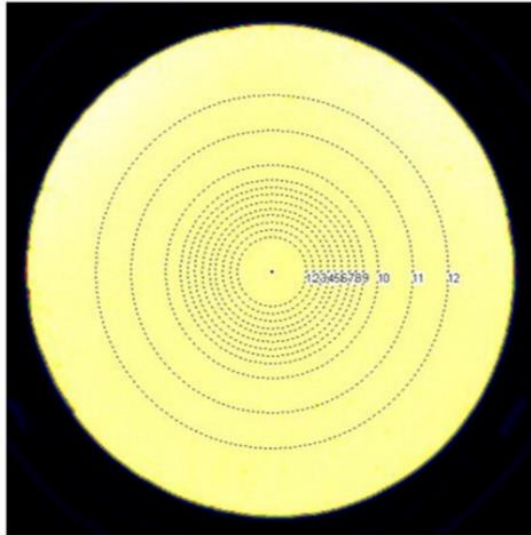
The source was dimmed and evaluated at different *L* values, but only two examples of the tests done are shown.

Measurement



Sample results

Circle N#	<i>L</i> _{average} (cd/m ²)		
3	630.9		
4	635	<i>L</i> _{max} (cd/m ²)	635.0
5	632.7	<i>L</i> _{min} (cd/m ²)	630.9
6	631.5		
7	632.2	Uniformity within:	
8	634.2	0.6499%	
9	634.8	(<i>L</i> _{max} - <i>L</i> _{min})/ <i>L</i> _{min}	
10	633.7		
11	634.8		



Circle N#	Diameter (mm)	$L_{average}$ (cd/m ²)	L_{max} (cd/m ²)	L_{min} (cd/m ²)
1	5	29.79		
2	6	29.79	29.91	
3	7	29.82		29.79
4	8	29.82		
5	9	29.82		
6	10	29.82		
7	11	29.82		
8	12	29.82		
9	13	29.84		
10	15	29.84		
11	20	29.89		
12	25	29.91		

Uniformity within:
0.4028%
 $(L_{max}-L_{min})/L_{min}$

Sample results: analysis of maximum, minimum, average, uniformity and standard deviation of Luminance.

2 Advertising – Luminous Signal

Spanish regulation (ROYAL DECREE 1890/2008, of November 14) for the energy efficiency in outdoor lighting installations	Measurement of luminance and analysis of uniformity on dynamic luminous signals used in advertising
---	---

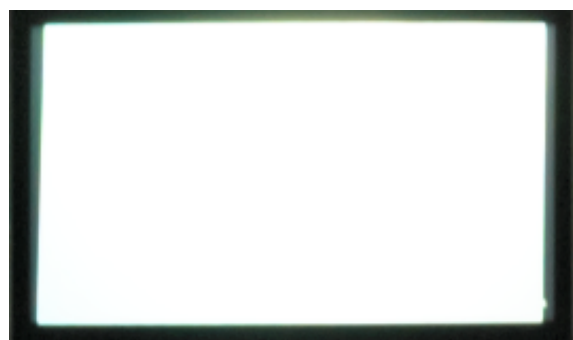
ILMD Type	I
Measurand	cd/m ²
FOV / (mm/°)	1° to 10° aprox.
Lens type	
Resolution	
<i>L</i>_{min}, <i>L</i>_{max}	50, 10000
Contrast local/ contrast global	

Type of Light Source	Projection systems using different types of sources, as special halogen lamps, HID, or others. Other advertising panels based on LED technology can be analyzed
Measurement conditions	On-site measurements: outdoor Laboratory measurements: typical lab conditions
Required Uncertainty / Traceability	Absolute measurements
Parameters during the measurement	Constant Varying FOV, configuration of exposure time and aperture, temperature (specially for in situ outdoors measurements)
Quality indices	<i>L</i> _{max} , <i>L</i> _{average}

Sample image with evaluation regions:

Any advertisement with luminous parts, static or dynamic. In the case of screens with variable pictures, the worst case scenario is a white homogeneous screen.

Blank screen projected on storefront (left: from indoors; right: as seen out-doors) where different advertisements or messages are played.



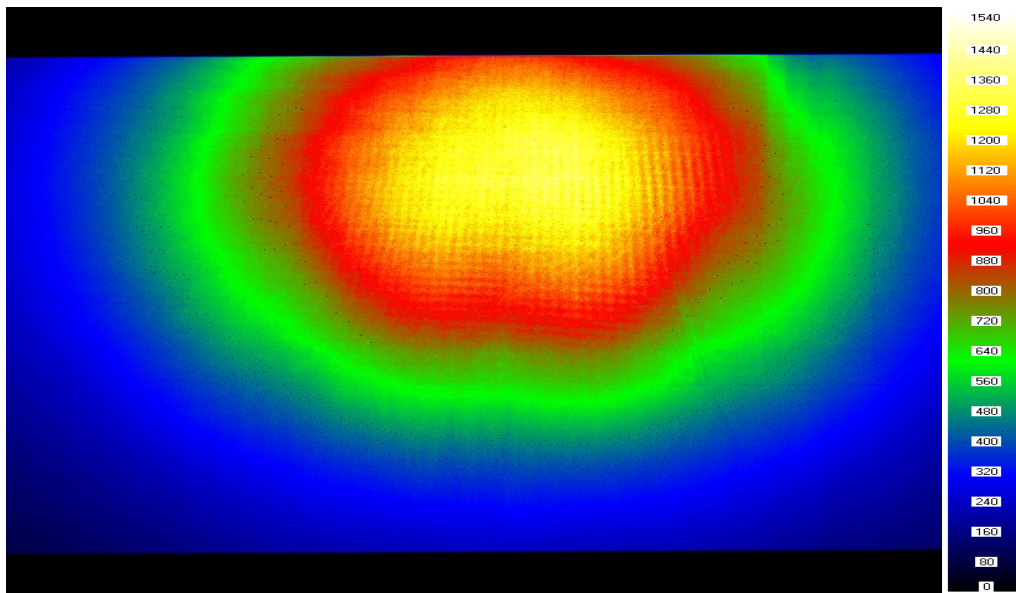
Uniformity of Luminance is an important quality parameter. Nevertheless, the maximum luminance provided by the luminous signal is the regulated parameter. The limit value depends on the dimensions of the screen and the

zone where the signal is located (zones 1 to 4, being 1: natural spaces, flora or fauna protection zones, and 4: urban centre, commercial area).

The maximum luminance value is regulated or subject to control of switching on, dimming and switching off in different time periods.

Measurement

On axis capture of the area of interest in the different working conditions (regulations of the product). Calculation of the maximum luminance and the average luminance.



Sample results:

Sample results (worst case: 100 % regulation level):

$L_{\text{average}} = (412.5 \pm 2.5) \text{ cd/m}^2$
$L_{\text{maximum}} = (1538 \pm 10) \text{ cd/m}^2$

3 BlackMURA

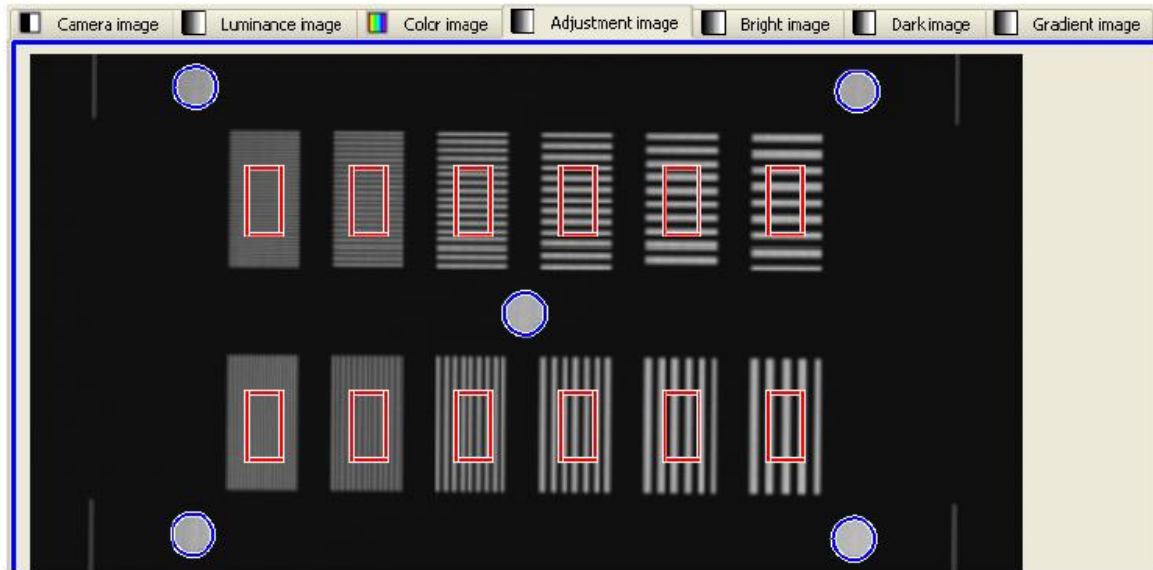
<i>Uniformity Measurement Standard for Displays V 1.2.</i> Pforzeim: DFF e.V. (DEUTSCHES FLACHDISPLAY-FORUM e.V.)	Evaluation of the uniformity of displays especially for the dark state according to (DFF, 2017)
---	---

ILMD Type	I
Measurand	BU: L_{min}/L_{max} Gradient in %/mm; or % / pix (Dark Image) Evaluation for Bright and Dark image separately
FOV / (mm/°)	Completely depending on display size (Display captured in one shot)
Lens type	E
Resolution	Camera Pixels / Display Pixels >1
L_{min}, L_{max}	$L_{min} > 0.1 \text{ cd/m}^2$ (Dark Image) $L_{max} > 1000 \text{ cd/m}^2$ (Bright Image))
Contrast local/ contrast global	Local contrast: a few % / mm; Global contrast < 5:1

Type of Light Source	Information Display (usually broad spectra, LCD or OLED), Modulation and Polarization possible; Curved Information Display Warm-up period which bases on luminance stability important as well Sometimes mounting position dependency
Measurement conditions	Precise Geometrical Alignment (perpendicular Alignment of ILMD relative to Display surface and centered) Distance and Lens selection with respect to DUT Field angle influence (try and error test procedure required) → minimal Distance (Lens) Defocus (to Avoid Aliasing) Mean of 10 images
Required Uncertainty / Traceability	All values are relative measurements Practical required uncertainty depends on region of BU For low and high BU; higher uncertainty is sufficient For mid BU (40% till 60%) lower uncertainty is usually required
Parameters during the measurement	Constant: Geometrical Alignment 25 °C ambient temperature Dark Room Varying: Distance (boundary), lens type, Focus setting, Reproduction Scale, Integration time
Quality indices	F1', F21, F31, F32, F8, F12

Sample image with evaluation regions:

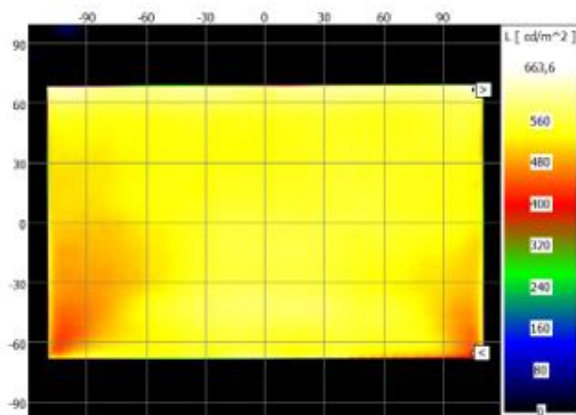
Setup:



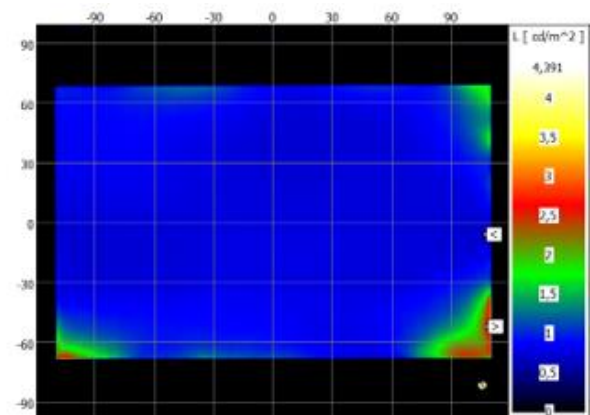
Camera and display related setup (angular adjustment, measurement of reproduction scale, modulation measurement)

Measurement:

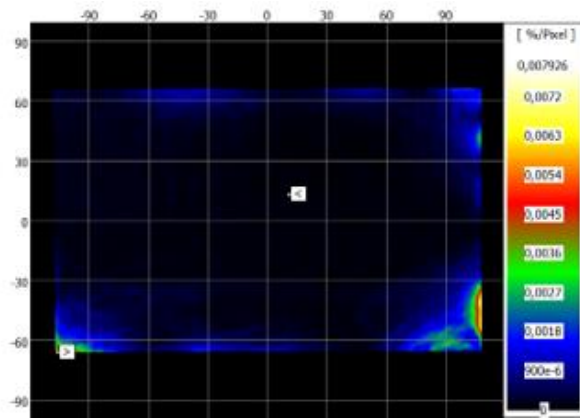
Bright State



Dark state



Gradient calculated from dark state



Sample results:

Parameter	Image	Value	Unit
Mean	Dark image	0.87	cd/m ²
Minimum	Dark image	0.71	cd/m ²
Maximum	Dark image	2.59	cd/m ²
Uniformity	Dark image	27.4	%
Maximum W	Gradient image	0.008	%/px
Maximum B	Gradient image	4.951	%/px
Mean	Bright image	543	cd/m ²
Minimum	Bright image	432	cd/m ²
Maximum	Bright image	637	cd/m ²
Uniformity	Bright image	68	%

References

DFF. (2017). *Uniformity Measurement Standard for Displays V 1.2*. Pforzeim: DFF e.V. (DEUTSCHES FLACHDISPLAY-FORUM e.V.).

4 TI (Threshold Increment)

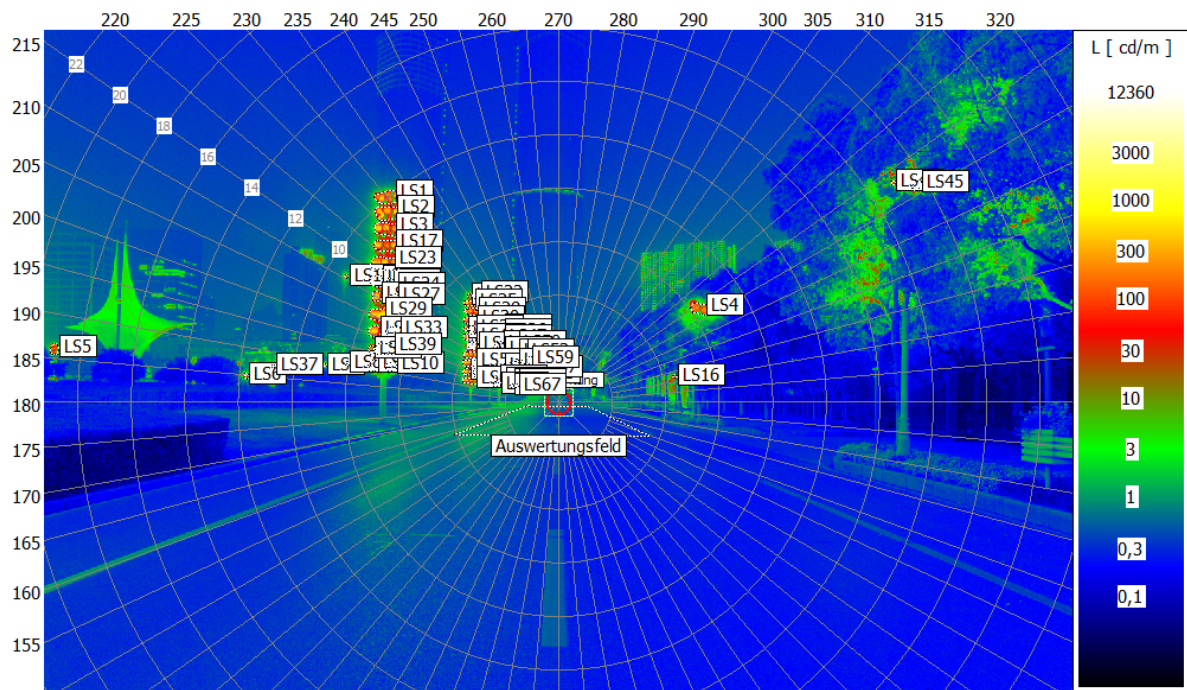
EN13201 – 3: 2016 - Road lighting - Part 3: Calculation of performance	Measuring luminance (cd/m^2) of lighting fixtures and road surface under fixed viewing position for specific viewing direction
--	--

ILMD Type	I / II
Measurand	%
FOV / (mm/°)	$\leq 20^\circ$
Lens type	E (wide angle)
Resolution	
L_{\min}, L_{\max}	0.01, 100
Contrast local/ contrast global	Local

Type of Light Source	Road reflectance and street lighting fixture
Measurement conditions	outdoor
Required Uncertainty / Traceability	
Parameters during the measurement	Constant Varying x
Quality indices	

Sample image with evaluation regions:

Measurement:



5 L20 - Measure: Example 1

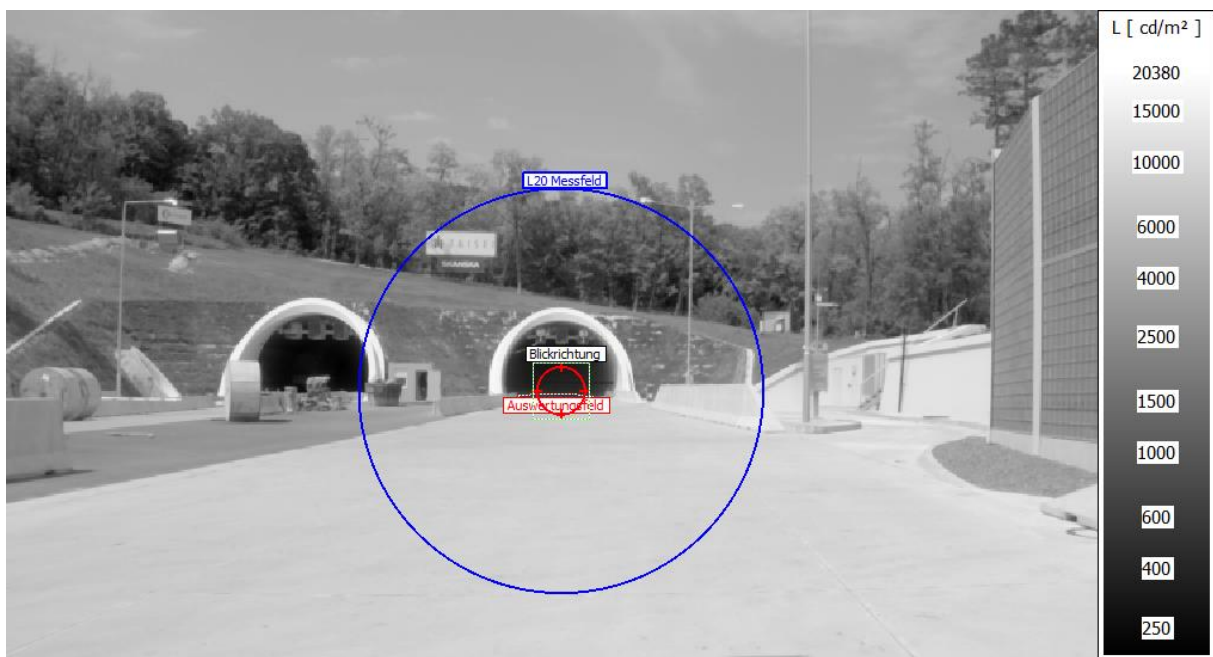
CIE Publ. 88 Guide for the lighting of road tunnels and underpasses	Measuring average luminance (cd/m^2) from the surrounding of tunnel entrance lighting fixtures and road surface under fixed viewing position for specific viewing direction
---	---

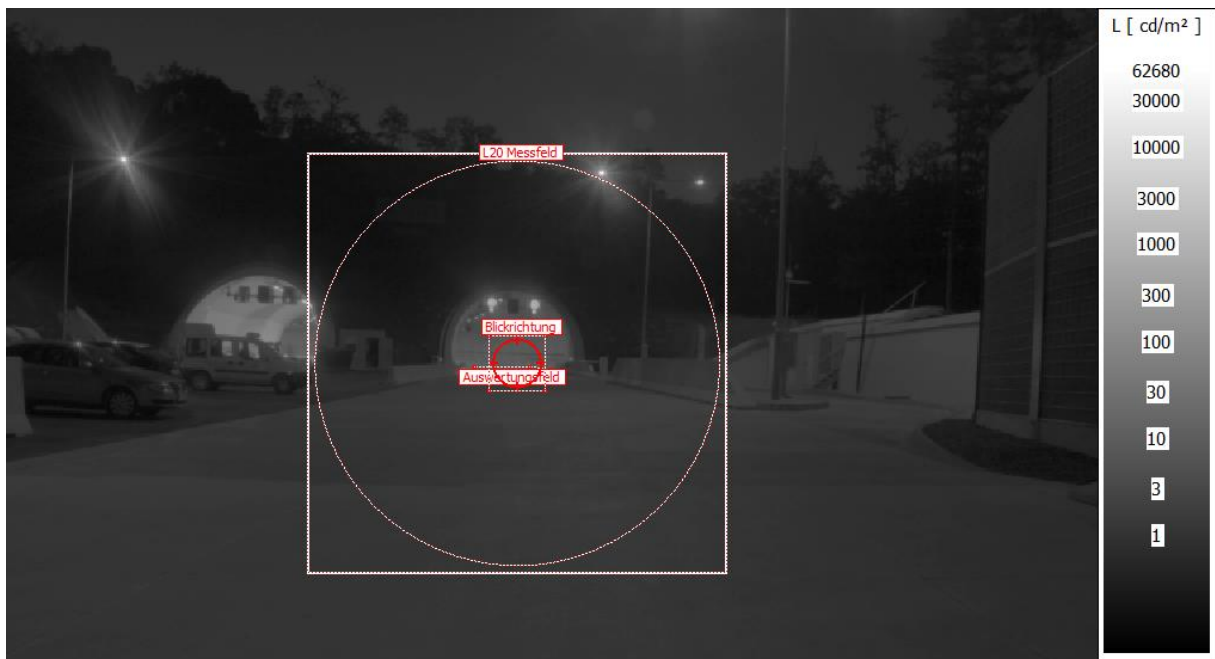
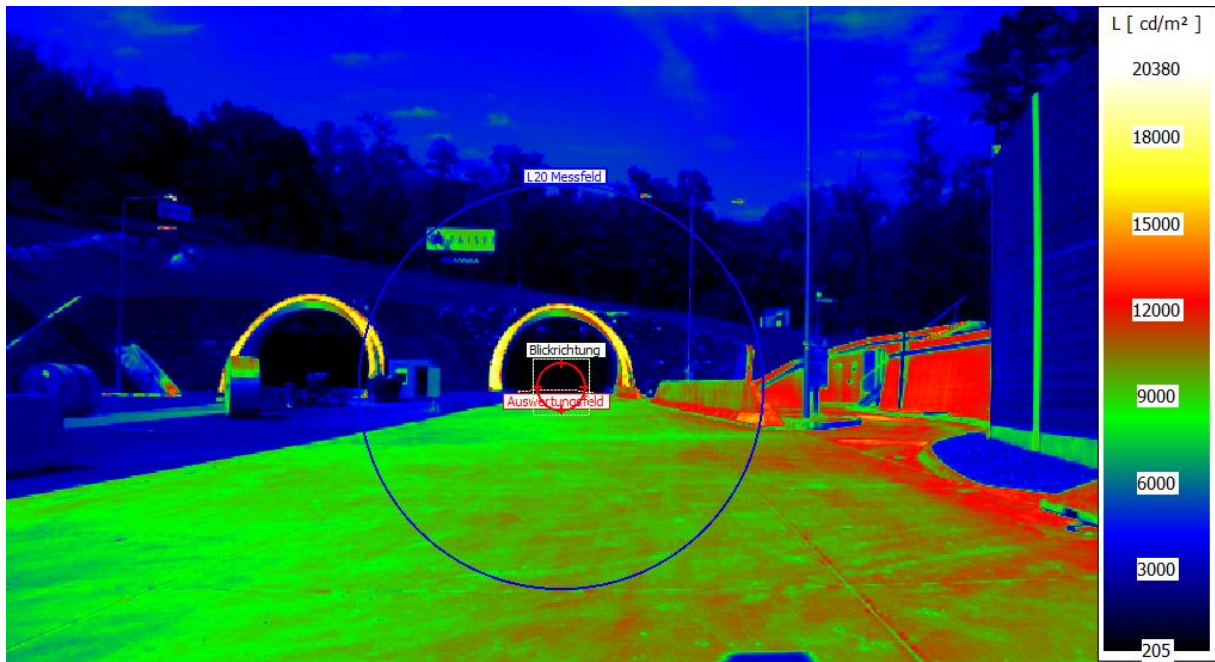
ILMD Type	I / II
Measurand	cd/m^2
FOV / (mm/°)	$\leq 20^\circ$
Lens type	E (wide-angle)
Resolution	
L_{\min}, L_{\max}	0.01, 100 000
Contrast local/ contrast global	global

Type of Light Source	Road reflectance and street lighting fixture
Measurement conditions	outdoor
Required Uncertainty / Traceability	
Parameters during the measurement	Constant
	Varying x
Quality indices	

Sample image with evaluation regions:

Measurement







Sample results:

L20 Messfeld	Geschwindigkeit (km/h)	Schwellwertfaktor k	$L(th) = k * L20$	L(mittel) Auswertungs-feld
5690	≤ 60 km/h	0,05	285	657,4
	60-80 km/h	0,06	342	657,4
	80-120 km/h	0,1	569	657,4

6 L20 – Measure: Example 2

CIE Publ. 88 Guide for the lighting of road tunnels and underpasses	Measuring luminance values of road surface on tunnel entrance under fixed viewing position for specific viewing direction, for FOV $\leq 20^\circ$
UNE EN-13201-4: 2016, Road lighting. Part 4: Methods for measuring photometric performance	
Spanish regulation (ROYAL DECREE 1890/2008, of November 14) for the energy efficiency in outdoor lighting installations and its complementary technical instructions EA-01 to EA-07	

ILMD Type	I
Measurand	cd/m ²
FOV / (mm/°)	$\leq 20^\circ$
Lens type	
Resolution	
L_{min}, L_{max}	0.01, 100 000
Contrast local/ contrast global	Global

Type of Light Source	Road reflectance and tunnel lighting fixtures
Measurement conditions	Outdoor
Required Uncertainty / Traceability	Absolute measurement
Parameters during the measurement	Constant FOV (20°) Varying configuration of exposure time and aperture; temperature (outdoors measurement)
Quality indices	

Sample image with evaluation regions

L₂₀ is the average value of luminance within 20° (FOV) at the entrance of a tunnel from the stopping distance, which depends on the maximum allowed speed and other road parameters. The measurement is used to define the lighting needs of the tunnel. This value should be obtained at least in the worst-case (considering the orientation of the tunnel as well as day / time with maximum levels of natural light), it can also be evaluated in different conditions to obtain different configurations for the artificial lighting regulation.



Sample results:

L20 3090 cd/m²



L20 2843 cd/m²

7 UGR Measurement

UNE-EN 12464-1:2012 Light and lighting - Lighting of work places - Part 1: Indoor work places	Measurement of background luminance and luminance produced by each luminaire, from each point and direction of interest
Technical Building Code, section HE3 "Energy Efficiency of Lighting Installations"	

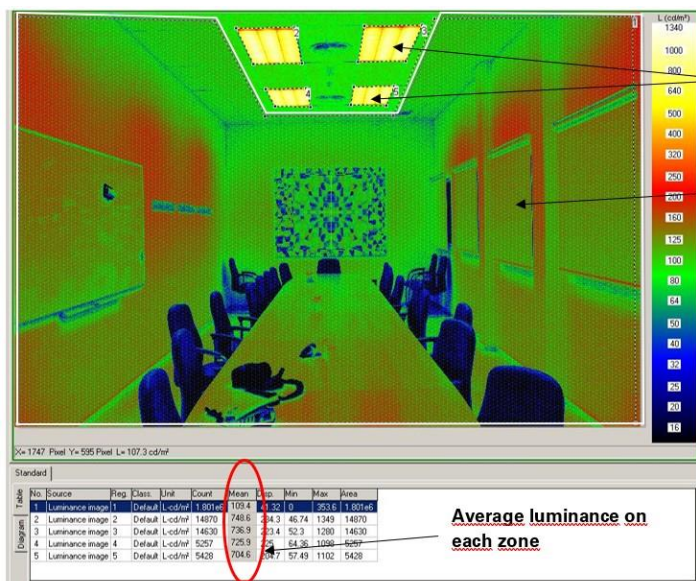
ILMD Type	I
Measurand	UGR value, based on measurement of $L(\text{cd}/\text{m}^2)$, position of sources and other geometrical data
FOV / (mm/°)	variable
Lens type	
Resolution	
L_{\min}, L_{\max}	0.01, 100000
Contrast local/ contrast global	Local / Global

Type of Light Source	Any (currently: typically LED luminaire, white, 3000 K to 5400 K)
Measurement conditions	indoor
Required Uncertainty / Traceability	Absolute measurements
Parameters during the measurement	Constant Varying FOV, measurement position and direction, configuration of exposure time and aperture, Temperature (in-situ measurements)
Quality indices	

Sample image with evaluation regions:

On each room (or space) to be evaluated, the points and directions of interest should be defined. Each value of UGR corresponds to one position and sight direction and evaluates the luminance measured from each luminaire as well as the background luminance.

Measurement



Sample results

Ref. point	UGR
N. 1	16
N. 2	14
N.3	11
N. 4	14
N. 5	11

8 Luminance Measurements in Tunnels

CIE Publ. 88 Guide for the lighting of road tunnels and underpasses	Measuring luminance (cd/m^2) of road surface on tunnel entrance and transit zones under fixed viewing position for specific viewing direction
UNE EN-13201-4: 2016, Road lighting. Part 4: Methods for measuring photometric performance	
Spanish regulation (ROYAL DECREE 1890/2008, of November 14) for the energy efficiency in outdoor lighting installations and its complementary technical instructions EA-01 to EA-07	

ILMD Type	I
Measurand	cd/m^2
FOV / (mm/°)	6' (vertical) \times 20' (horizontal)
Lens type	E (wide-angle)
Resolution	
L_{\min}, L_{\max}	0.01, 10 000
Contrast local/ contrast global	Local / Global

Type of Light Source	Tunnel lighting fixtures and emergency lighting
Measurement conditions	outdoor
Required Uncertainty / Traceability	Absolute measurements
Parameters during the measurement	Constant: Measurement position and FOV (in each zone to be evaluated)
	Varying: Direction of measurement for the different points. Configuration of exposure time and aperture. Temperature (out doors measurements)
Quality indices	

Sample images in different parts along the tunnel, with different lighting configurations (entrance, transit, emergency):

Measurement and results

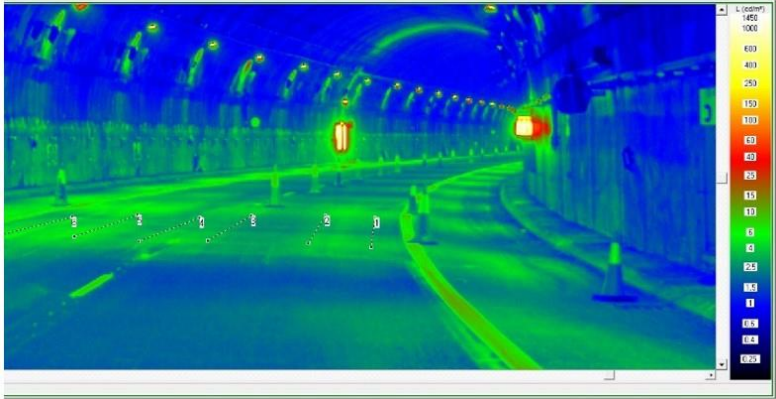
Measurements of luminance along three lines on each lane. Average values and uniformity are calculated.

Entrance of the tunnel:



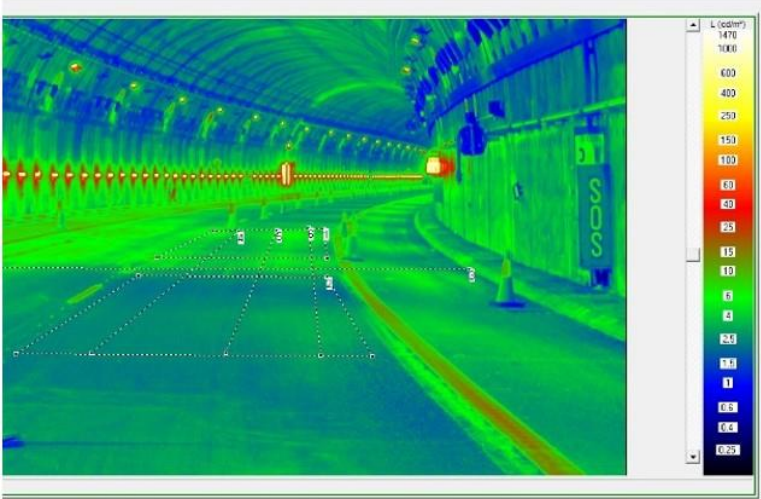
Zone#	$L_{\text{average}} (\text{cd}/\text{m}^2)$
4	196.0
5	181.6
6	173.6

Inside part of the tunnel:



Zone#	<i>L</i> _{average} (cd/m ²)
1	3.460
2	3.708
3	3.456

Inside part of the tunnel with emergency lighting:



Zone#	<i>L</i> _{average} (cd/m ²)
4	2.990
5	3.409
6	3.522

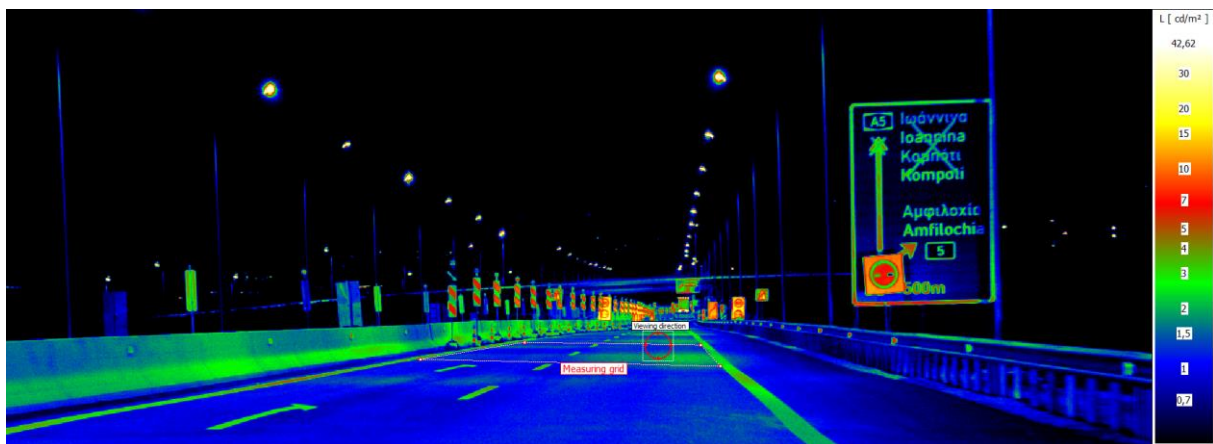
9 Street Lighting EN13201 Measuring grid

EN 13201-3:2015 Road lighting - Part 3: Calculation of performance	Measuring luminance (cd/m^2) of road surface under fixed viewing conditions for specific point grid raster
---	--

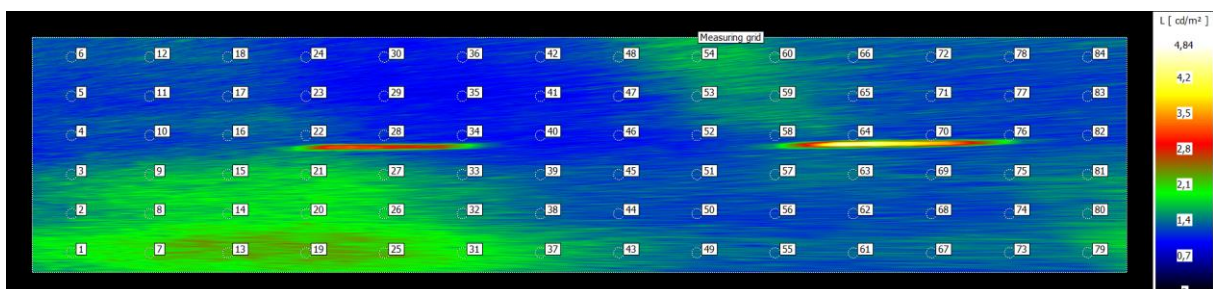
ILMD Type	I / II
Measurand	cd/m^2
FOV / ($\text{mm}/^\circ$)	$\leq 20^\circ$
Lens type	E (telecentric)
Resolution	
L_{\min}, L_{\max}	0.01, 100
Contrast local/ contrast global	Global

Type of Light Source	Road reflectance of street lighting fixture
Measurement conditions	outdoor
Required Uncertainty / Traceability	
Parameters during the measurement	Constant
	Varying: x
Quality indices	

Sample image with evaluation regions:



Sample results:



Number of grid lines	1	2	3	4	5	6	7	8	9	10	11	12	13	14	L_Max	L_Min	L_Avg	Lengthwise Uniformity	Overall Uniformity
6	1.32	1.37	1.34	1.16	1.07	1.08	1.17	1.37	1.63	1.52	1.36	1.31	1.29	1.28	1.63	1.07	1.4	0.658	0.696
5	1.24	1.24	1.25	1.11	1	0.971	1.03	1.12	1.43	1.47	1.32	1.26	1.2	1.22	1.47	0.971		0.659	
4	1.28	1.22	1.33	1.29	1.13	1.04	1.06	1.09	1.2	1.32	1.3	1.21	1.24	1.21	1.33	1.04		0.778	
3	1.48	1.67	1.7	1.78	1.68	1.4	1.32	1.28	1.29	1.37	1.42	1.33	1.38	1.44	1.78	1.28		0.721	
2	1.52	1.75	1.81	1.84	1.77	1.54	1.39	1.26	1.24	1.22	1.24	1.25	1.27	1.45	1.84	1.22		0.664	
1	1.89	2.06	2.21	2.22	2.21	1.96	1.66	1.52	1.41	1.37	1.38	1.38	1.39	1.5	2.22	1.37		0.618	

10 Photobiological safety

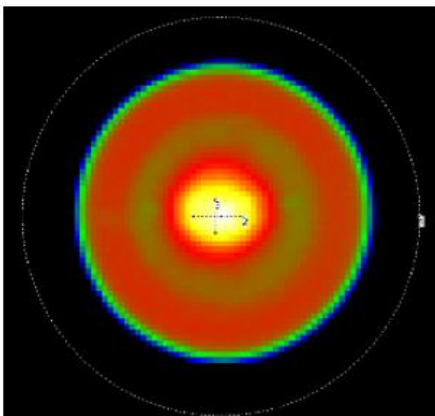
Dimensional measurement of the luminous area with emission above 50% of maximum, identification of the FOV to be evaluated in different configurations	UNE-EN 62471:2009: Photobiological safety of lamps and lamps systems
UNE-EN 62471:2009: Photobiological safety of lamps and lamps systems	

ILMD Type	I
Measurand	cd/m ²
FOV / (mm/°)	1.7 mrad to 100 mrad
Lens type	
Resolution	
L_{min}, L_{max}	50, 100 000; neutral filter needed in some cases
Contrast local/ contrast global	Local

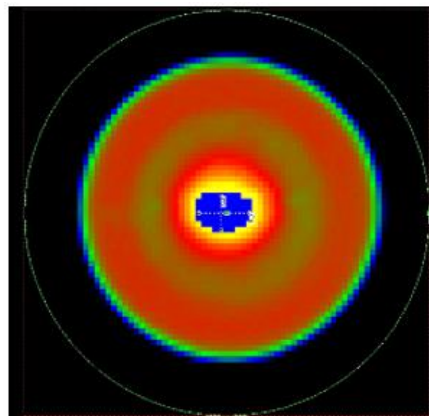
Type of Light Source	Any (typically LED sources: white or color)
Measurement conditions	Typical laboratory conditions
Required Uncertainty / Traceability	Relative measurements
Parameters during the measurement	Constant Varying: FOV, configuration of exposure time and aperture accordingly to the characteristics of the product
Quality indices	Area with Luminance above 50% of maximum luminance

Examples of evaluation in different products

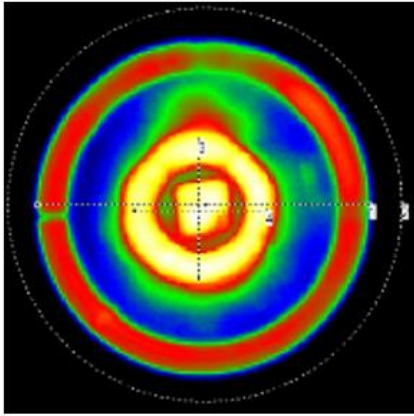
The emitting surface of the source is analysed, the actual dimensions of the area with luminance $\geq 50\%$ of the maximum luminance allows the classification of the source as “small” or “non-small”, which conditions how the blue light hazard should be evaluated, obtaining radiance or irradiance values, having different limiting values per risk category.



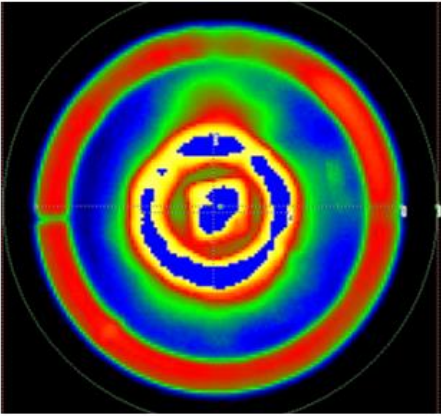
Luminance image



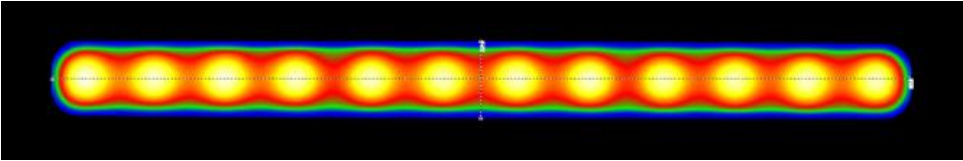
Processed image: $L \geq 50\% L_{\max}$ in solid blue central area



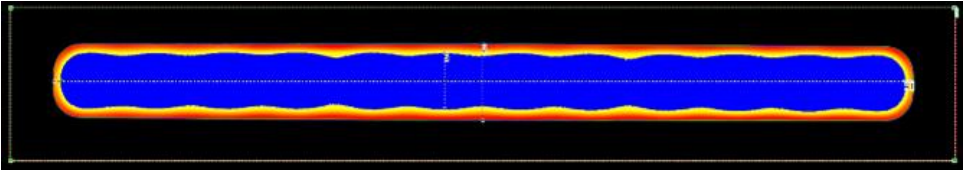
Luminance image



Processed image: $L \geq 50\% L_{max}$ in solid blue areas



Luminance image



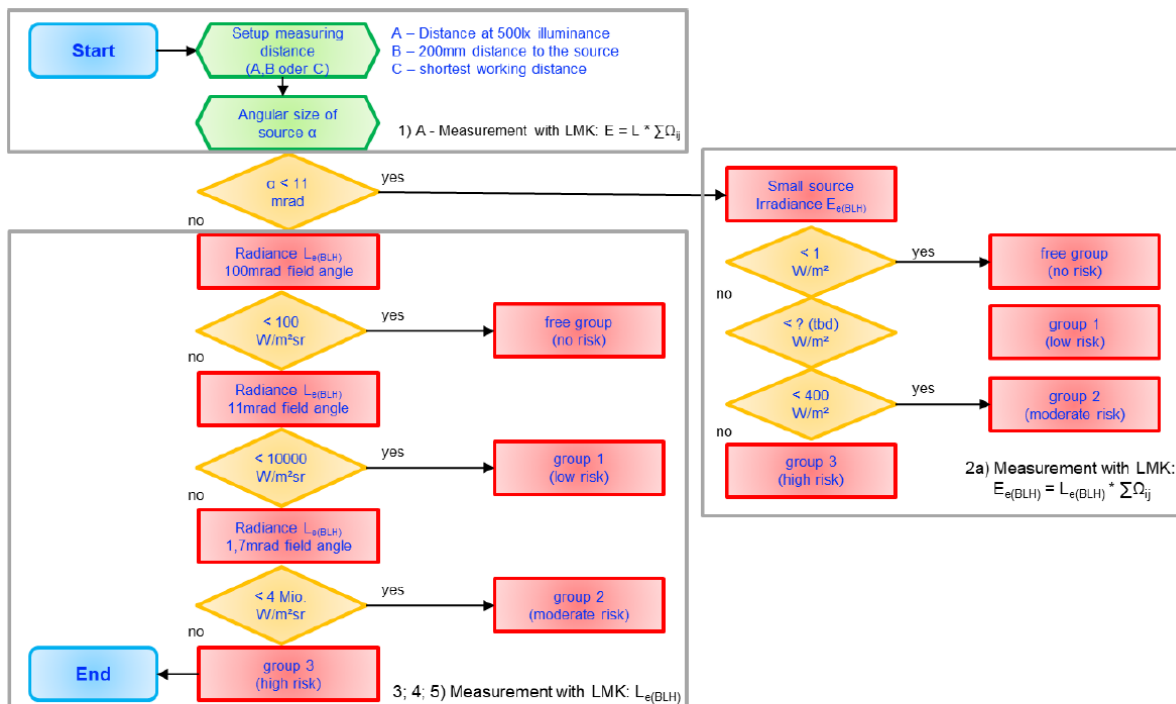
Processed image: $L \geq 50\% L_{max}$ in solid blue area

11 BLH – Blue light hazard

EN 62471 – photobiological safety of lamps and lighting systems	Measuring radiance $W/(m^2 \cdot sr)$ and irradiance (W/m^2) of lighting fixtures under fixed direct viewing conditions into the light source
---	---

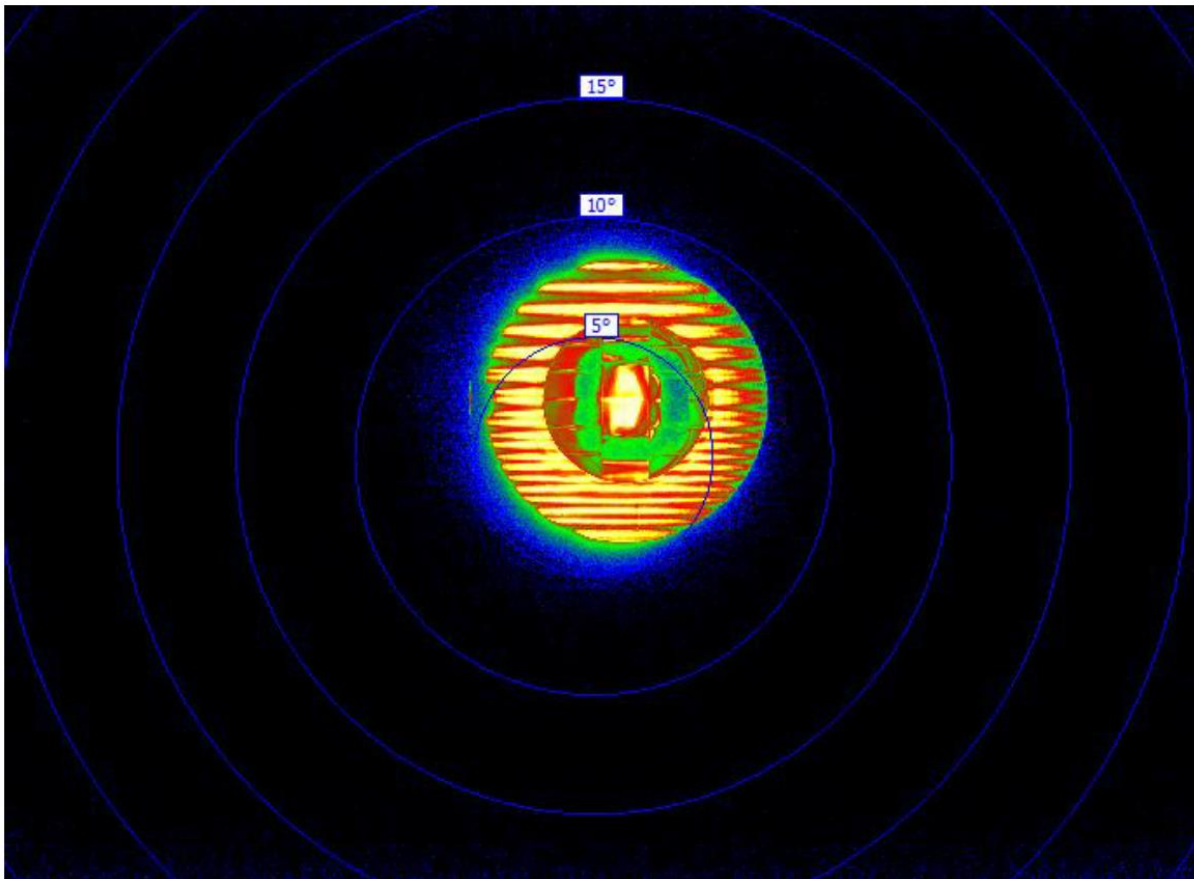
ILMD Type	I / II
Measurand	$W/(m^2 \cdot sr)$
FOV / (mm/°)	
Lens type	E
Resolution	certain measurement angles or aperture angles must be used: 100 mrad (5.73°); 11 mrad (0.63°) or 1.7 mrad (approx. 0.1°)
L_{min}, L_{max}	
Contrast local/ contrast global	Local

Type of Light Source	Not specified
Measurement conditions	Test set up
Required Uncertainty / Traceability	
Parameters during the measurement	Constant x
	Varying
Quality indices	

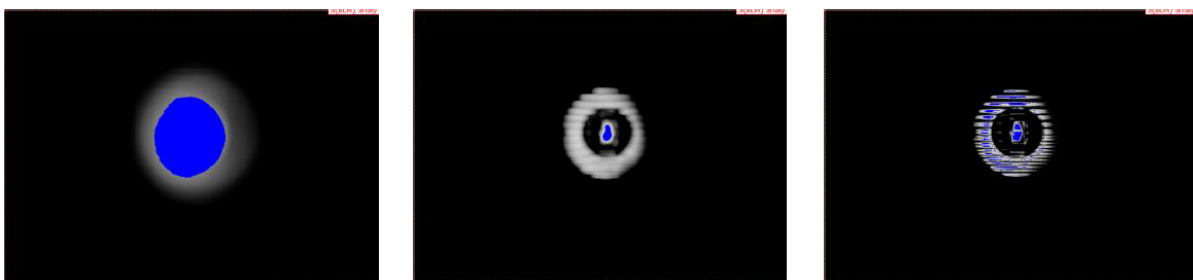


Overview of the standardized sorting into risk groups of EN 62421

Sample image with evaluation regions:



BLH filtered/weighted image with 100 mrad (left), 11 mrad (middle) and 1.7 mrad (right) aperture combined with the display (blue coloured) of the 50 % emission threshold to determine the size of the active angular area α in mrad:



Sample results:

Stat.No.	Parameter	Image	Region	Class	Area	Min	Max	Mean	Disp	BLH Irradiance (W/m ²)	BLH angular size (mrad)
					pix ²	W/sr ² m ²					
1	Lum_Gr[91]	BLH image 100 mrad	S(BLH) analysis	> 212.75 W/sr ² m ²	519900	212,8	425,5	296,9	61,31	7,053	174
2	Lum_Gr[92]	BLH image 11 mrad	S(BLH) analysis	> 1203.0 W/sr ² m ²	11880	1203	2406	1678	318,6	0,911	26,29
3	Lum_Gr[93]	BLH image 1.7 mrad	S(BLH) analysis	> 1528.5 W/sr ² m ²	46090	1529	3057	1847	300,7	3,888	51,78



19NRM02 “RevStdLED”

**Good Practice Guide
for
Setting up an Uncertainty Budget for the
Measurement of Luminance Distributions
Part 2
Measurement Uncertainty Contributions
Originating From the Scene**

This project has received funding from the EMPIR programme co-financed by the Participating States and from the European Union’s Horizon 2020 research and innovation programme.



The EMPIR initiative is co-funded by the European Union's Horizon 2020 research and innovation programme and the EMPIR Participating States

Table of Contents

Scope	3
Introduction.....	3
1 General Notation.....	5
2 Model evaluation	6
2.1 Modelling DUT (source).....	8
2.2 Modelling the luminance standard source.....	9
2.3 Modelling of the measurement	10
2.4 Modelling interaction	10
2.5 Summary.....	10
Summary of overall model	11
3 Collecting information.....	11
3.1 Noise and stabilisation	12
3.2 Adjustment factor	14
3.3 Temperature Dependence	14
3.4 Ageing information.....	15
3.5 Spectral mismatch	16
3.6 Linearity index, f_3	18
4 Parameter Estimation.....	19
4.1 General Models	19
4.2 Examples.....	21
4.3 Light source stability.....	22
4.4 Temperature Coefficient	23
4.5 Ageing of a luminance standard.....	26
4.6 Non-uniformity of a light source	27
4.7 Non-Linearity Correction.....	29
5 Monte Carlo Simulation	31
5.1 Basics	31
5.2 Code Example.....	32
6 References.....	33

Scope

In the following, based on a simple model of a photometric measurement, it is shown how corrections or characterisation can be performed and added to the model and how the measurement uncertainty of the resulting quantity can be determined.

Reference is made to the notation and models described in the normative document (CIE 198:2011, 2011), hereafter called *CIE198*, and its supplements (CIE198-SP1.3:2011, 2010; CIE198-SP1.1:2011, 2011; CIE198-SP1.2:2011, 2011; CIE198-SP1.4:2011, 2011; CIE 198-SP2:2018, 2018) hereafter referred to as *CIE198-SP1* and *CIE198-SP2*.

The knowledge of the documents (JCGM 100:2008, 2008; JCGM 101:2011, 2011; JCGM 102:2011, 2011) and (JCGM106:2020, 2020) hereafter called *GUM*, *GUMS1*, *GUMS2* and *GUMS6* and the *CIE198*, incl. supplements, is assumed in broad outline.

The general approach based on Monte Carlo Simulations (MCS, *GUMS1*) is used to determine the measurement uncertainty so that no further explanations (partial derivatives, etc.), as used in the original *GUM*, are necessary here after the modelling and determining the model parameters.

Introduction

Measurement uncertainties play a key role in establishing comparability and metrological traceability of measurement results. Stating measurement uncertainties along with measurement results is therefore not only considered good practice but is most often a normative requirement of many measurement or application standards.

This good practice guide was written as part of the EMPIR project 19NRM01 RevStdLED to assist users in photometry in setting up measurement uncertainty calculations for their applications. The document focuses on practical guidance for situations where the available information about the measuring instrument is used and, if necessary, further estimations by an additional application-relevant characterisation are performed to allow parametrization of the measurement process, where the instrument is part of the measurement setup, to determine the measurement uncertainties. This is often the case for users of commercial measurement instruments, where only limited information about the inner workings of the instruments, especially the kind of applied corrections for significant internal and external influences, is available from the manufacturer and the user can at most perform a limited number of simple characterisation measurements. In such situations, the methods and models described in many other existing documents, especially from the CIE 198 series, can be difficult to apply, which largely motivated the writing of this document.

The objective of this document is to provide practical guidance for the estimation of measurement uncertainties for photometric measurements using largely effective models based on typical information available from calibration-/test certificates, data sheets and simple characterisation methods. The document's focus is on measurements with **Imaging Luminance Measurement Devices (ILMDs)**, but much of the provided information can be readily applied also to other photometric measurements. The target audience are users performing their measurements with calibrated commercial measurement instruments using the readings of their instruments mostly "as is", that is without applying extensive characterisations to implement corrections beyond that already internally provided by the manufacturers and covered by an uncertainty considering the critical contributions, cf. Part 1 of this GPG. Characterisation effort is limited to finding residual deviations of the corrected signals that might have application-relevant effects.

The provided information will also be useful for users working at calibration labs or NMIs. Methods to determine corrections to measurement results and their associated uncertainties are not covered in full detail by this document (cf. Part 1 of this GPG), as this would in many cases require to go beyond the described effective models and to acquire more detailed information about the details of the processes inside a measurement instrument leading to the indicated measurement result (i.e. reading from the ILMD) and the luminance distribution to be measured (i.e. the lamp). Applying corrections that go beyond these require to parametrize a quite complex measurement model, i.e. as defined by an equivalent circuit of the pixel and signal processing block diagram. This is especially also true where corrections implemented by the manufacturer (e.g. a look up table rather than a parametrized low order function) cannot be bypassed to fully cover the parameter range or perform reverse engineering. Consequently, also the process of instrument adjustment, calibration and estimation of the associated uncertainties will not be covered in full detail.

It should also be noted that the required effort to determine the uncertainty also depends on the required quality of the measurement, i.e. not every contribution has to be taken into account if only very low requirements are placed on the uncertainty. Critical contributions from the ILMD itself and their correlation between different measurements are identified in Part 1 of this GPG.

This document (Part 2 of the GPG) describes and promotes measurement uncertainty evaluations by Monte Carlo methods. This approach is not only considered the most general and conceptually rigorous one, but, with nowadays freely available software tools, it is often also more easily implemented than a standard GUM calculation. Still, the document assumes that the reader is familiar with the basic concepts of measurement uncertainty and the standard GUM methods for measurement uncertainty evaluation.

This document is organised as follows:

Chapter 1 introduces the terminology and notation conventions usually used in measurement uncertainty calculations and photometric measurements. A very short introduction on the general concept of measurement uncertainty and standard methods for its evaluation is given.

Chapter 2 introduces a general model of evaluation that is the starting point for measurement uncertainty calculation. Based on this model and the outset of this document the workflow and governing principles of estimating measurement uncertainties is described.

Chapter 3 provides general guidance for identifying potential uncertainty contributions, setting up a corresponding uncertainty budget and establishing a hierarchy of uncertainty contribution that allows to select significant contributions that will have to be characterized in detail.

Chapter 4 introduces describes how the standard measurement uncertainty can be derived from the model of evaluation and the individual contributions from Chapter 4 using Monte Carlo methods.

1 General Notation

The notation of the quantities and models follows the *CIE198* as closely as possible. Where possible, direct reference is also made to the corresponding chapters.

According to *CIE198*, we can model a photometric measurement of a number of $k = 1 \dots N$ physical output quantities Y_k represented by a number of $l = 1 \dots n$ output values $y_{k,l}$ based on the measurement of $i = 1 \dots M$ physical input quantities X_i provided by $j = 1 \dots m$ input values $x_{i,j}$ using a general model:

$$(Y_1, \dots, Y_N) = F(X, \dots, X_M) \tag{1}$$

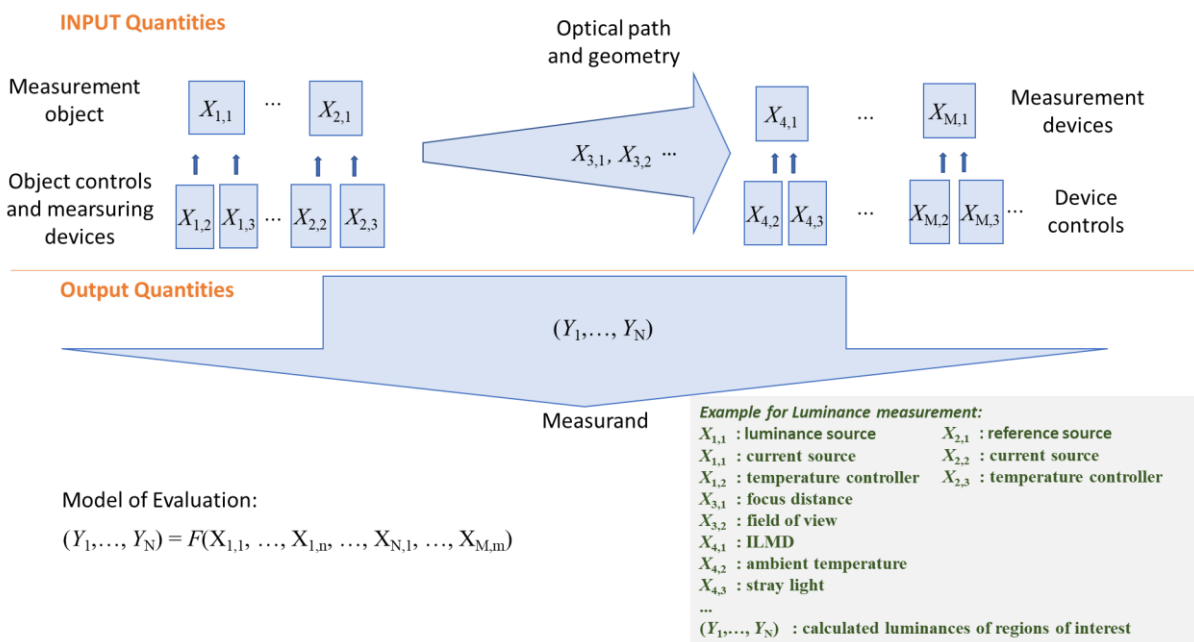


Figure 1: General modelling of the measurement by a model of evaluation

It is also possible to describe this modelling in more general terms by using vector the notation $\mathbf{X} = (X_1, \dots, X_M)$ and $\mathbf{Y} = (Y_1, \dots, Y_N)$. In this case, input and output quantities are described by $\mathbf{F}(\mathbf{X}, \mathbf{Y}) = \mathbf{0}$.

To measure a model input quantity X_i we typically collect at first multiple readings $x'_{i,j}$ of the input quantity. Based on the multiple readings and possibly sometimes also on the basis of internal adjustment factors, we calculate the input quantity X'_i . However, if e.g. the environmental condition of the measurement was different from the absolute calibration condition, we have to correct X'_i to get the input quantity X_i we need in the model of evaluation for the measurement. Therefore, the quantity X_i denotes the expected input quantity.

$$X_i = c_i \cdot X'_i \tag{2}$$

The use of the quantities with and without prime is used as a general concept in this document:

Primed quantities always represent the value of a quantity/indication **without correction**, as read (for measuring instruments) or as realised (for standards, i.e. under the currently given conditions). Quantities **without prime** represent **corrected** measured values (for measuring instruments) or reference

values at calibration/reference conditions (for standards or DUTs). The details are explained and applied step by step below.

According to GUM, the true value of a measured quantity is never known. The maximum knowledge we may get about a quantity, instead, is a distribution of measurement values, e.g. $x_{i,j}$, around an arithmetic mean value, \bar{x}_i , where the distribution of measurement values is characterized by the standard deviation, $s(x_{i,j})$, of measured values. A different set of measurement data will typically result in a different arithmetic mean value. Therefore, the associated uncertainty is defined as the experimental standard deviation of the mean value, $u(x_i) = s(\bar{x}_i)$.

Also, in case of a measurement simulation, we start with the known uncertainty of an input quantity and its arithmetic mean value. Within the framework of the Monte Carlo simulation of a measurement, we generate individual measured values that deviate from the mean value by random amounts that lie within the measurement uncertainty interval of the measurand. However, if we simulate a measurement, we are able to draw (i.e. to generate) as much simulated random measurement values, x^r , as we want. Therefore, the arithmetic mean value of a real measurement turns into an expectation value of a probability distribution, $\mathcal{G}(\mu, \sigma(x))$ of possible (measurement) values with an expectation value, $\mu \hat{=} \bar{x}_i$, and a standard deviation, $\sigma(x) \hat{=} u(x_i)$. The important difference between real measurements and simulated ones is, that the shape of the distribution of a real measurement is given by the distribution of the measured values while the distribution in a Monte Carlo simulation needs to be stated in advance based on the knowledge of the behaviour of the measurement process of the respective input quantity.

Further general notations used in this document:

T_a	ambient temperature
T_{aR}	reference ambient temperature (nominal value) <ul style="list-style-type: none"> • The subscript "R"¹ will always be used to state reference conditions / nominal values. • Nominal values have "A zero" uncertainty. (CIE198-SP1, 1.4).
$\Delta T_a = T_a - T_{aR}$	temperature difference <ul style="list-style-type: none"> • All differences are stated as the difference of the current value minus the reference value.
$\alpha_{T,X}$	temperature coefficient of the quantity X
$\alpha_{T,X,rel}$	relative temperature coefficient of the quantity X
$\mathcal{N}(x, u(x))$	Normal distribution with expectation value x and standard deviation $u(x)$ A random number for the MCS will be named $x^r \sim \mathcal{N}(x, u(x))$
$\mathcal{U}(x, \Delta x)$	Uniform distribution over the interval $[x - \Delta x, x + \Delta x]$ A random number for the MCS will be named $x^r \sim \mathcal{U}(x, \Delta x)$

2 Model evaluation

Measurement task:

An LMD/ILMD is calibrated with a luminance standard having a spectral distribution (SD) similar to CIE standard illuminant A. In the second step, the luminance of another luminance source, e.g. with the SD of a phosphor-type white LED, is determined. In this respect, the ILMD is an indicating device that needs to be linear and spectrally matched. (Type of calibration: Lamp calibrates lamp)

¹ This is different to CIE198, where the subscript "0" was used. The subscript "0" is used for the dark signal in this document.

Following an idea by Georg Sauter (Sauter, 2012), published with examples and details in (Krüger *et al.*, 2014), the measurement uncertainty budget of a measurement can be summarised very clearly in the following way and then refined step by step.

Consistent to Part 1 of the GPG, this document is written from a "luminance/photometric signal" in contrast to a "count/raw signal" perspective. This is a so-called "Black Box" approach for the complete device with respect to its indicated output quantity, meaning that we use measurement instruments with proper internal adjustment and model only minor deviations and imperfections rather than the underlying signal processing which is covered by the estimate for critical uncertainty contributions. On the other hand, this approach means that we can usually not use equivalent models motivated by the physical implementation, but we only have to model the observations by mathematical functions that are approximating the effective characteristic.

The starting point is the model equation (noted here without the restriction of generality for luminance or luminance distributions measured with LMD's (luminance measuring devices) or ILMD's), respectively:

$$\frac{L'_Z}{L'_C} = \frac{Y_Z}{Y_C} \quad (3)$$

$$L'_Z = L'_C \cdot \frac{Y_Z}{Y_C}$$

$$L_Z = \frac{c_{L,Z}}{c_{L,C}} L_C \cdot \frac{c_{Y,Z} Y'_Z}{c_{Y,C} Y'_C}$$

Where

L_Z	luminance (distribution) of the light source to be measured (DUT)
L'_C	indicated luminance (distribution) of the luminance standard for calibration under the given condition
L_C	Luminance (distribution) of the luminance standard (Calibration certificate)
Y_Z	Corrected measured quantity for the luminance (distribution) of the DUT
Y_C	Corrected measured quantity for the luminance (distribution) of the luminance standard
Y'_Z	indicated quantity for the luminance (distribution) of the DUT
Y'_C	indicated quantity for the luminance (distribution) of the luminance standard
$c_{L,Z}, c_{L,C}, c_{Y,Z}, c_{Y,C}$	Correction factors provided by the manufacturer or derived from characterising measurements

The approach is explained step by step in deriving the individual model components. This model equation describes the absolute calibration of the measuring device and the measurement as a whole. It should also be noted that in nearly all cases, the measured values of the ILMDs are already provided as luminance values (readings). However, the physical measurement process with ILMDs is typically a counting process of collected photons and extensive signal processing which residual errors and related critical uncertainty contributions are considered in Part 1 of this GPG. This becomes especially important if linearity properties and their contributions to the MU are discussed. However, count values are often hidden in the manufacturer's software and not directly accessible by the user. How to deal with linearity will be shown in Chapter 4.7. The correction factors determined and provided by the manufacturer are typically implemented in the software of the measurement devices. In this case, the factors appear in the model of the user as unity with a given uncertainty, which may still depend on the application.

Remark: The modelling could also be done by describing the physical processes in a measuring device/light source by an equivalent circuit and a block diagram. However, this is increasingly problematic (also for the manufacturers) because not enough information about the pixel sensor is provided for this, and the measurement systems are becoming more complex. The BlackBox approach is probably the only method of describing current measuring systems and light sources. But even with this Black-Box approach, it is possible to model different levels so that, for example, the manufacturer can access further internal data that is no longer made available to the user in his modelling.

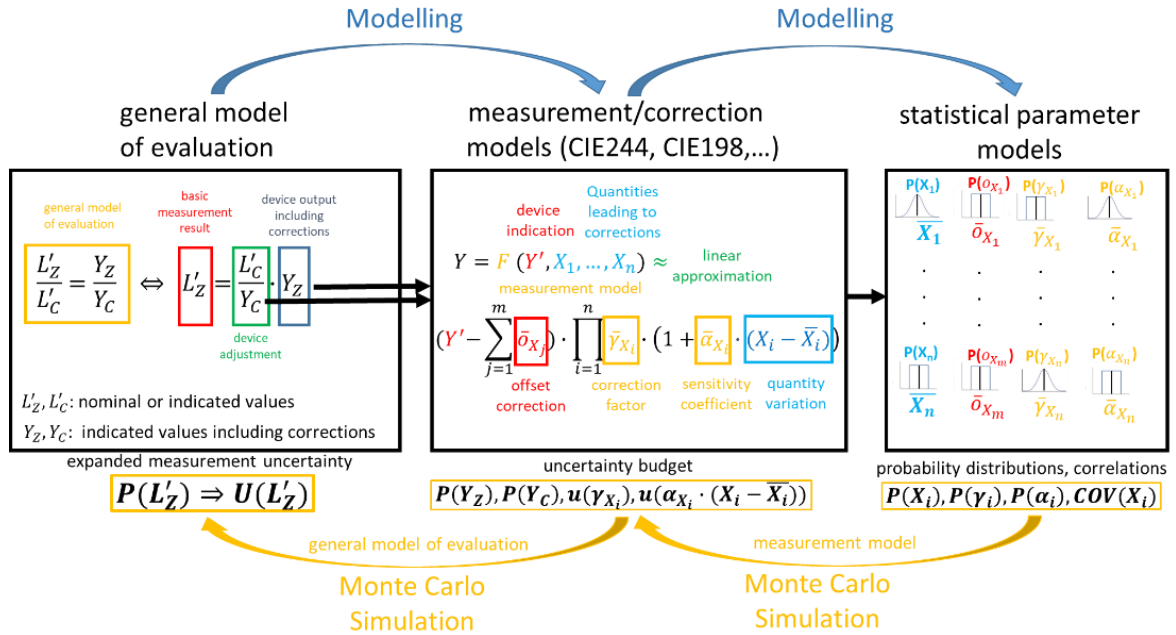


Figure 2: Detailed description of the modelling

2.1 Modelling DUT (source)

The following model can be used as a general model for measuring the light source (DUT). Whereby the Luminance L_Z under defined boundary conditions is to be determined from the measured luminance L'_Z under the current measurement conditions by multiplication with a correction factor.

$$L_Z = L'_Z c_{L,Z} \quad (4)$$

This also applies analogously to the other variables from equation (3).

The correction factor can be broken down in detail step by step.

$$c_{L,Z} = (1 - \alpha_{T,Z} \Delta T_Z - \alpha_{\theta,Z} \Delta \theta_Z - \alpha_{J,Z} \Delta J_Z - \gamma_{U,Z} - \gamma_{t,Z} \dots) \quad (5)$$

The relative sensitivity coefficients are described with α , where the first letter of the index describes the variable to be changed, and the second letter represents the object (e.g. Z for the DUT, C for the calibration light source, etc.). The sensitivity is valid for the measurement quantity we observe, which is the luminance in this example. A sensitivity is connected to a second parameter, describing the change of the influencing variable. Example $\alpha_{T,Z} \Delta T_Z$: In this case $\alpha_{T,Z}$ is the sensitivity in 1/K describing the relative luminance change for every degree change of the reference temperature. And the ΔT_Z is describing that temperature change (or a possible range of temperatures with a random variable).

The values in the models depicted with γ represent model parameters without an additional scaling like temporal noise or uniformity.

T_Z	The temperature of the DUT (depending on the measurement, the ambient temperature T_a or the temperature at a specific point $T_{p,Z}$ on the enclosure is relevant here).
ΔT_Z	Difference to the reference Temperature $\Delta T_Z = T_Z - T_{ZR}$
$\alpha_{T,Z}$	Relative sensitivity for the luminance change with respect to the temperature change of the DUT
$\alpha_{\vartheta,Z}$	Relative sensitivity for luminance change with respect to angular dependence of the luminance
$\Delta \vartheta_Z$	Angular difference to the normal view
$\gamma_{U,Z}$	Non-uniformity of the DUT surface (e.g. if a different spot size with respect to the calibration condition is measured; zero degree)
$\gamma_{t,Z}$	Stability of the DUT after burn-in (remaining instability)
$\alpha_{J,Z}$	Sensitivity regarding the current setting of the device (e.g. if an external source is needed)
ΔJ_Z	Difference to the reference current $\Delta J_Z = J_Z - J_{ZR}$, (e.g. if an external source is needed)

Further influencing variables can be added here depending on their relevance. In the very first step, one can start with $c_{L,Z} = 1$ and just estimate its uncertainty by a value covering typical characteristics.

The term noise is used here in a very general way. First of all, of course, for the description of quantities whose repeated observation allows to infer mean value, standard deviation and possibly the probability distribution function (GUM Type A). But then also for quantities about which e.g. limits are known from other sources or other information is available (GUM Type B).

For the modelling to be done here via MCS, however, the difference in the treatment during the modelling is not relevant, so that here both types of quantities are modelled equivalently. In the first case, normal distributed random variables are modelled. In the second case, one often meets with equally distributed random variables, e.g. if only the range is known. Furthermore, it does not matter for the modelling whether there is really a random process behind it or whether it is a systematic deviation/variation.

2.2 Modelling the luminance standard source

The luminance standard can generally be described similarly. However, more properties are usually known for this light source, so the modelling can be somewhat more complex:

$$L_C = L'_C \cdot c_{L,C} \tag{6}$$

$$c_{L,C} = (1 - \alpha_{T,C} \Delta T_C - \alpha_{\vartheta,Z} \Delta \vartheta_Z - \alpha_{p,C} \Delta p_C - \gamma_{U,C} - \gamma_{t,C} \dots)$$

$\alpha_{p,C}$	Relative ageing coefficient of the luminance value
Δp_C	Accumulated time of operation since the last calibration (together with the ageing coefficient $\alpha_{p,C}$, the ageing of the calibration source luminance value caused by its operation can be corrected here).

2.3 Modelling of the measurement

The determination of the luminance values Y_Z and Y_C (the actual measurements) can be described similarly, whereby the corrections and especially their uncertainties are to be applied and respected depending on the measurement technique used for the application.

$$\begin{aligned} Y_Z &= Y'_Z c_{Y,Z} \\ Y_C &= Y'_C c_{Y,C} \end{aligned} \quad (7)$$

The correction factors can be modelled as in (5) and (6) with extension based on focus, linearity and size of source properties.

$$c_{Y,Z} = (1 - \alpha_{T,C} \Delta T_C - \gamma_{U,Y} - \gamma_{t,C} - \textit{Focus} - \textit{Linearity} - \textit{Size of Source} - \dots)$$

$$c_{Y,C} = (1 - \alpha_{T,C} \Delta T_C - \gamma_{U,Y} - \gamma_{t,C} - \textit{Focus} - \textit{Linearity} - \textit{Size of Source} - \dots)$$

Since the measurement of the DUT and the reference light source is carried out with the same *measuring* instruments and usually under the same or at least very similar conditions, some influences of the measuring instrument and the actual measurement conditions (if measured concurrently) may cancel each other out. Therefore, during numerical modelling, special care must be taken to ensure that logically related measured values (e.g. ambient temperatures) are modelled with the same random variables to represent these correlations adequately.

2.4 Modelling interaction

In addition to modelling the measurement and the corrections described in the previous sections, the interaction between the measurement system and the measured object must also be described. Here the spectral matching and the influence of stray light are essential to be considered, whereby “stray light” is usually modelled as an offset (not viewed further here as covered in Part 1 of the GPG).

As described by (Krüger *et al.*, 2022), the spectral mismatch correction factor $F(S_C(\lambda), S_Z(\lambda))$ for a photometer calibrated with a relative spectral distribution (SD) $S_C(\lambda)$ measuring a different relative SD of the DUT $S_Z(\lambda)$ can be written as:

$$F_{C,Z} = F(S_C(\lambda), S_Z(\lambda)) = \frac{\int_{360 \text{ nm}}^{830 \text{ nm}} S_Z(\lambda) V(\lambda) d\lambda}{\int_{\lambda_{\min}}^{\lambda_{\max}} S_Z(\lambda) s_{\text{rel},C}(\lambda) d\lambda} \quad (8)$$

Attention: Compared to other equations (e.g. in (ISO/CIE 19476:2014, 2014)) the normalised spectral responsivity $s_{\text{rel},C}(\lambda)$ here is calculated from the relative spectral responsivity $s_{\text{rel}}(\lambda)$ using a weighting with the relative SD of the calibration light source to make the evaluation much easier.

$$s_{\text{rel},C}(\lambda) = \frac{\int_{360 \text{ nm}}^{830 \text{ nm}} S_C(\lambda) V(\lambda) d\lambda}{\int_{\lambda_{\min}}^{\lambda_{\max}} S_C(\lambda) s_{\text{rel}}(\lambda) d\lambda} s_{\text{rel}}(\lambda) \quad (9)$$

2.5 Summary

The individual modelling steps of the previous sections can then be summarised as follows:

$$L_Z = c \cdot L_C \cdot \frac{Y'_Z}{Y'_C} \quad \text{with} \quad c = \frac{c_{L,Z} c_{Y,Z}}{c_{L,C} c_{Y,C}} F_{C,Z} \quad (10)$$

This means one gets the luminance L_Z of the DUT using the luminance of the calibration source L_C (certificate of calibration), the measurement values (readings) during the calibration/adjustment Y'_C and the measurement values Y'_Z at the time of the DUT measurement, applying a couple of corrections.

Using a different notation introducing an adjustment factor² k_Y :

$$k_Y = \frac{L_C}{Y'_C} \cdot \frac{1}{c_{L,C} \cdot c_{Y,C}} \quad (11)$$

$$L_Z = c_S \cdot k_Y \cdot Y'_Z \quad \text{with} \quad c_S = c_{L,Z} c_{Y,Z} F_{C,Z} \quad (12)$$

In this case, the calibration/adjustment of the measurement device can be separated from the DUT measurement. However, one should consider the correlations (e.g. using the same thermometer) which make it reasonable to set up a joint model for calibration and measurement whenever possible.

However, all correction factors and adjustment factors as well as the reading of the ILMD comes with an uncertainty, which need to be determined to finally calculate the combined uncertainty of the measurement process.

Summary of overall model

$$L_Z = \frac{c_{L,Z}}{c_{L,C}} \frac{c_{Y,Z}}{c_{Y,C}} F_{C,Z} \cdot L_C \cdot \frac{Y'_Z}{Y'_C}$$

with

$$c_{L,Z} = (1 - \alpha_{T,Z} \Delta T_Z - \alpha_{\theta,Z} \Delta \theta_Z - \alpha_{J,Z} \Delta J_Z - \gamma_{U,Z} - \gamma_{t,Z} \dots)$$

$$c_{L,C} = (1 - \alpha_{T,C} \Delta T_C - \alpha_{\theta,Z} \Delta \theta_Z - \alpha_{p,C} \Delta p_C - \gamma_{U,C} - \gamma_{t,C} \dots)$$

$$c_{Y,Z} = (1 - \alpha_{T,C} \Delta T_C - \gamma_{U,Y} - \gamma_{t,C} - \text{Focus} - \text{Linearity} - \text{Size of Source} - \dots)$$

$$c_{Y,C} = (1 - \alpha_{T,C} \Delta T_C - \gamma_{U,Y} - \gamma_{t,C} - \text{Focus} - \text{Linearity} - \text{Size of Source} - \dots)$$

$$F_{C,Z} = (1 - k f'_1)$$

3 Collecting information

In the following chapters, we will collect the information we need for the modelling and to derive the components making up the correction factors $c_{L,C}, c_{Y,C}$ and $c_{Y,Z}, c_{L,Z}$ of the measuring device and the sources step by step.

The information we need for the modelling we can get from (the order does not represent an assessment of importance):

- Calibration sheets and the calibration history (e.g. of a luminance standard)
- Literature as well as specifications (e.g. as issued by the manufacturer)
- Characterisation of measurement devices used to perform the measurement
- Quality indices of luminance meter used
- Measurements

² Attention: The adjustment factor is sometimes also defined in the reciprocal version. The version used in this document facilitates its application in the correction, which is then really a factor.

According to (ISO/CIE 19476:2014, 2014; CIE244:2021, 2021), several quality indices are defined for LMDs and ILMDs. These quality indices have been developed to assign characteristic values to photometers including LMDs and ILMDs to allow users to identify the capabilities of such devices under specific measurement conditions. Some of these quality indices can be used to estimate the uncertainty contribution, but they cannot be used for correction. In the following, this will be mentioned for every possible contribution.

3.1 Noise and stabilisation

For the description of the remaining instability γ_t (see equations 5 and 6), a distinction must be made between effects belonging to the light sources and those belonging to the measuring devices.

3.1.1 Light source including power supply

A light source has a slight permanent drift or instability after a specific burn-in time. The burn-in time was therefore defined in CIES025 4.4.1.:

“Specific requirement: The DUT shall be operated for at least 30 min and it is considered as stable if the relative difference of maximum and minimum readings of light output and electrical power observed over the last 15 minutes is less than 0,5 % of the minimum reading. If the DUT is pre-burned, it does not need to be operated for 30 min, and it is considered stable if the readings of the last 15 min meet above requirement.”

However, no distinction is made here between noise (random instability after reaching a stable operating point) and a small remaining drift.

It is therefore recommended to examine the light to be used in detail. For luminance standards, this should be self-evident. With unknown DUTs, the situation is different.

In this guide, a relative instability factor is used to model the residual instability $\gamma_{t,C}$ or $\gamma_{t,Z}$. To handle it in the context of MCS, a random variable $\gamma_{t,C}^r \sim \mathcal{N}(0, \sigma_{t,C})$ is introduced with an expectation value of zero and the standard deviation $\sigma_{t,C}$.

3.1.2 Measurement device

The situation is similar for the measuring instruments. Here, too, a specific warm-up time must be waited for before measurements can be started. But even then, you do not get the same measured value for every measure, but different measured values that fluctuate around an average value.

Care must be taken to ensure that the scatter of the measured values is sufficiently large and that one is not limited by the quantisation noise (Sripad and Snyder, 1977). In the following, the quantisation step is denoted as Δ_{ADC} in units of the evaluated Quantity $[Y]$.

Another point is to pay attention to temporal light modulation. Here, the frequency bandwidth settings in the measuring devices or the selected integration times may have to be adjusted accordingly. This can be checked by recording a series of measured values in close succession and examining them for mean value, standard deviation and (low/high frequency) fluctuations.

3.1.2.1 LMD

For an LMD, N measured values Y_i are to be recorded and the mean value \bar{Y} and experimental standard deviation of the mean value $u(\bar{Y}) = \sigma(Y)/\sqrt{N}$ are included in the further evaluation.

Hence, in our MCS, we model the measurement value Y as the realization of a random number $Y^r \sim \mathcal{N}(\bar{Y}, \sigma(Y)/\sqrt{N})$, i.e. as a normal distributed number around the mean value with the uncertainty (i.e. the experimental standard deviation of the mean) used as a parameter to describe the width of the distribution.

Attention: If the noise is too low ($\sigma < \Delta_{\text{ADC}}/3$), an additional contribution for the consideration of the quantization resolution has to be included ($u(\bar{Y}) = \Delta_{\text{ADC}}/3$). The measurement value Y in the MCS is then the realization of a random number $Y^r \sim \mathcal{N}(\bar{Y}, \Delta_{\text{ADC}}/3)$ without an influence of the number of measurements. An alternative solution is to model with $Y^r \sim \mathcal{U}(\bar{Y}, \Delta_{\text{ADC}}/2)$ in this case. The quantisation resolution Δ_{ADC} must be determined experimentally or provided by the manufacturer.

3.1.2.2 ILMD

For ILMDs, what has been said for LMDs applies analogously. The quantization noise does not usually play a role here, as the quantization resolution is usually sufficiently good. In addition to the number of measurements N , the size of the evaluation region M (macro pixel, containing M physical camera pixel) also plays a role. One, therefore, averages over $N * M$ values so that the experimental standard deviation of the mean value is reduced accordingly by the factor $1/\sqrt{N * M}$. However, it should be checked here whether an enlargement of the measurement region or an increase in the number of images taken also leads to a reduction in the experimental standard deviation of the mean value or whether correlations prevent this. For $N * M > 1000$, a noise reduction can usually no longer be achieved in practice.

3.1.2.2.1 Difference Image Method

The user of an ILMD usually finds it difficult to access the physical model parameters. These are usually also changed by the correction algorithms of the manufacturer, so it is better to make investigations with the luminance images themselves.

Here, one can work in the same way as with LMDs with short-time standard deviations, i.e. one takes a series of measured values and analyses the temporal standard deviations of the values for a defined time range.

With ILMDs, however, the difference image method can also be used. Here, two images are acquired quickly after each other, and the difference image is determined. The temporal noise σ_t of the ILMD measurement data can now be determined from the spatial noise σ_o in the difference image, where $\sigma_t = \sigma_o/\sqrt{2}$. The $\sqrt{2}$ comes from the difference image. The difference image represents a random number based on the difference of two random numbers with the standard deviation σ_t . Therefore, the difference image itself has a standard deviation of $\sqrt{2}\sigma_t$.

Using this approach, we will get for the signal to be modelled by MCS: $Y^r \sim \mathcal{N}(\bar{Y}, \sigma_o/\sqrt{2})$

3.1.2.2.2 Photon Transfer Method

The standard deviation can be estimated by measurements or based on the physical properties of the sensor (assuming that the camera electronics itself is not the limiting factor). This modelling is usually done by the photon transfer method (PTM, (Janesick, Klaasen and Elliott, 1985)) and described in detail in (EMVA, 2016).

A very short summary for a physical model using the signal Y as direct ADC counts: In an image sensor, the incident photons are converted into electrons, which can be read out in very different ways. In principle, however, due to the Poisson distribution of shot noise generated by the electron flow, one obtains the relationship that the variance of the signal shot noise σ_Y^2 corresponds to the mean value \bar{Y} of the signal shot noise. From this relationship, the model parameters system transmission factor, k_{sys} , and dark signal noise, σ_0 , can then be derived. A further refinement of this modelling can be found in (EMVA, 2016), hereafter denoted as *EMVA1288*.

This results in the following for the modelling of the signal noise for a single pixel $M = 1$ in a single capture $N = 1$:

$$\sigma^2(Y) = k_{\text{sys}}Y + \sigma_0^2 \quad (13)$$

Using multiple image captures and or larger regions, the noise can be reduced accordingly.

$$\sigma(\bar{Y}) = \sqrt{\frac{k_{\text{sys}}Y + \sigma_0^2}{M * N}}$$

The signal for the MCS can be modelled $Y^r \sim \mathcal{N}\left(\bar{Y}, \sqrt{\frac{k_{\text{sys}}Y + \sigma_0^2}{M * N}}\right)$

Attention: This is only true for the ADC counts of the conversion process. For the luminance readings, which the user usually only has access to, several other effects also play a role (e.g. dark signal, defect pixel, and shading correction) so that the relationship mentioned above only represents the lower noise limit.

3.2 Adjustment factor

Using an adjusted instrument, we have an adjustment factor k_Y and its uncertainty. That means we can use the luminance reading of our measurement device Y'_C and apply the adjustment factor:

$$L'_C = k_Y Y'_C = Y_C \quad (14)$$

In our MCS, we model the adjustment factor as the realization of a random number $k_Y^r \sim \mathcal{N}(k_Y, u(k_Y))$

There are several possibilities for getting information about the adjustment factor:

- Using a adjusted instrument with a calibration sheet, one can assume that one can use $k_Y^r \sim \mathcal{N}(1, U(k_Y)/2)$. That means we assume the factor is one, and we use half of the expanded measurement uncertainty stated in the calibration sheet of the luminance meter as standard deviation.
- Using a known adjustment factor (usable if one adjusts in the in-house laboratory). In this case, one can use the adjustment factor for the luminance meter as measured and its uncertainty $k_Y^r \sim \mathcal{N}(k_Y, u(k_Y))$.
Attention: Do not apply the factor twice in this case!
- Using the information from the characteristic value initial adjustment index f_{adj} .
 $k_Y^r \sim \mathcal{N}\left(1, \sqrt{f_{\text{adj}}^2 + u^2(f_{\text{adj}})}\right)$.

Using the characteristic value:

The initial adjustment index, f_{adj} , (typical or individual value from the luminance meter) (ISO/CIE 19476:2014, 2014) is defined as (with the notation of this document):

$$f_{\text{adj}} = \left| \frac{Y}{Y_0} - 1 \right| = \left| \frac{Y_C}{L'_C} - 1 \right| \quad (15)$$

From the practical point of view, the value itself should be zero after the initial adjustment process. But the uncertainty $u(f_{\text{adj}})$ has to be stated, too and can be used in a measurement budget.

3.3 Temperature Dependence

Influence of ambient or device temperature change. Here we can use the same procedures for light sources and measurement devices. The explanation will be done with the luminance of a light source.

$$L = c_T L' \quad (16)$$

The temperature dependence can be modelled generally according to³

$$X = c_T X' = (1 - \alpha_T \Delta T_a) X' \quad (17)$$

The relative temperature coefficient α_T and its uncertainty should be estimated by a linear regression model (see 4.1.1).

1. In the case that the data for α_T and ΔT_a are only typically known and may not be corrected, c_T must be set to 1, and the typical information for α_T and ΔT_a must be integrated into the MU of c_T .

$$c_T = \mathcal{U}(1, |\alpha_T \Delta T_{a,\max}|) \quad (18)$$

Where $\Delta T_{a,\max}$ is the maximal temperature deviation, e.g. based on a tolerance interval ($\Delta T_{a,\max} = 1.2 \text{ K}$ in *CIES025*, see 4.2.2).

2. One source of information, in this case, is the quality index $f_{6,T}$. This index states the absolute value of 10 times the relative temperature coefficient. Therefore, one gets:

$$c_T = \mathcal{U}\left(1, \left|\frac{1}{10} f_{6,T} \Delta T_{a,\max}\right|\right) \quad (19)$$

3. In the case that α_T and ΔT_a are known (with expectation value and MU), one can generate the random numbers for $\alpha_T^r = \mathcal{N}(\alpha_T, u(\alpha_T))$ and $\Delta T_a^r = \mathcal{N}(\Delta T_a, u(\Delta T_a))$ and use (17) for the MCS.

Using the characteristic value:

The quality index, $f_{6,T}$, describing the temperature dependence of the photometer is defined as:

$$f_{6,T} = \left| \frac{Y(T_2) - Y(T_1)}{Y(T_R)} \frac{\Delta T}{T_2 - T_1} \right| \quad (20)$$

With $T_2 = 40^\circ\text{C}$, $T_1 = 5^\circ\text{C}$, $T_R = 20^\circ\text{C}$ and $\Delta T = 10^\circ\text{C}$. This means $f_{6,T}$ represents the absolute value of 10 times the relative temperature coefficient α_T .

3.4 Ageing information

Information about the ageing of sources and detectors can only be obtained through many years of experience and the evaluation of calibration certificates (for example, see 4.5). Some indications can also be found in the literature.

- The ageing of light sources is usually described as a function of the operating hours.
- The ageing of detectors is usually described as a function of a lifetime (time since the last calibration).
- Controlled standards, common for luminance standards, can be an exception here, as the ageing of the detector is usually the dominant variable.

If no information is available from your calibration certificates, you can ask the manufacturer or use the typical values from the literature.

Example values from literature:

³ The sign in this equation is different from CIE198-SP1:1.4.

- CIE198-SP1.2 2.8 (ageing of a luminous intensity standard lamp depending on the operation time) $\rightarrow 0.0007$ 1/h
- CIE198-SP1.2 2.9 (ageing of a luminance meter depending on the time since the last calibration) $\rightarrow 0.002$ 1/year

In addition, ageing is typically spectrally nonuniform. This may affect the calibration of spectroradiometers and light sources for spectral radiance/irradiance.

3.5 Spectral mismatch

A photometer should be matched to the $V(\lambda)$ -function. If this match is not ideal and the SD of the DUT differs from the SD of the light source used for calibration a correction may be necessary or the correction is set to one and the possible spectral mismatch correction factor is used to determine the measurement uncertainty of the spectral mismatch.

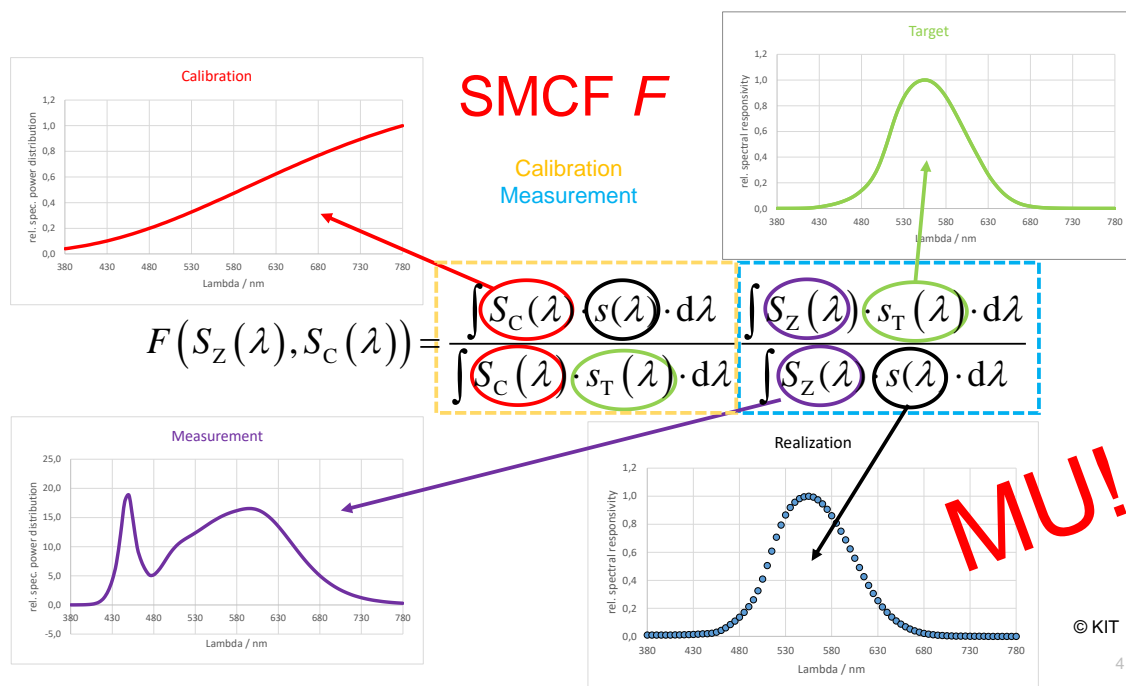


Figure 3: Calculation of the Spectral Mismatch Correction Factor (SMCF)

We have to deal with the calibration and the measurement state, and we have to describe the MU of integrated quantities, which was investigated in this project for the conference paper (Krüger *et al.*, 2023), which will be submitted to the peer review journal "Lighting Research & Technology".

A more general way to calculate the SMCF:

$$F(S_Z(\lambda_Z), S_C(\lambda_C)) = \frac{F_{C,N} F_{M,N}}{F_{C,D} F_{M,D}}$$

$$F_{C,N} = \int S_C(\lambda_C) s(\lambda_s) d\lambda$$

$$F_{C,D} = \int S_C(\lambda_C) s_T(\lambda) d\lambda$$

$$F_{M,N} = \int S_Z(\lambda_Z) s_T(\lambda_s) d\lambda$$

$$F_{M,D} = \int S_Z(\lambda_Z) s(\lambda_s) d\lambda$$

$$F(S_Z(\lambda_Z), S_C(\lambda_C)) = \frac{\int S_C(\lambda_C) s(\lambda_s) d\lambda}{\int S_C(\lambda_C) s_T(\lambda) d\lambda} \frac{\int S_Z(\lambda_Z) s_T(\lambda) d\lambda}{\int S_Z(\lambda_Z) s(\lambda_s) d\lambda}$$

Calibration
Measurement

Symbol	Description
$F(S_Z(\lambda_Z))$	SD DUT
λ_Z	wavelength scale for the measurement of SD DUT
$F(S_C(\lambda_C))$	SD Calibration
λ_C	wavelength scale for the measurement of SD Calibration
$s(\lambda_s)$	the (rel.) spectral responsivity of the detector
λ_s	wavelength scale for the spectral responsivity measurement
$s_T(\lambda)$	the spectral responsivity of the target function (e.g. $V(\lambda)$)
λ	nominal wavelength scale

Using the characteristic value:

The general $V(\lambda)$ mismatch index, f_1' , uses a general calculation not directly related to the spectral mismatch correction factor. However, as demonstrated in (Krüger *et al.*, 2022), one can use a statistical method to analyse the relationship between the index and the spectral mismatch correction factor.

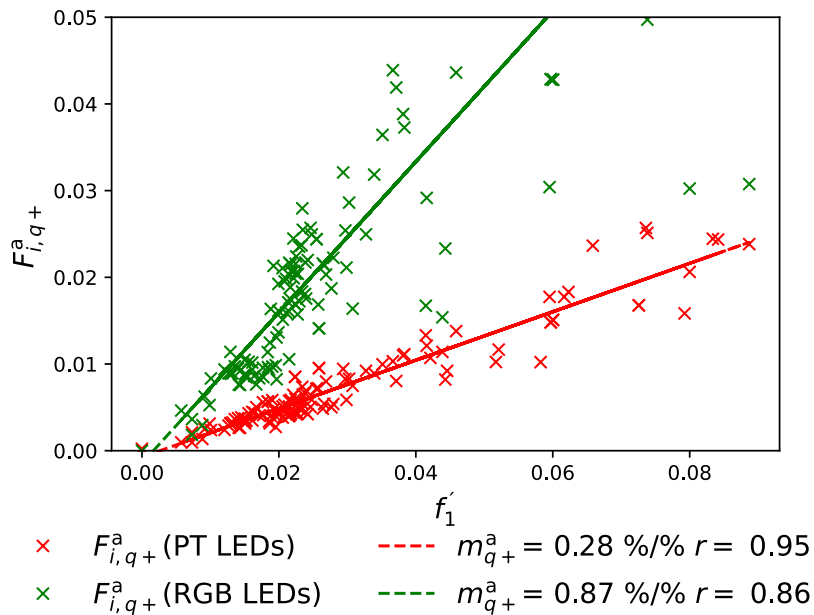


Figure 4: Relation between the absolute deviation due to spectral mismatch and the f_1' value for phosphore type white LEDs and RGB-based white LEDs. (Krüger *et al.*, 2022)

The quantity $F_{i,q+}^a$ represents the 95 % quantile (index q+) for the absolute (upper index a) deviation of the spectral mismatch correction factor minus one ($|F - 1|$) for the photometer i based on a large test set of spectral distributions. The slope of the points is given by the m-values in Figure 4, whereas the r-value represents the square root of the coefficient of determination for the regression.

Example: Using this information in a measurement uncertainty budget, the spectral mismatch correction factor F can be modelled as $F_{\text{PT}} \sim \mathcal{U}(1, 0.28 \cdot f_1')$ for measurements of phosphor-type white LEDs and $F_{\text{RGB}} \sim \mathcal{U}(1, 0.87 \cdot f_1')$ for measurements of RGB-type white LEDs.

3.6 Linearity index, f_3

With the notation of this document, the linearity index is defined based on the relative deviation between actual value and the given value at a certain input setting:

$$f_3(Y) = \left| \frac{Y}{Y_{\max}} \frac{X_{\max}}{X} - 1 \right| \quad (21)$$

This means for the output value Y (with the full range value Y_{\max} in the observed measurement range) and the corresponding input value X we calculate the value $f_3(Y)$. In this case the full range value Y_{\max} is corresponding to X_{\max} input value.

The linearity index f_3 is defined as:

$$f_3 = \max_{Y=0.1Y_{\max} \dots Y_{\max}} [f_3(Y)] \quad (22)$$

Meaning that we look for the maximum $f_3(Y)$ value in a specific measurement range from 10% full range value to the full range value.

The characteristic function $f_3(Y)$ agrees with the definition of non-linearity of (CIE 237:2020, 2020):

$$N_L = \frac{s(Z) - s(Z_R)}{s(Z_R)} \quad (23)$$

With the sensitivity $s(Z)$ and the reference sensitivity $s(Z_R)$. However, no characteristic values based on this function are defined there.

For the following, we will have a look at some properties of the $f_3(Y)$ definition above.

Properties and remarks:

- $f_3(Y_{\max}) = 0$ (This is more or less an adjustment to define a working point.)
- $f_3(Y \rightarrow 0)$ is not defined or significantly depending on the MU of the input values X . Therefore, the calculation is limited to the range $Y = 0.1Y_{\max}$ to Y_{\max} .

If one attributes the correction of the non-linearity of a system to multiplication with a correction factor dependent on the output level (Ferrero, Campos and Pons, 2006) then one must use

$$c_{\text{NL}}(Y) = \frac{X}{Y} = \frac{L_R}{L} \quad (24)$$

multiply so that with $X_{\max} = Y_{\max}$, $f_3(Y)$ can be written as:

$$f_3(Y) = \frac{1}{c_{\text{NL}}(Y)} - 1 \quad (25)$$

Whereas L_0 is the luminance of a luminance standard or other known reference (generally X) and L the luminance measurement result for the corresponding setting L_R (generally Y).

Thus, with the determination of $c_{NL}(Y)$ one has determined both the correction function including their uncertainty $u(c_{NL}(Y))$ and the characteristic value, whereby the measurement uncertainty and the influence of the non-linearity correction on the measurement result can also be described.

All this information is not usable in a MU budget. However, with some additional assumptions, one can estimate the influence of the non-linearity roughly.

The manufacturer and, with a few exceptions, the user can also use the information from a linearity measurement, which is needed to determine the non-linearity correction and its test, to estimate a “residual error”. However, it makes sense to implement the correction not as a factor but as an offset. This offset correction must be carried out before applying further correction factors.

$$Y = c_Y(Y' - Y_0) \quad (26)$$

4 Parameter Estimation

4.1 General Models

4.1.1 Linear Regression

Linear regression will be used often to estimate model parameters, e.g.

- relative temperature coefficients with value pairs (temperature, value)
- dark signal generation rates (integration time, signal @ dark condition)
- evaluation of high dynamic range information (integration time, signal @ light condition)

Calculating the slope α and intercept β from the measurement value pairs, the measurement uncertainty of the slope $u(\alpha)$ has to be estimated too.

Let's start with a linear model:

$$y = \alpha \cdot x + \beta \quad (27)$$

From the device characterization, we get value pairs and measurement uncertainties $(x_i, y_i), (u(x_i), u(y_i))$. Using the standard ordinary least squares approach (OLS), we reach for the slope α :

$$\alpha = \frac{S_{xy}}{S_{xx}} \quad (28)$$

Using the standard notation of summation in this case:

$$S_{xy} = \sum_{i=1}^n (x_i - \bar{x})(y_i - \bar{y}) \quad (29)$$

$$S_{xx} = \sum_{i=1}^n (x_i - \bar{x})(x_i - \bar{x}) \quad (30)$$

But what about $u(\alpha)$? Here we have three different possibilities:

- Using the empirical standard deviation, we get from the OLS regression model.
- Calculating $u(\alpha)$ using a MC-Simulation
- Using the approach of (Matus, 2005)

4.1.1.1 Empirical standard deviation

In the first approach, the empirical standard deviation, $s(\alpha)$, (every regression algorithm will return) will be used. This value describes how the model fits (independent from $u(x)$ and $u(y)$!).

$$s(\alpha) = \frac{S_y}{\sqrt{S_{xx}}} \quad (31)$$

$$s_y^2 = \frac{1}{n-2} \sum_{i=1}^n (y_i - \beta - \alpha x_i)^2 = \frac{S_{xx}S_{yy} - S_{xy}^2}{(n-2)S_{xx}} \quad (32)$$

4.1.1.2 Monte Carlo Simulation

In the second approach, one can use the MCS. Generating random numbers $(\mathcal{N}(x_i, u(x_i)), \mathcal{N}(y_i, u(y_i)))$ and calculate the slope α in every trial. The standard deviation of α can be calculated after the simulation. This straightforward but time-consuming approach should be avoided in a complex model.

4.1.1.3 Matus

In the third case, the approach of (Matus, 2005) is used, calculating the slope's standard deviation and the measurement uncertainty information from the input data. This results in the following formulas:

$$\begin{aligned} u^2(\alpha) &= \sum_{i=1}^n \left(\frac{\delta\alpha}{\delta x_i} \right)^2 u^2(x_i) + \sum_{i=1}^n \left(\frac{\delta\alpha}{\delta y_i} \right)^2 u^2(y_i) \\ &= \sum_{i=1}^n c_{xi}^2 u^2(x_i) + \sum_{i=1}^n c_{yi}^2 u^2(y_i) \end{aligned} \quad (33)$$

$$\begin{aligned} c_{xi} &= \frac{(y_i - \bar{y}) - 2\alpha(x_i - \bar{x})}{S_{xx}} \\ c_{yi} &= \frac{(x_i - \bar{x})}{S_{xx}} \end{aligned} \quad (34)$$

This results in two interesting, exceptional cases:

Table 1: $u(\alpha)$ for different settings

	$u(x_i) \equiv u(x)$	$u(x_i) \equiv 0$
	$u(y_i) \equiv 0$	$u(y_i) \equiv u(y)$
$u(\alpha) =$	$\frac{\sqrt{S_{yy}}}{S_{xx}} u(x)$	$\frac{1}{\sqrt{S_{xx}}} u(y)$

How to compare $u(\alpha)$ and $s(\alpha)$ (see also GUM H 3.2):

$u(\alpha)$:

- Is identical to the results of a MCS (standard deviation of α)
- But more efficient in the calculation (available in front of a MCS)
- Using $u(\alpha)$ equations, one can make design decisions for the experiments (usable also for General Least Square Models GLS)

$s(\alpha)$:

- Empirical standard deviation, describing how the model fits (independent from $u(x)$ and $u(y)$)

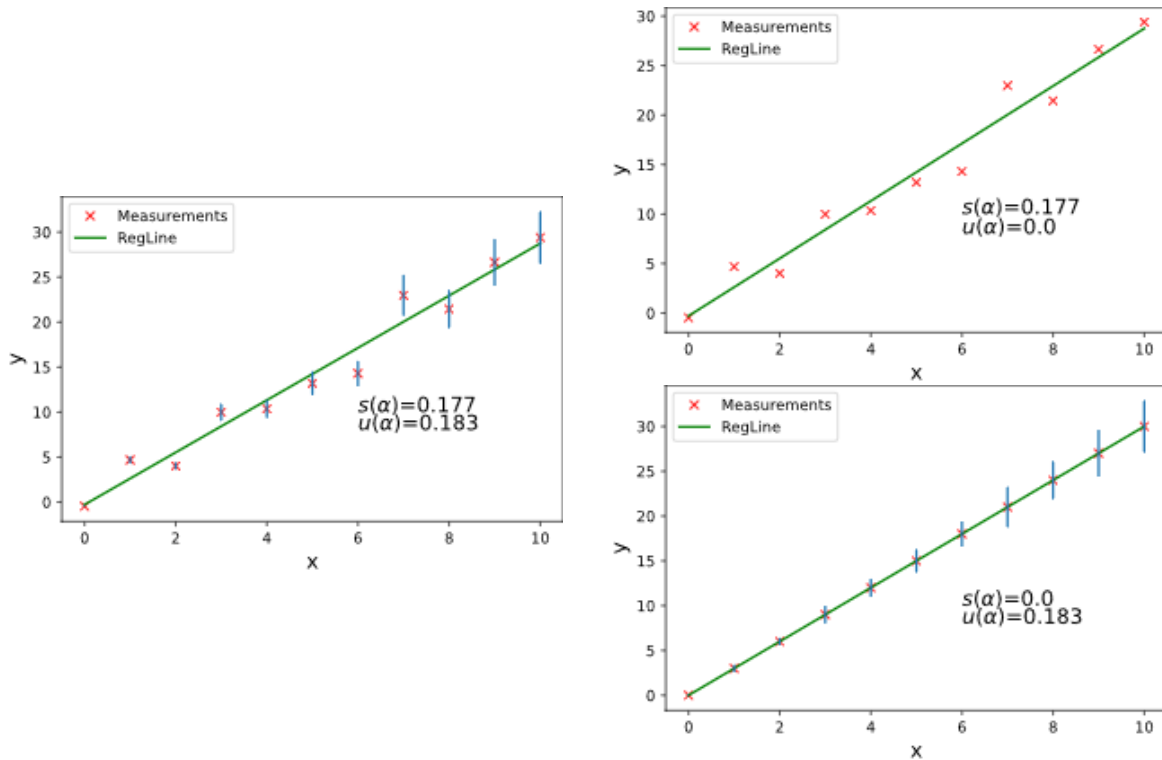


Figure 5: $u(\alpha)$ and $s(\alpha)$ for different settings

I.e. for a simple, practical approach, especially if enough points are available for the regression, one will be able to use $s(\alpha)$. Here, however, one must be aware that one does not use the measurement uncertainty of the points and must trust that due to the large number of measurement points, the realization of the random variables is implicitly included in the regression.

Above all, one must be able to rely on the fact that the mathematical model used represents the underlying physics (see, for example, the use of a polynomial function to generate a wavelength scale for a spectroradiometer from individual measurements of spectral lines).

On the other hand, Matus' approach (Matus, 2005) can be realized quickly so that one can get to the slope and its MU without MCS.

4.2 Examples

For all experiments to investigate the characteristic of ILMDs, great care should be taken to separate the dependency you want to determine from other possible influences. This is not always easy, as the following examples demonstrate.

Problems arise in particular with (some examples for luminance measurements):

- Changing the luminance without changing the spectral distribution of the light source.
- Changing the size of luminous surfaces without changing the luminance.
- Determining angular dependencies (i.e. response non-uniformity) without considering the effect of any angular (or spatial) dependence of the light source.

Furthermore, the following procedure is helpful for experiments (with examples of the temperature sensitivity of a luminance meter):

1. Draw up an essential process for the measurement.
 - What quantity is to be measured? [*luminance*]
 - Which influencing variable [*temperature of the luminance meter*] is to be changed, in which range [*15°C ... 35°C*] is this to happen, and how will the change take place (values [*temperature in 5K steps*], times [*settling time about two hours*⁴], control variables [*device temperature, flow and return temperature of the climate control, additional temperature sensor*]?)
 - Which critical influencing variables must be kept constant? [*luminance of the reference source*]
2. Carry out a few measurements, test the planned evaluation, and validate the original assumptions (waiting times, etc.). In any case, you should also check the reproducibility when approaching specific measuring points.
3. Generate an automatic process for the measurement and evaluation to get a higher data density.

4.3 Light source stability

The stability of the light sources is determined in so-called burn-in tests. The measurement of a luminance standard is prepared with a stable LMD/ILMD (sufficiently run-in, high repeatability is needed). Shortly after switching on the luminance standard, the measurement starts, whereby as many measurements as possible (small time interval) should be made.

From the data, one can then make specifications for the necessary burn-in time and determine the remaining residual noise for modelling.

4.3.1 Burn-In Conditions for luminance standards

The burn-in process of a luminance standard (SD CIE standard illuminant A) is illustrated in Figure 6. From the data, a necessary run-in time of 3-5 min can be derived. The "residual noise" is $<2e-5$, whereby at this order of magnitude, it is no longer possible to distinguish between the residual noise of the DUT and that of the measuring device.

⁴ When determining temperature dependencies, long settling times are often required so that the temperature conditions in the device stabilise. In this case, it makes sense to record measured values at short intervals (e.g. one minute) in order to observe the transient behaviour. For the evaluation of the actual measurement, the mean value of the last measurements (before setting the next temperature) can be used.

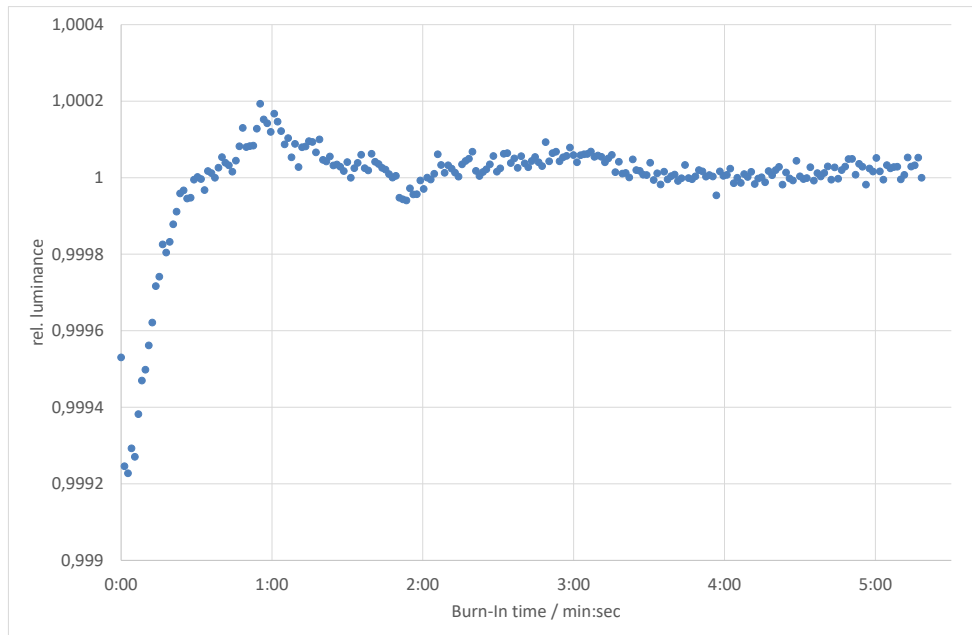


Figure 6: Burn-in results for a luminance standard

4.3.2 Burn-In Observation for DUT's

The burn-in process of a DUT (SD phosphore type LED) is illustrated in Figure 7. From the data, a necessary run-in time of only 1 min can be derived. The "residual noise" is 2.5×10^{-5} , whereby at this order of magnitude it is no longer possible to distinguish between the residual noise of the DUT and that of the measuring device.

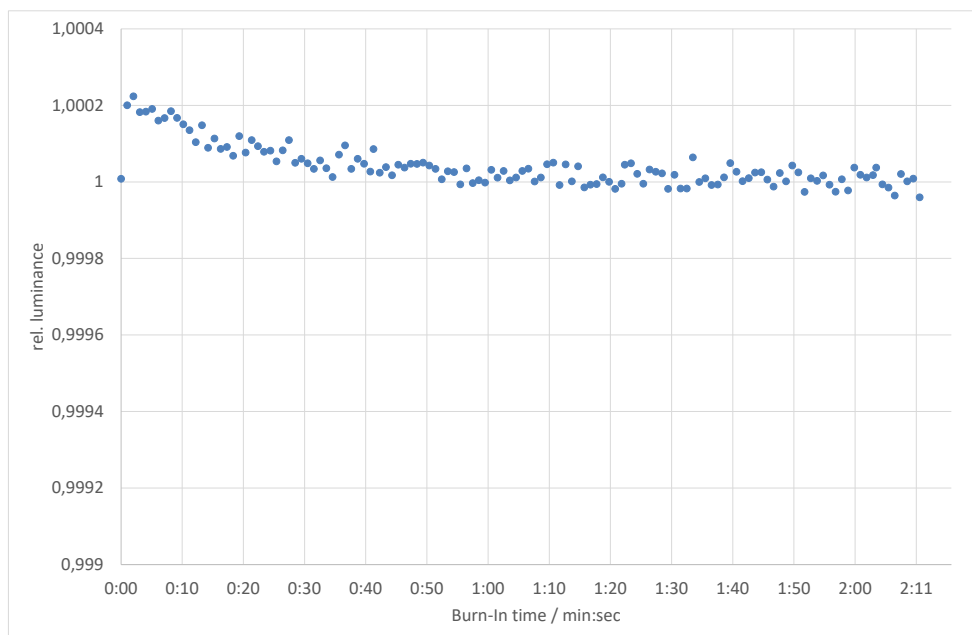


Figure 7: Burn-in results for a DUT

4.4 Temperature Coefficient

For the estimation of the temperature coefficient of a reading x' with respect to a temperature T (ambient temperature T_a or device temperature T_D) usually, a measurement in a temperature chamber is recommended for exact measurements. For rough estimations, measurements during self-heating are also possible.

The measurement design for a linear regression model (see 4.1.1) should be made over the complete temperature operating range for the device. Furthermore, the choice of temperature steps and settling times should ensure that the device under investigation is already in thermal equilibrium during the measurement. This can be guaranteed by so-called pyramid measurements, in which a specific temperature is realized both in the direction of rising and falling temperature.

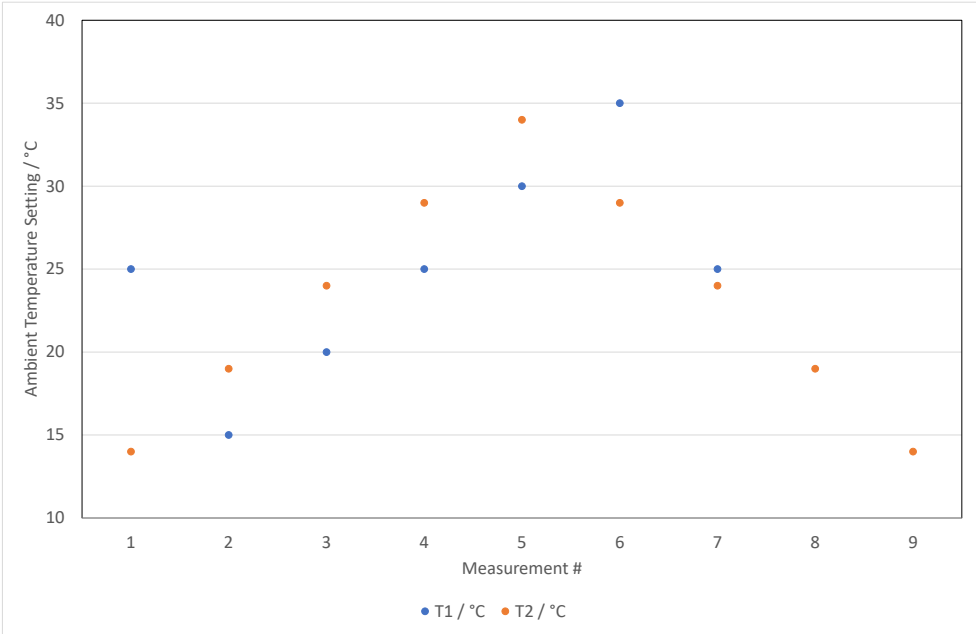


Figure 8: Temperature settings for a pyramid design (T2) and modified pyramid design (T1)

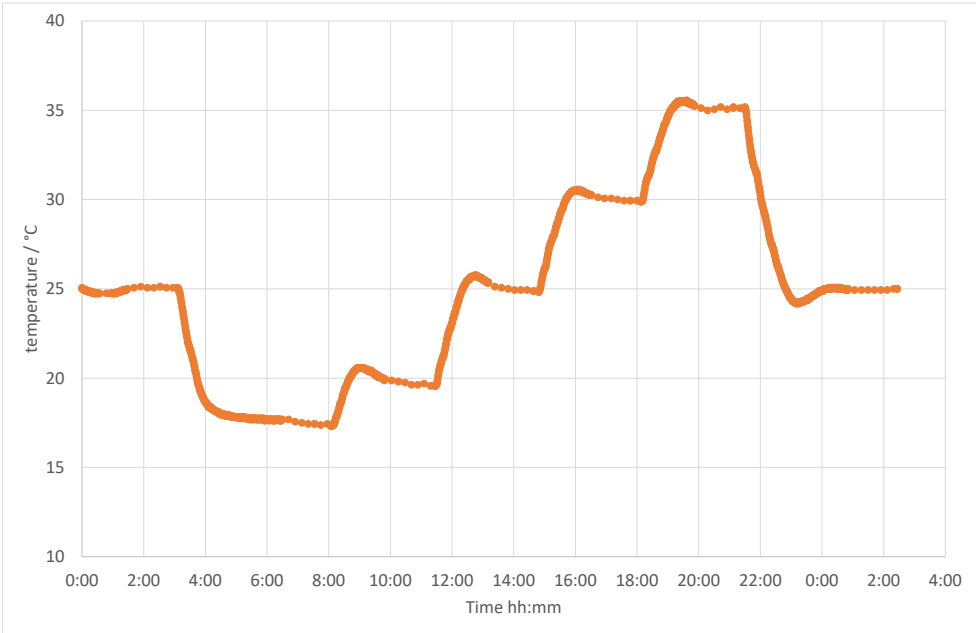


Figure 9: Example temperature profile for the T1-Design from Figure 8

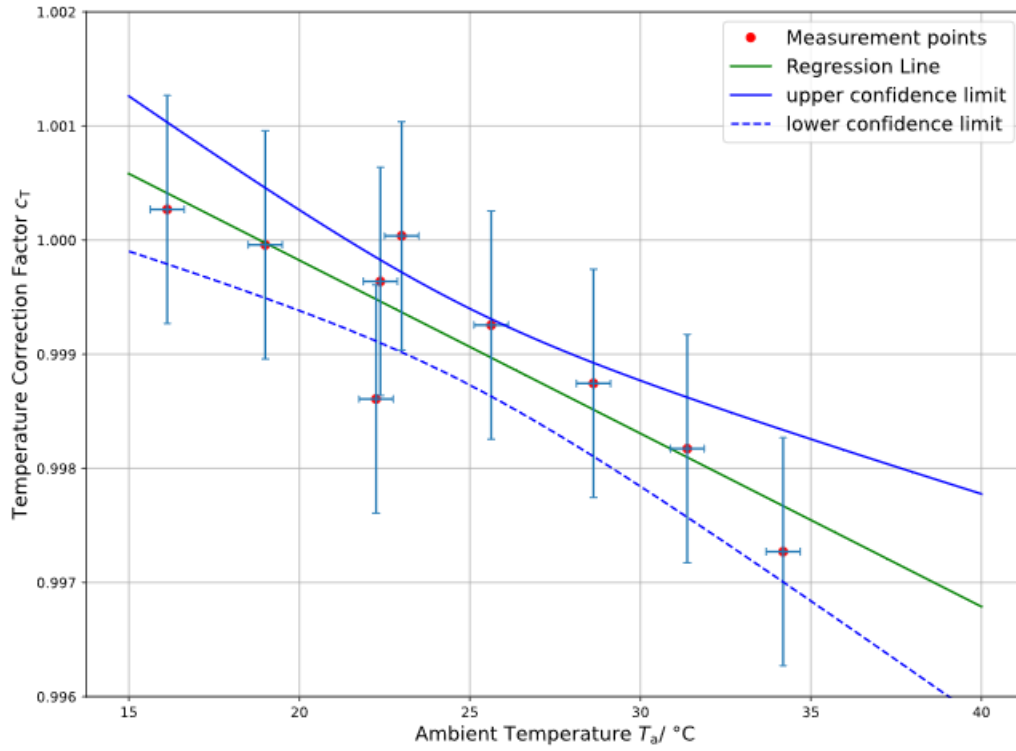


Figure 10: Regression line and confidence interval for a relative temperature coefficient evaluation

Table 2: Measurement data and results for the sample temperature coefficient

	T / °C	Y / A.U.
u(.)	0,5	0,001
α	- 0,00015254	
u(α) Matus	6,095E-05	
u(α) MCS	6.070E-05	
s(α)	2,8703E-05	
	22,25	0,998607574
	16,125	1,000268825
	19	0,999958121
	22,375	0,999638246
	25,625	0,999255214
	28,625	0,998744568
	31,375	0,998172623
	34,1875	0,997269868
	23	1,000037044

The Y values in Table 2 represent relative values only. One can normalize the reading to the reference temperature reading, the mean value or other calculations. The only precondition is that the relative values are close to 1 at the end.

For the MU of Y only the repeatability was taken into account. All fully correlated contributions do not affect the measurement uncertainty of the slope.

4.5 Ageing of a luminance standard

One can proceed similarly to describe the ageing of a luminance standard, i.e. the change in luminance between calibrations as a function of time or operating hours.

For this purpose, a table with the date of calibration, current operating hours counter, luminance and standard measurement uncertainty of the luminance is used. In the following, the luminance is normalized to the last known value from the calibration certificates.

The uncertainty in calibrations contains, at least in the case of NMI's, large correlated portions that result from the traceability of the unit. It is, therefore, not sensible in this case to use the MU of the calibrations in the regression analysis, as these would have to be modelled correlated in this case, which leads to no contribution to MU in the slope.

It may therefore make sense to use the empirical standard deviation $s(\alpha)$ from the regression as uncertainty for the slope.

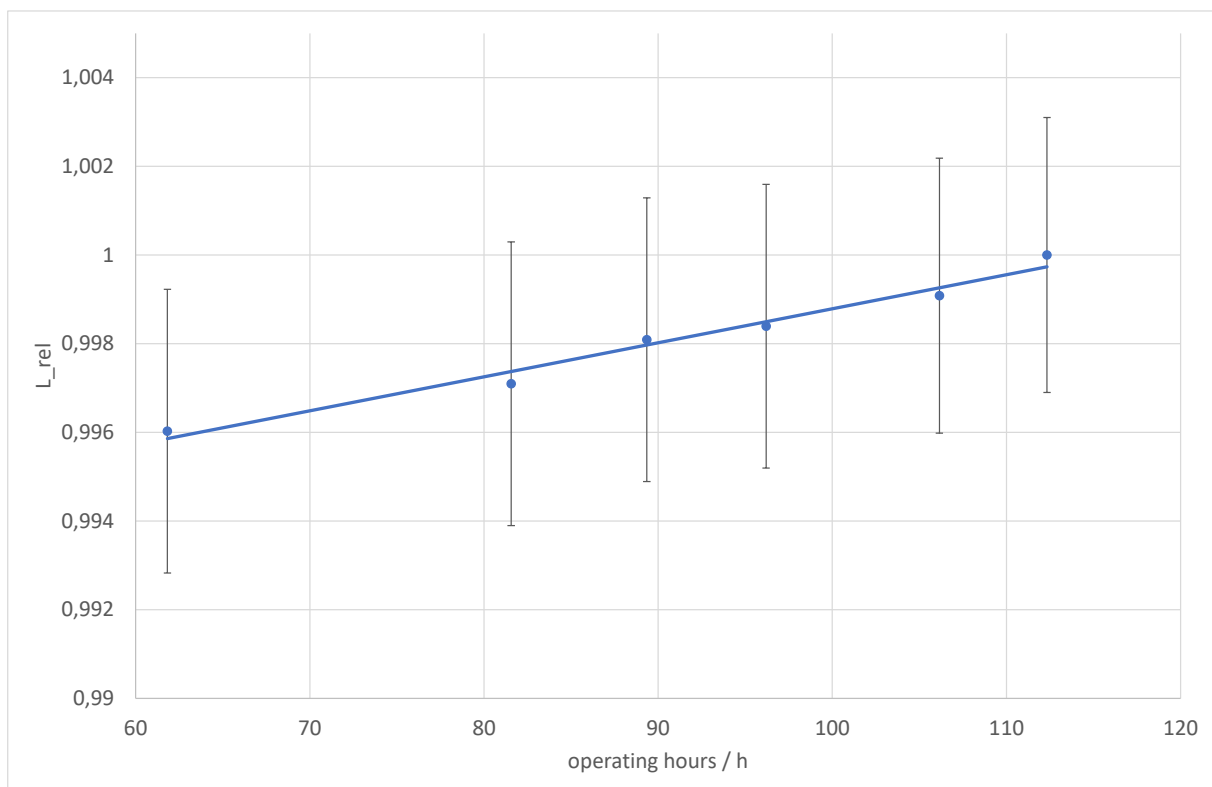


Figure 11: Ageing of a luminance standard over 50 operation hours with standard uncertainties from the calibration sheets

Table 3: Collecting data from calibration certificates of a luminance standard

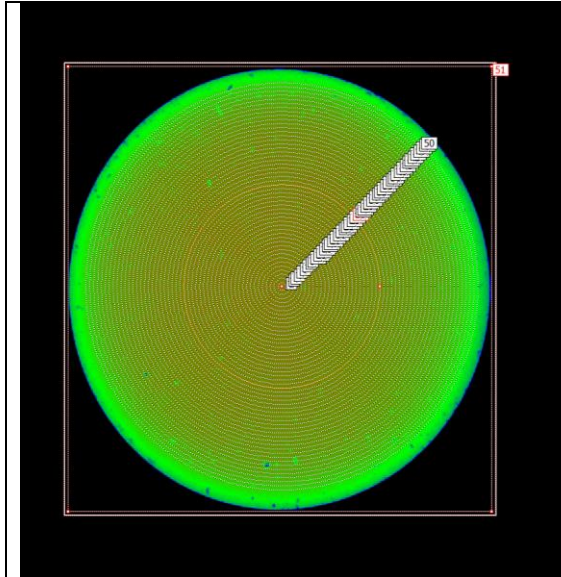
$\alpha_{p,C}$	0,0077%	1/h	
$s(\alpha_{p,C})$	0,00006%	1/h	
r^2	0,977		
t / days	t_{op} / h	L_{rel}	$u(L_{rel})$
3500	112,33	1,0000	0,0031
2788	106,15	0,9991	0,0031
2106	96,20	0,9984	0,0032
1469	89,35	0,9981	0,0032
728	81,56	0,9971	0,0032
0	61,82	0,9960	0,0032

4.6 Non-uniformity of a light source

In addition to the run-in behaviour, the radiation behaviour of the luminance standards also plays a role for the measurement, which must be described.

The following influences must be examined:

1. How does the average luminance depend on the size of the evaluation region?
2. How does the average luminance change if the evaluation region is not positioned precisely in the centre?
3. How does the luminance change if the measurement is not exactly perpendicular to the surface of the luminance standard?



In the first step, the luminous surface of the luminance standard is captured with an ILMD, and the average luminance of circular regions of different sizes is evaluated (see picture). Then the relative mean luminance is plotted as a function of area and the area surrounding the calibration conditions (1/4 of the total area) is examined. If you want to calculate the homogeneity properties of the ILMD, you can also combine different images that show the luminance standard on different areas of the ILMD (multiple displacement of the ILMD relative to the luminance standard while maintaining the perpendicular position). As a rule, however, this is not necessary.

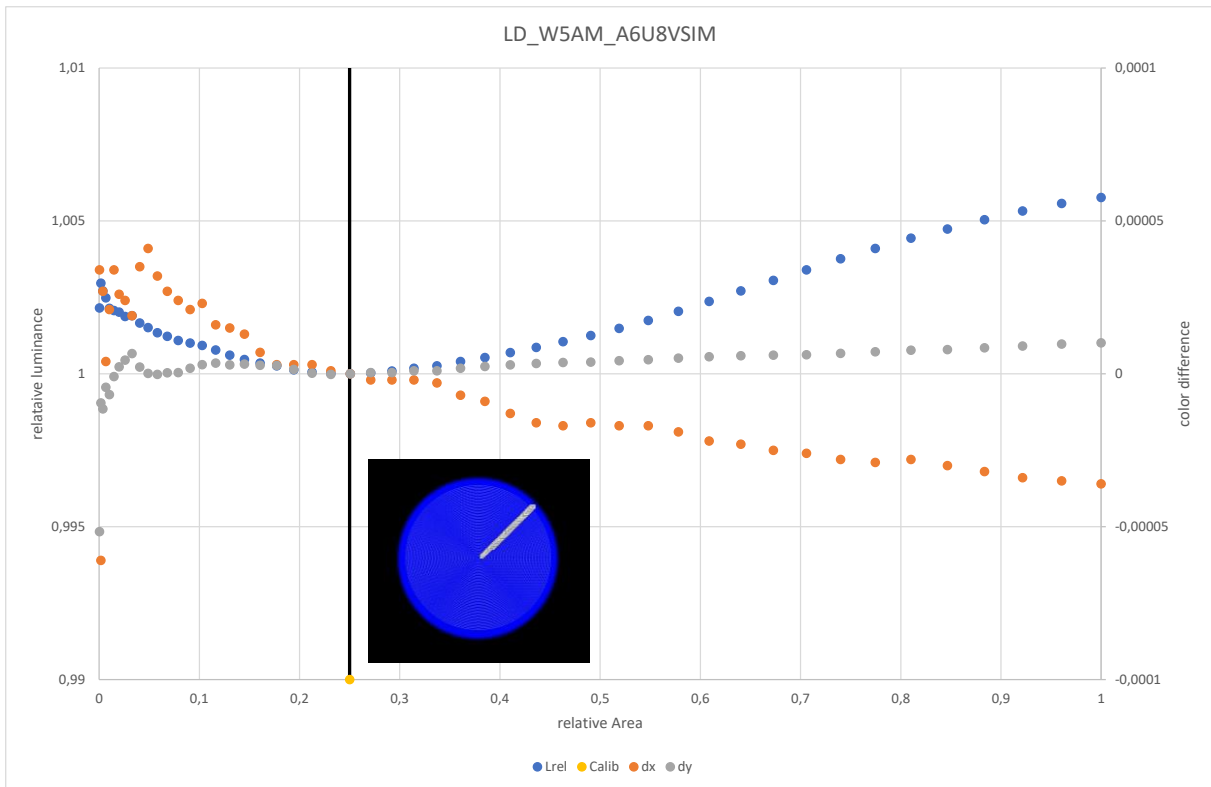


Figure 12: Relative luminance change for different evaluation region sizes (L^3 luminance standard)

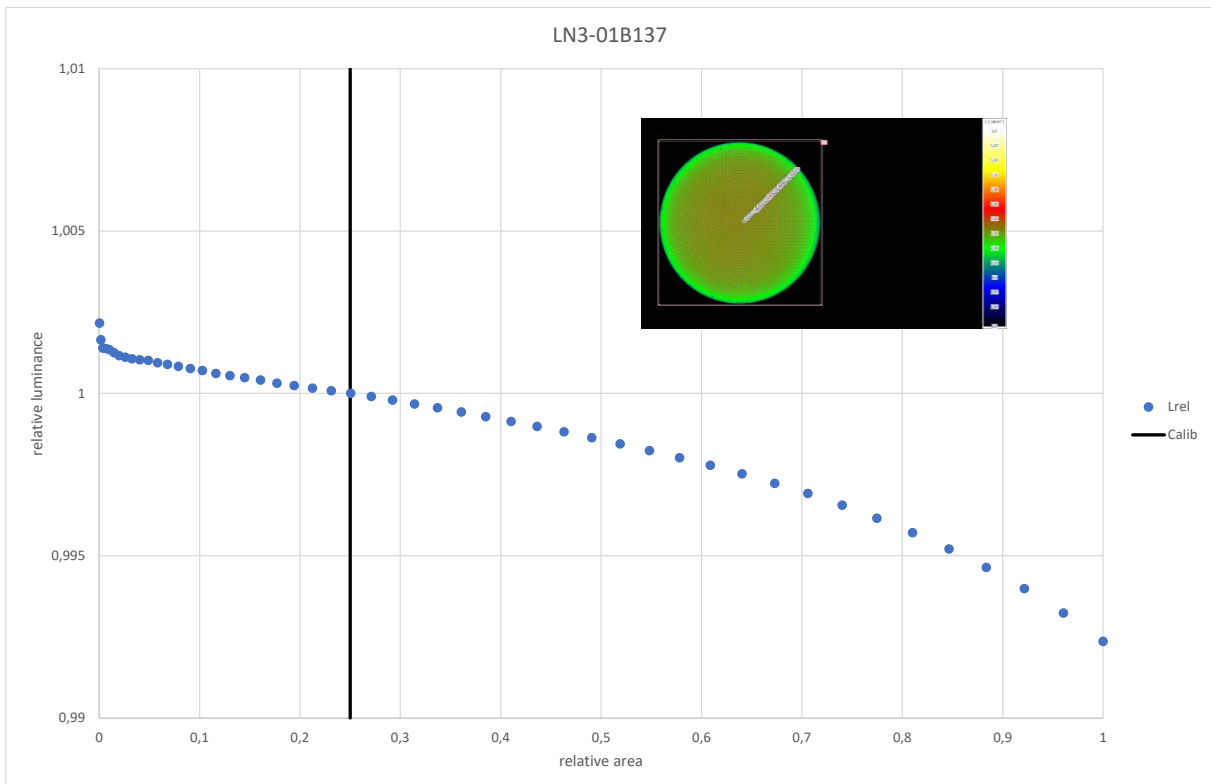


Figure 13; Relative luminance change for different evaluation region sizes (LN3 luminance standard)

4.7 Non-Linearity Correction

Let's assume we make several measurements of a luminance standard with different integration times of the luminance measuring device:

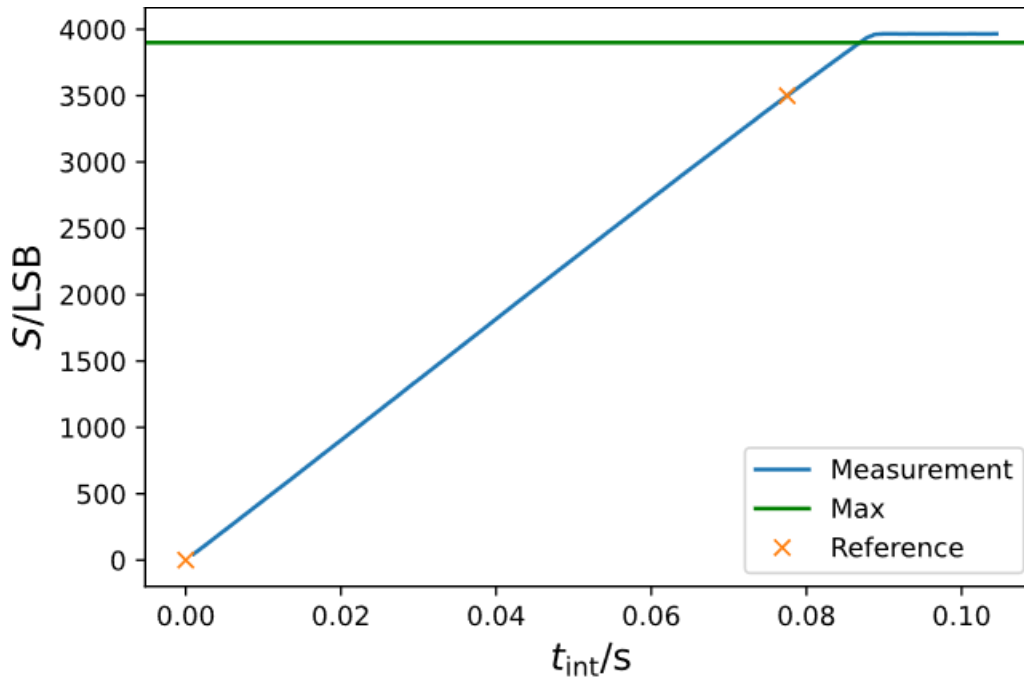


Figure 14: Measurement of a luminance standard with different integration times

We define a maximum load and two reference values. The line through the reference points represents the ideal behaviour of the device. Any deviation from this line is called non-linearity.

Remark: The manufacturer will do this (as demonstrated in Figure 12) with the Analogue-Digital-Converter readings (called counts and stated in digital numbers (DN) or least significant bit (LSB)) and not with the final measurement results. In this case, the manufacturer can avoid a range change and probably use the non-linearity information for different measurement ranges. If this is impossible, the manufacturer can switch between different non-linearity corrections for different measurement ranges (amplifier gain settings).

The corrected value S of the internal measurement can be described based on the reading S' with $S = f_{NL}(S')$. The correction function f_{NL} can be described using a polynomial or a look-up table. The use of the polynomial is described here.

$$f_{NL}(x) = \sum_{i=0}^{N_p} \alpha_i x^i \quad (35)$$

With α_i the polynomial coefficients of the polynomial with grade N_p and x is the variable of the domain, used for evaluation.

Remark: The dark signal correction should be applied before, e.g. $S = f_{NL}(S' - S'_0)$

The question for the MU evaluation is now how to implement this correction. We have two possibilities here:

- Use a MCS for the regression and estimate the polynomial coefficients, including their correlation.
- We can use the range calibration approach (Kessel, Kacker and Sommer, 2010)

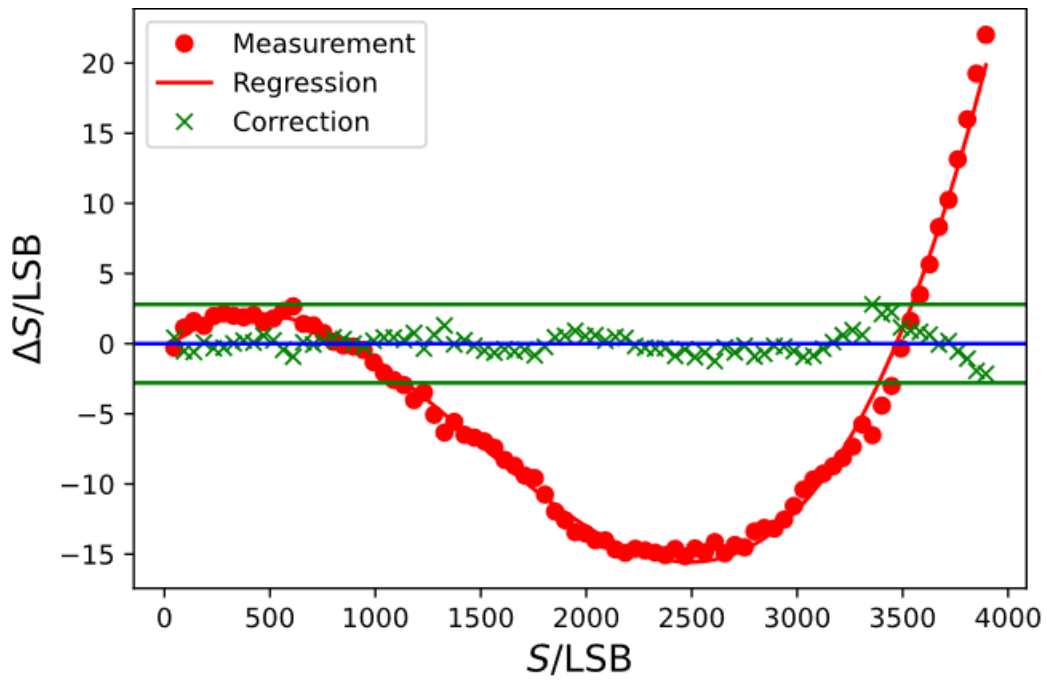


Figure 15: Description of the non-linearity and the result of a non-linearity correction

Table 4: Coefficients of the full regression polynomial for Figure 13 (with domain scaling $[0,4000] \rightarrow [-1,1]$)

Coef.	x^0	x^1	x^2	x^3
Mean	2004,20	1986,10	-1,55	16,65
StdDev	0,47	0,64	0,40	0,81
Rel.StdDev	0,02%	0,03%	-25,93%	4,88%

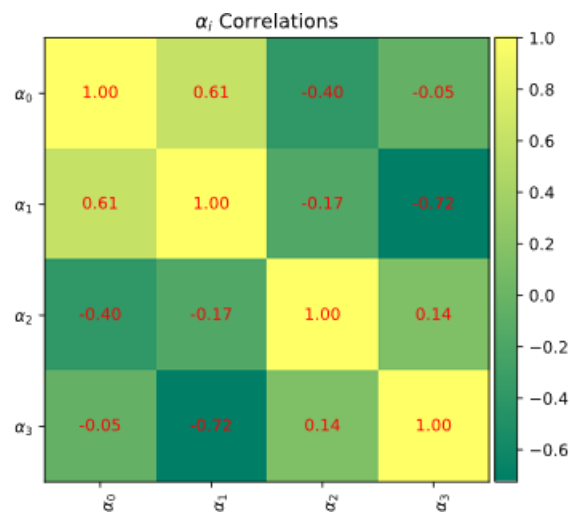


Figure 16: Coefficients of correlation for the polynomial coefficients

5 Monte Carlo Simulation

According to *GUMS1* the Monte Carlo Simulation (MCS) is one way to calculate the measurement uncertainty of a measurand.

This is neither the place to explain the mathematical foundations of MCS nor to go into its subtleties. The following is only a plausible basic introduction, which should be sufficient to carry out and evaluate the first MCS on your own.

The reader will find a more detailed introduction on the engineering level with practical examples (including source code) in (Amelin, 2015; Ciaburro, 2020; Dunn and Shultis, 2022; Stevens, 2022).

5.1 Basics

Assume we have a series of measurements with N readings taken one after the other. Now we can determine the mean and the standard deviation of these readings.

$$\hat{\mu} = \bar{x} = \sum_{i=1}^N x_i \quad \hat{\sigma} = \sqrt{\frac{1}{N} \sum_{i=1}^N (x_i - \bar{x})^2} \quad (36)$$

With the MCS as it is used for the determination of the combined uncertainty of a measurement, we do precisely the opposite. We know the value (mean) and the uncertainty (standard deviation) of the measured input variable (e.g. from the readings and calibration sheets) and generate a series of individual values (assuming a probability density function (PDF) - often the PDF of a normal distribution) representing the possible spread of values for this simulated quantity which might be seen in real measurements. We calculate the output quantity or variables via the measurement model with these individual values (usually from different input variables). Now we can again determine the mean value and standard deviation for the output variable and then have an estimate for our output variables and their measurement uncertainty.

Table 5: Analogy between multiple measurements (left) and the generation of random numbers in an MCS (right)

Index	Measurement		μ	9,973
1	9,986		σ	0,117
2	10,001		Index	Simulation
3	9,968		1	9,789
4	9,976		2	10,11
5	9,885		3	10,136
6	10,141		4	9,965
7	10,133		5	9,646
8	9,738		6	10,158
9	9,858		7	9,959
10	10,047		8	10,102
		9	9,919	
$\hat{\mu}$	9,973	10	9,927	
$\hat{\sigma}$	0,117			
		$\hat{\mu}$	9,971	
		$\hat{\sigma}$	0,156	

The numerical examples in Table 5 roughly reproduce the procedure (with far too few numbers). First, you have ten measured values, from which you determine the mean and standard deviation (left half of the table). In the MCS (right half of the table), you then take these data and generate ten random numbers with the parameter's mean value and standard deviation using a random generator. If you determine the mean value and standard deviation for these generated random numbers, then you get approximately the values that you previously obtained in the evaluation of the measurement series. The more random numbers you generate, the better the agreement.

5.2 Code Example

The implementation of the MCS can be found in the GitHub repository of this project under the folder <https://github.com/empir19nrm02/empir19nrm02/tree/main/empir19nrm02/MC>

Examples for the usage can be found in the Jupyter Notebook https://github.com/empir19nrm02/empir19nrm02/blob/main/empir19nrm02/Jupyter/MCSim_PM.ipynb

6 References

- Amelin, M. (2015) *Monte Carlo Simulation in Engineering*. KTH Royal Institute of Technology. Available at: [https://www.kth.se/social/files/562dfd19f276544062a47ba1/Monte Carlo Simulation in Engineering.pdf](https://www.kth.se/social/files/562dfd19f276544062a47ba1/Monte_Carlo_Simulation_in_Engineering.pdf).
- Ciaburro, G. (2020) *Hands-On Simulation Modeling with Python: Develop simulation models to get accurate results and enhance decision-making processes*. Packt Publishing.
- CIE 198-SP2:2018 (2018) *Determination of Measurement Uncertainties in Photometry Supplement 2: Spectral measurements and derivative quantities*. Vienna. doi: 10.25039/TR.198SP2.2018.
- CIE 198:2011 (2011) *Determination of Measurement Uncertainties in Photometry*, CIE. Available at: <http://cie.co.at/publications/determination-measurement-uncertainties-photometry>.
- CIE 237:2020 (2020) *Non-Linearity of Optical Detector Systems*. Vienna. doi: 10.25039/TR.237.2020.
- CIE198-SP1.1:2011 (2011) *Determination of Measurement Uncertainties in Photometry. SUPPLEMENT 1: Modules and Examples for the Determination of Measurement Uncertainties. Part 1: Modules for the Construction of Measurement Equations*. Vienna: International Commission on Illumination. Available at: <https://cie.co.at/publications/determination-measurement-uncertainties-photometry-supplement-1-modules-and-examples-0>.
- CIE198-SP1.2:2011 (2011) *Determination of Measurement Uncertainties in Photometry. Supplement 1: Modules and Examples for the Determination of Measurement Uncertainties. Part 2: Examples for models with Individual Inputs*. International Commission on Illumination. Available at: <https://cie.co.at/publications/determination-measurement-uncertainties-photometry-supplement-1-modules-and-examples-0>.
- CIE198-SP1.3:2011 (2010) *Determination of Measurement Uncertainties in Photometry. Supplement 1: Modules and Examples for the Determination of Measurement Uncertainties. Part 3: Examples for the Solving of Systems of Equations*. Vienna: International Commission on Illumination. Available at: <https://cie.co.at/publications/determination-measurement-uncertainties-photometry-supplement-1-modules-and-examples-0>.
- CIE198-SP1.4:2011 (2011) *Determination of Measurement Uncertainties in Photometry. Supplement 1: Modules and Examples for the Determination of Measurement Uncertainties. Part 4: Examples for Models with Distributions*. Vienna: International Commission on Illumination. Available at: <https://cie.co.at/publications/determination-measurement-uncertainties-photometry-supplement-1-modules-and-examples-0>.
- CIE244:2021 (2021) *CIE 244:2021 Characterization of Imaging Luminance Measurement Devices (ILMDs)*. Vienna. doi: 10.25039/TR.244.2021.
- Dunn, W. L. and Shultis, J. K. (2022) *Exploring Monte Carlo Methods*. Elsevier Science; 2nd edition.
- EMVA (2016) *EMVA Standard 1288 Release 3.1*. doi: 10.5281/zenodo.235942.
- Ferrero, A., Campos, J. and Pons, A. (2006) "Low-uncertainty absolute radiometric calibration of a CCD," *Metrologia*, 43(2), pp. S17–S21. doi: 10.1088/0026-1394/43/2/S04.
- ISO/CIE 19476:2014 (2014) *Characterization and performance of illuminance meters and luminance meters*.
- Janesick, J., Klaasen, K. and Elliott, T. (1985) "CCD Charge Collection Efficiency And The Photon Transfer Technique," in Dereniak, E. L. and Prettyjohns, K. N. (eds.), p. 7. doi: 10.1117/12.950297.
- JCGM 100:2008 (2008) "Evaluation of measurement data — Guide to the expression of uncertainty in measurement," *International Organization for Standardization Geneva ISBN*, 50(September), p. 134.

Available at: <http://www.bipm.org/en/publications/guides/gum.html>.

JCGM 101:2011 (2011) "Evaluation of measurement data — Supplement 1 to the 'Guide to the expression of uncertainty in measurement' — Propagation of distributions using a Monte Carlo method," *International Organization for Standardization Geneva*, 101, p. 90.

JCGM 102:2011 (2011) "Evaluation of measurement data — Supplement 2 to the 'Guide to the expression of uncertainty in measurement' — Extension to any number of output quantities," *International Organization for Standardization Geneva*, 102(October), pp. 1–72.

JCGM106:2020 (2020) "Guide to the expression of uncertainty in measurement - Part 6: Developing and using measurement models," *International Organization for Standardization Geneva*, JCGM GUM-6, pp. 1–103. Available at: <https://www.bipm.org/en/publications/guides>.

Kessel, R., Kacker, R. N. and Sommer, K. D. (2010) "Uncertainty budgeting for range calibration," *ENBIS - IMEKO TC21 Workshop on Measurement Systems and Process Improvement 2010*, pp. 215–243.

Krüger, U. *et al.* (2014) "Messunsicherheit photometrischer Messungen unter Berücksichtigung der Anforderungen der prEN13032-T4 (Langversion)," in *Licht2014, Tagungsband*. Den Haag, Niederlande, pp. 711–725.

Krüger, U. *et al.* (2022) "Evaluation of different general V (λ) mismatch indices of photometers for LED-based light sources in general lighting applications," *Metrologia*. doi: 10.1088/1681-7575/ac8f4d.

Krüger, U. *et al.* (2023) "SENSITIVITY EVALUATION OF MEASUREMENT UNCERTAINTY CONTRIBUTIONS OF SPECTRAL DATA FOR CALCULATED INTEGRAL QUANTITIES," in *CIE x050:2023 Proceedings of the CIE symposium on Innovative Lighting Technologies, September 18-20, 2023, Ljubljana, Slovenia*. Vienna: CIE, pp. 20–33. doi: 10.25039/x50.2023.OP061.

Matus, M. (2005) "Koeffizienten und Ausgleichsrechnung: Die Messunsicherheit nach GUM. Teil 1: Ausgleichsgeraden (Coefficients and Adjustment Calculations: Measurement Uncertainty under GUM. Part 1: Best Fit Straight Lines)," *teme*, 72(10), pp. 584–591. doi: 10.1524/teme.2005.72.10_2005.584.

Sauter, G. (2012) *Model of evaluation for luminous flux measurement with integrating sphere method using an incandescent lamp as reference standard*.

Sripad, A. and Snyder, D. (1977) "A necessary and sufficient condition for quantization errors to be uniform and white," *IEEE Transactions on Acoustics, Speech, and Signal Processing*, 25(5), pp. 442–448. doi: 10.1109/TASSP.1977.1162977.

Stevens, A. (2022) *Monte-Carlo Simulation: An Introduction for Engineers and Scientists*. London, England: CRC Press.